INTERACTIONS OF TRIBLOCK COPOLYMERS WITH IONIC SURFACTANTS

Islamabad

A dissertation submitted to the Department of Chemistry, Quaid-i-Azam University, Islamabad, in partial fulfillment of the requirements for the degree of

Master of Philosophy

in

Physical Chemistry

by

Zaheer Ahmad

Department of Chemistry
Quaid-i-Azam University
Islamabad
2010

DECLARATION

This is to certify that this dissertation entitled **"Interactions of triblock copolymers with ionic surfactants".** submitted by ***Mr. Zaheer Ahmad*** is accepted in its present form by the Department of Chemistry, Quaid-i-Azam University, Islamabad, Pakistan, as satisfying the dissertation requirements for the degree of ***Master of Philosophy in Physical Chemistry.***

Supervisor:

Prof. Dr. M. Siddiq
Department of Chemistry
Quaid-i-Azam University
Islamabad.

External Examiner:

Dr. Habib Ahmad
Principal Scientific Officer
Chemical Technology Division
A. Q. Khan Research Labs.
P.O. Box 502
Rawalpindi

Head of Section:

Prof. Dr. M. Shahid Ansari
Department of Chemistry
Quaid-i-Azam University
Islamabad.

Chairman:

Prof. Dr. Saqib Ali
Department of Chemistry
Quaid-i-Azam University
Islamabad.

Dedicated to

My sweet Sauban & Rumeesa

ACKNOWLEDGEMENTS

All praises to almighty **ALLAH**, he benevolent, who bestowed upon me. His blessings and through the mediation of his beloved **Prophet Muhammad (peace be upon him)** whose guidance enlightened my way toward the right path and whose sayings enable me to find my research basics in the Quran.

I offer my humble thanks and pay my immense gratitude to my most respected and worthy supervisor **Professor Dr. Mohammad Siddiq**, who showed commendable alacrity in providing proper guidance and encouragement. His support through educative discussion and scientific suggestions made this research work to be an extremely purposeful venture for me personally.

I am also grateful to **Professor Dr. Saqib Ali, Chairman Department of Chemistry**, for providing me all necessary facilities during the course of my research work.

I am also thankful to **Professor Dr. Shaid Ansari, Head of Physical section, Department of Chemistry** for providing me all necessary facilities during the completion of my research work.

I cannot afford to forget my parents and family members for their consistent encouragement and support.

The last but not the least thanks to all my friends and lab-fellows, Abbas Khan, Muhammad Usman, Musammir Khan, Iram bibi, Noor Rehman, Sayyar Ali Shah and Irfan Haider and all the well-wishers who helped me in areas where I got stuck up during this research undertaking.

(Zaheer Ahmad)

ABSTRACT

The interactions of triblock copolymers $E_{30}B_{10}E_{30}$ and $E_{48}B_{10}E_{48}$ with anionic surfactant SDS and cationic surfactant CTAB were studied employing surface tensiometry, electrical conductivity, pyrene fluorescence probe and dynamic laser light scattering techniques. Using surface tensiometry and electrical conductivity techniques Critical Micelle Concentration (CMC) were determined. Electrical Conductivity technique was used to determine CMC, degree of ionization (α), degree of counter ion binding (β) and free energy of micellization (ΔG_m). The increase trend in CMC for ternary system both in the case of SDS and CTAB were observed. The increase in CMC in case of concentrated polymer solution is more as compare to dilute polymer solution both in the case of SDS and CTAB. In our case among the two triblock copolymers, $E_{30}B_{10}E_{30}$ is more hydrophobic (B/E = 0.166) as compare to $E_{48}B_{10}E_{48}$ (B/E = 0.104) that is why $E_{48}B_{10}E_{48}$ cause more delay in the CMC of surfactants and greater increase were observed in this case. The CMC of the mixed system determined by surface tensiometry and electrical conductivity are in close agreement with an increasing trend. The increase trends were observed for degree of ionization in case of SDS as compare to CTAB. Degree of counter ion binding increase in case of CTAB as compare to SDS. The free energy of micellization remains negative both in the case of SDS and CTAB predicting that the process is spontaneous.

Pyrene Fluorescence technique was used to calculate first and third vibronic ratio I_1/I_3, micelle aggregation number (N_{agg}), Binding sites (n), Binding constant (K_b) and free energy of binding (ΔG_b). The 1st and 3rd vibronic ratio for pure CTAB is more as compare to SDS confirming more hydrophobic nature of CTAB. In the presence of triblock copolymers the I_1/I_3 ratio is more for SDS as compare to CTAB, predicting that the micro polarity of the solvent decrease in the case of CTAB. The aggregation number decrease both in the case of SDS and CTAB.

Dynamic laser light scattering was used to determine the apparent hydrodynamic radius (R_h). Decrease in the aggregates size (R_h) in the presence of surfactants (SDS) were confirmed from dynamic laser light scattering.

TABLE OF CONTENTS

LIST OF TABLES

LIST OF FIGURES

Chapter – 1

INTRODUCTION

Chapter - 1
INTRODUCTION

1.1 Polymer

The word *polymer* is derived from the Greek words (*poly*), meaning "many" and (*meros*), meaning "part". The term was coined in 1833 by "Jons Jakob Berzelius Jöns". Thus polymer is a large molecule (macromolecule) built by the repetition of small chemical units. Polymers are materials which consist of repeating units whose molecular weights are in the range of tens to hundreds of Daltons. The majority of water soluble polymers, whether natural or synthetic are carbon based. Generally the solubility of these polymers is due to the presence of polar oxygen groups while sometimes the polar groups are nitrogen based. The polar group and hydrophobic centers on the polymer represent sites for possible interaction with added surfactants. The mobility of the polymer or the polymer segments in aqueous solution is important. Due to high molecular weight of the polymer, the diffusion coefficient of polymers is less than that of simple solutes by a hundred or thousands fold or more. However, the mobility of individual monomer groups within the polymer can be large, especially in the polymer molecules that adopt a random configuration in solution. This point is quite important in understanding polymer/surfactant interaction mechanism. Open configuration and higher monomer mobility are encouraged in "good solvents" while more closed configuration and lower monomer mobility are encountered in "poor solvents".

1.1.1 Historical Background

Starting in 1811, Henri Braconnot did pioneering work in derivative cellulose compounds, perhaps the earliest important work in polymer science. The development of vulcanization later in the nineteenth century improved the durability of the natural polymer rubber, signifying the first popularized semi-synthetic polymer. In 1907, Leo Baekeland created the first completely synthetic polymer, Bakelite, by reacting phenol and formaldehyde at precisely controlled temperature and pressure. Bakelite was then publicly introduced in 1909. Despite significant advances in synthesis and characterization of polymers, a correct understanding of polymer molecular structure did not emerge until the 1920s. Before that time, scientists believed that polymers were clusters of small molecules (called colloid), without definite molecular weights, held

together by an unknown force, a concept known as association theory. In 1922, Hermann Staudinger proposed that polymers consisted of long chains of atoms held together by covalent bonds, an idea which did not gain wide acceptance for over a decade and for which Staudinger was ultimately awarded the Nobel Prize. Work by Wallace Carothers in the 1920s also demonstrated that polymers could be synthesized rationally from their constituent monomers. An important contribution to synthetic polymer science was made by the Italian chemist Giulio Natta and the German chemist Karl Ziegler, who won the Nobel Prize in Chemistry in 1963 for the development of the Ziegler-Natta catalyst. Further recognition of the importance of polymers came with the award of the Nobel Prize in Chemistry in 1974 to Paul Flory, whose extensive work on polymers included the kinetics of step-growth polymerization and of addition Polymerization, chain transfer, excluded volume, the Flory-Huggins solution theory, and the Flory convention.

1.1.2 Applications of Polymers

Synthetic polymer materials such as nylon, polyethylene, Teflon, and silicone have formed the basis for a burgeoning polymer industry. These years have also shown significant developments in rational polymer synthesis. Most commercially important polymers today are entirely synthetic and produced in high volume on appropriately scaled organic synthetic techniques. Synthetic polymers today find application in nearly every industry and area of life. Polymers are widely used as adhesives and lubricants, as well as structural components for products ranging from children's toys to aircraft. They have been employed in a variety of biomedical applications ranging from implantable devices to controlled drug delivery. Polymers such as poly (methyl methacrylate) find application as photoresist materials used in semiconductor manufacturing and low-k dielectrics for use in high-performance microprocessors. Recently, polymers have also been employed as flexible substrates in the development of organic light-emitting diodes for electronic displays.[1]

1.1.3 Classification of Polymers

Like the old story about the elephant and the blind men, the way people classify polymers depends on their experience. For example, an organic chemist is interested in the detailed arrangement of atoms in the chain, while a structural engineer only considers a table of physical attributes such as tensile strength or density. There is no uniform system of classification of polymers.[2]

Polymers can be classified in many different ways.

1. Classification on the basis of origin

A. Natural Polymers

Natural polymers are of two types:

a. Biological origin: All conversion processes occurring in our body are due to the presence of enzymes, nucleic acids and proteins which are polymer of biological origin. These polymers have normally very complex structures.

b. Plant origin: cellulose, natural rubber is the examples of plant origin and has relatively simpler structures than those of enzymes and proteins.

B. Synthetic Polymers

There are large number of synthetic polymers (man-made) consisting of various families like fibers, elastomers, plastic, adhesive etc.

2. Classification on the basis of synthetic way

A. Addition Polymer

An addition polymer is the one which is formed by addition reaction where many monomers bond together via rearrangement of bonds without the lost of any atom or molecule. For addition polymerization a carbon-carbon double bond is required to be present in monomer.

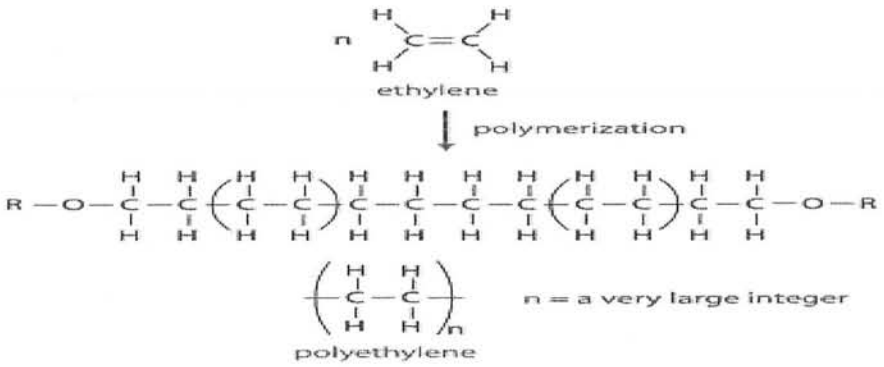

Fig. 1.1: Schematic representation of addition polymerization

B. Condensation Polymers

Any kind of polymer formed through a condensation reaction, releasing small molecule as by-product such as water or methanol. Condensation polymerization is a form of step-growth polymerization.

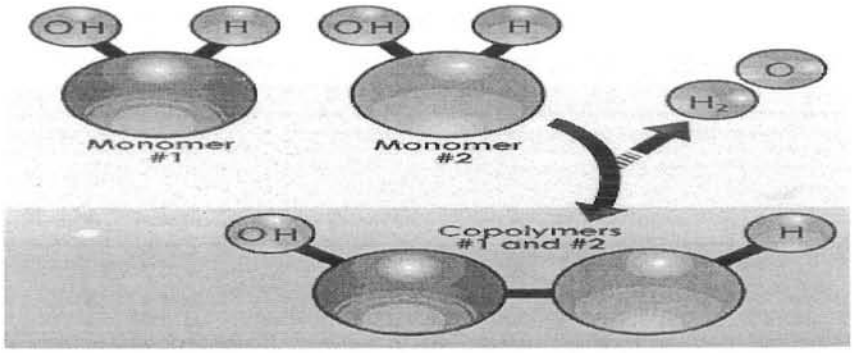

Fig. 1.2: Schematic representation of condensation polymerization

3. Classification on the basis of heating effect

A. Thermoplastic polymers

B. Thermosetting polymers

4. Classification on the basis of nature

A. Organic polymer

B. Inorganic polymer

5. Classification on the basis of mechanical strength

A. Elastomers

B. Plastomers

C. Fibers

6. Classification on the basis of conductivity

A. Conducting polymers

B. Non-conducting polymers

7. Classification on the basis of morphology

A. Crystalline polymers

B. Semi crystalline polymers

C. Amorphous polymers

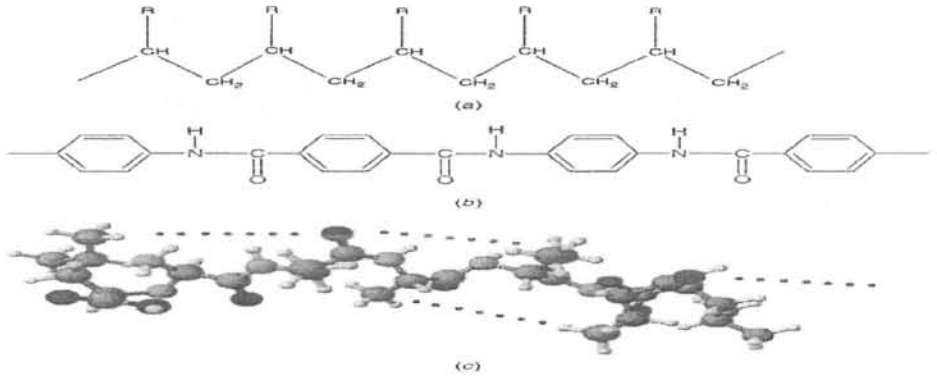

Fig. 1.3: Three different types of polymeric liquid crystals (a) vinyl type; (b) Kevlar polymer; (c) polypeptide chain

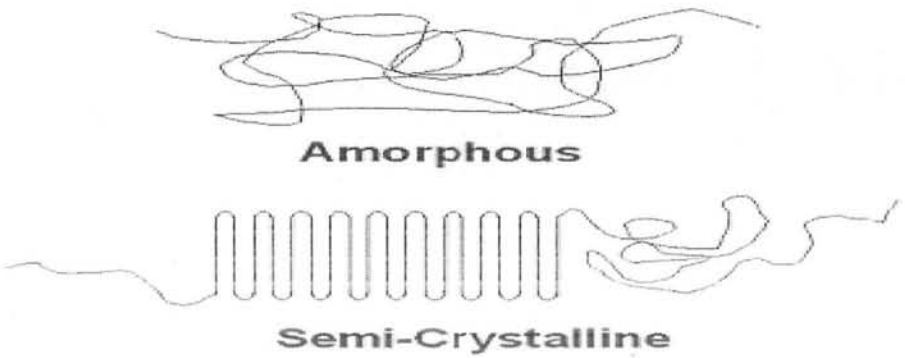

Fig. 1.4: Schematic representation of amorphous and Semi-Crystalline polymer

8. Classification on the basis of stereochemistry

A. Isotactic polymers
B. Syndiotactic polymers
C. Atactic polymers

9. Classification on the basis of molecular arrangement

A. Linear polymers
B. Branched polymers
C. Cross linked polymers
D. Network (three dimensional) molecular structure

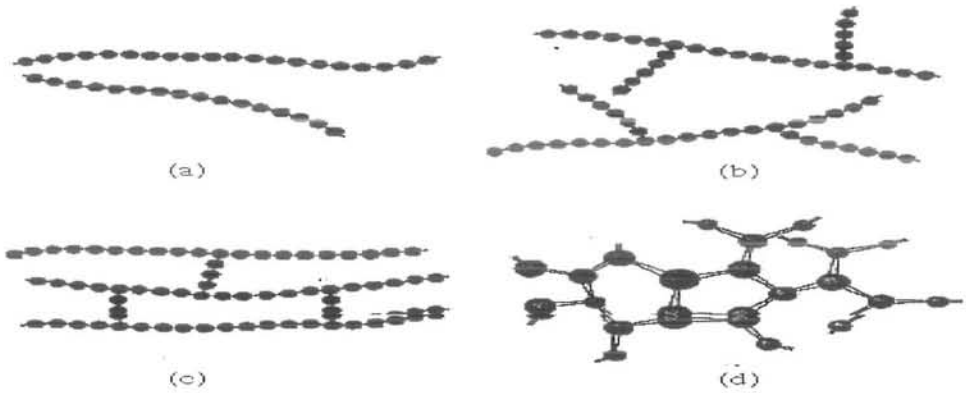

Fig. 1.5: Schematic representation of (a) linear polymer; (b) branched polymer; (c) Cross-linked polymer; (d) Network molecular structure

10. Classification on the basis of type of monomers

A. Homopolymers

B. Heteropolymers or Copolymers

Copolymers

A polymer consists of two or more than two different monomers called copolymers. These polymers are also called hetero polymers. The simultaneous polymerization (copolymerization) of two or more monomers was not investigated until about 1911, when copolymer of olefins and di olefins were found to have rubbery properties and was more useful than homopolymers made from single monomers.[3]

Types of Copolymers

Since copolymer consist of two types of constitutional units (not structural), copolymers can be classified based on how these units are arranged along the chain. Following are the important types of copolymers.

A. Alternating copolymers

"That type of copolymer which consist of alternating A and B units are called alternating copolymers".

-A-B-A-B-A-B-A-B-A-B-A-B-A-B-

B. Periodic copolymers

"That type of copolymers in which A and B units are arranged in repeating sequence called periodic copolymers".

$(A\text{-}B\text{-}A\text{-}B\text{-}B\text{-}A\text{-}A\text{-}A\text{-}A\text{-}B\text{-}B\text{-}B)_n$

C. **Statistical copolymers**

"Copolymers in which the sequence of monomer residues follows a statistical rule". If the probability of finding a given type monomer residue at a particular point in the chain is equal to the mole fraction of that monomer residue in the chain, then the polymer may be referred to as a truly random copolymer.

-A-B-B-B-A-B-A-B-A-A-

D. **Block copolymers**:

"Comprise two or more homopolymer subunits linked by covalent bonds". The union of the homopolymer subunits may require an intermediate non-repeating subunit, known as a junction block. Block copolymers with two or three distinct blocks are called diblock copolymers and triblock copolymers, respectively.

-A-A-A-A-B-B-B-B-A-A-A-A-B-B-B-B-

E. **Graft copolymers**

"A special type of branched copolymer in which the side chains are structurally distinct from the main chain. The illustration depicts a special case where the main chain and side chains are composed of distinct homopolymers. However, the individual chains of a graft copolymer may be homopolymers or copolymers. Note that different copolymer sequencing is sufficient to define a structural difference, thus an A-B diblock copolymer with A-B alternating copolymer side chains is properly called a graft copolymer.

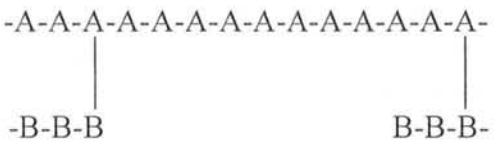

Block Copolymers

Block copolymers are a special type of polymer in which each molecule consists of two or more segments of simple polymers (blocks) joined in some arrangement. In block copolymers, the different monomers are organized into distinct segments, or blocks. Block copolymers with two, three, and more blocks are called diblocks, triblocks, and multiblocks. Some arrangements are linear, in which the blocks are connected end-to-end, and some of them are star like in which all of the blocks are connected via one of their ends at a single junction. Of course more complicated arrangements are also

possible. The number of monomer types in a block copolymer may be less than or equal to the number of blocks. Thus, an ABC linear triblock consists of three monomer types, whereas an ABA linear triblock consists of two monomer types. The following diagram shows the arrangement of blocks in an AB diblock (1), an ABA triblock (2), an ABC triblock (3), and a star block (4).

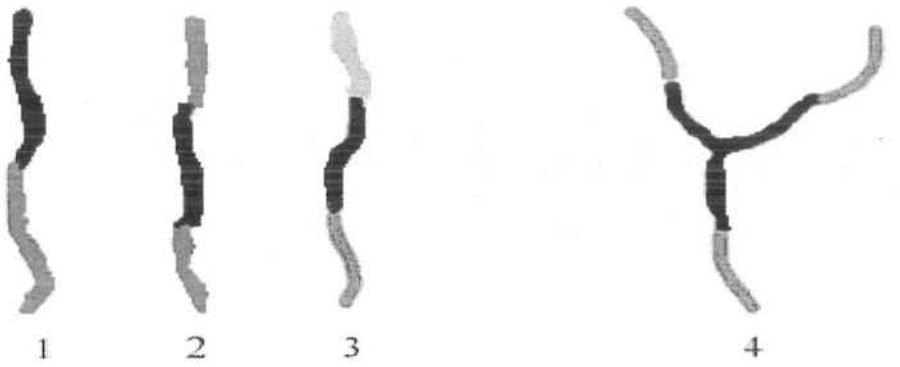

Fig 1.6: (1) AB diblock copolymer; (2) ABA triblock copolymer; (3) ABC triblock copolymer; (4) Star block copolymer.

1.2 Surfactants

"Surfactants (surface active agents) are organic compounds with at least one lyophilic (solvent loving) group and one lyophobic (solvent-fearing) group in the molecule.[4]"

OR

"A substance that, when present at low concentration in a system, has the property of adsorbing onto the surface or interface of the system and of altering to the marked degree the surface or interfacial free energies of those surfaces (or interfaces).[5] If we are using water as a solvent then the respective terms hydrophilic and hydrophobic are used.

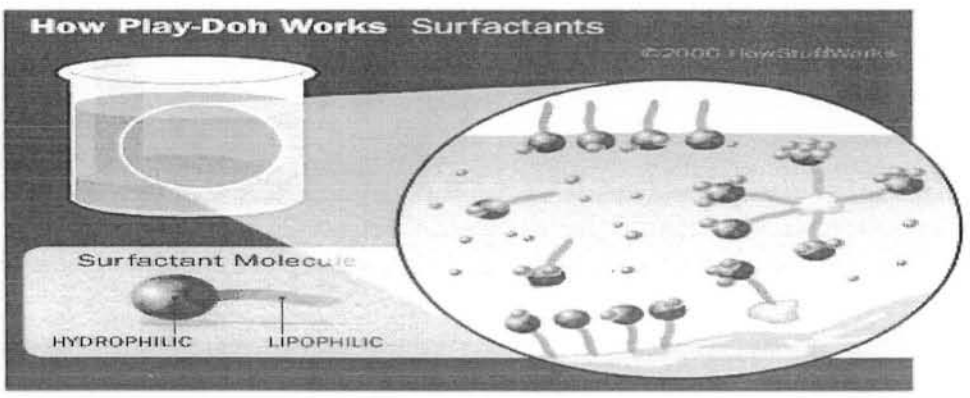

Fig 1.7: General structure of Surfactant.

1.2.1 Classification of Surfactants

Numerous variations are possible within the structure of both the head group and tail of surfactant. The head group can be charged or neutral, compact in size or a polymeric chain. The tail is usually single, double, straight or branched hydrocarbon chain, but may also be a fluorocarbon or siloxane or contain aromatic rings.

Depending on the nature of hydrophilic group, surfactants are classified as:

1. Anionic

The surface-active portion of the molecule bears a negative charge, for examples, $RCOO^-Na^+$ (soap), $RC_6H_4SO_3^-Na^+$ (alkyl benzene sulfonate), and SDS etc.

2. Cationic

The surface-active portion bears a positive charge, for examples, $RNH_3^+Cl^-$(salt of long-chain amine), $RN^+(CH_3)_3Cl^-$ (quaternary ammonium chloride), CTAB etc.

3. Zwitter ionic

Both positive and negative charges may be present in the surface-active portion, for example, $R^+NH_2CH_2COO^-$ (long chain amino acid), $RN^+(CH_3)_2CH_2CH_2SO_3^-$ (sulphobetaine) etc.

4. Non-ionic

The surface-active portion bears no apparent ionic charge, for example, $RCOOCH_2CHOHCH_2OH$ (mono glyceride of long-chain fatty acid), $RC_6H_4(OC_2H_4)xOH$ (poly oxyethylenated alkyl phenol) etc.

Differences in the nature of the hydrophobic groups are usually less pronounced than in the nature of the hydrophilic group. Generally, they are long-chain hydrocarbon residues. However, they include such different structures as:

1. Straight-chain alkyl groups (C_8-C_{20})
2. Branched-chain, alkyl groups (C_8-C_{20})
3. Alkyl benzene residues.
4. Alkyl naphthalene residues (C_3 and greater-length alkyl groups).
5. Rosin derivatives.
6. High-molecular weight propylene oxide polymers (polyoxypropylene glycol derivatives).

7. Long-chain perfluoroalkyl groups.
8. Polysiloxane groups.

1.2.2 Aggregation or Micellization

Surfactants are ultimate example of amphiphilic structure. They combine a long chain alkyl group, which is hydrophobic, with an ionic group, which is highly hydrophilic. In ionic surfactants the two groups are covalently bonded in the same molecule. If such a molecule is exposed to water, the powerful forces of hydration will attempt to drive the molecule into the solution, but at the expense of exposing the attached hydrocarbon chains to an unfavored aqueous media. In trying to minimize contact of their alkyl chains with water, surfactant molecules will adsorb at:

1. Solid/water interfaces (as in wetting and detergency)
2. Air/water interfaces, lowering the surface tension (as in foaming and wetting)
3. Oil/water interface, lowering interfacial tension (as in emulsification)

In these processes of adsorption, the hydrocarbon group loses energy by reducing contact with water and by association with one another. The ultimate process for the reduction of hydrocarbon/water contact is the micellization.

Important aspects of micellization

1. The process of aggregation and de aggregation for pure surfactant like SDS is very fast even in microseconds to milliseconds.[6]

2. The enthalpy change of micellization is generally small.[7, 8] The small enthalpy change is due to energy lost in decreasing contact between hydrocarbon chain and water which is offset by the energy gained in the electrical repulsion of ionic head groups brought into proximity in the micelle periphery.

3. Addition of salt reduces the repulsive forces between head groups of surfactant, or lengthening the "R" group of the surfactant, which increases the energy loss on eliminating the hydrocarbon chains/water interface, can sharply reduce the CMC.

4. In non-ionic surfactants due to absence of electrostatic repulsive forces at the micellar periphery, aggregations take place at a much lower concentration. For the same R group the CMC of a non-ionic surfactant can be two orders of magnitude lower than that of anionic surfactant. In solution surfactant shows the phenomena of adsorption and aggregation. To limit the contact between water

and surfactant hydrophobic part, the surfactant molecules aggregates in the bulk solution with the hydrophilic group oriented towards the aqueous phase. The aggregation process is called micellization and the aggregates are called micelles.A micelle is an aggregate of surfactant molecules dispersed in a liquid colloid. Micelles are colloidal-sized clusters. Micellization is an alternative to interfacial adsorption for removing of hydrophobic group from contact with the aqueous environment, which reduces the free energy of the system. In micelle the hydrophobic groups are directed toward the centre of the surfactant aggregates while the hydrophilic groups are oriented outside toward the aqueous phase.

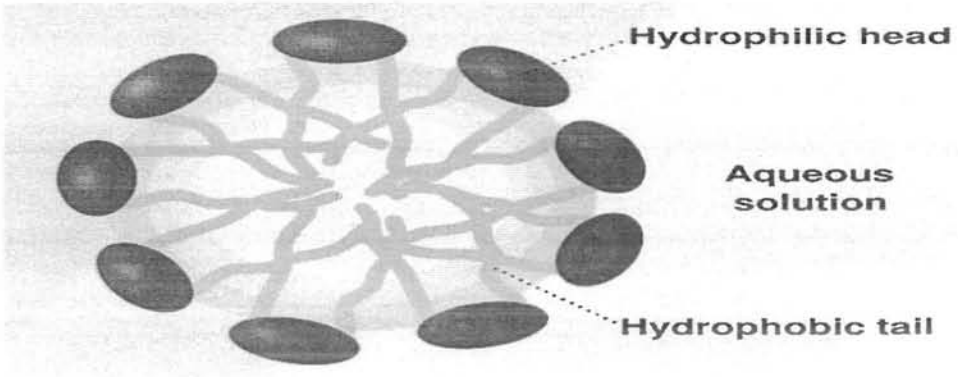

Fig 1.8: Typical structure of Micelle

Micelles are dynamic species and there is a constant rapid interchange of the surfactant molecules between the micelle and the bulk phase. Micelles thus cannot be regarded as rigid structures with well defined shapes, although an average micellar shape may be considered. The shape and sizes of the micelles in the micellar solution depend upon the architecture of surfactant molecule, surfactant concentration and solution temperature. The main types of micelles recognized are spherical, elongated cylindrical, rod like micelles with hemispherical ends etc.

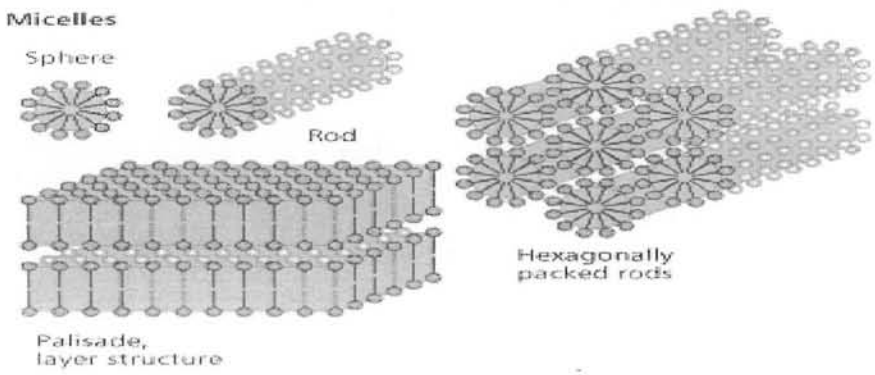

Fig 1.9: Different shapes of micelles.

1.2.3 Critical Micelle Concentration

The critical micelle concentration (CMC) is defined as the concentration of surfactants above which micelles are spontaneously formed. Upon introduction of surfactants (or any surface active materials) into the system they will initially adsorb at the interface, reducing the free energy of the system by

a) Lowering the energy of the interface (calculated as area × surface tension) and

b) By removing the hydrophobic parts of the surfactant away from water.

Subsequently, when the surface coverage by the surfactants increases and the surface free energy (surface tension) has decreased, the surfactants start aggregating into micelles, thus again decreasing the system free energy by decreasing the contact area of hydrophobic parts of the surfactant with water. Upon reaching CMC, any further addition of surfactants will just increase the number of micelles (in the ideal case).

There are several theoretical definitions of CMC. One well-known definition is that CMC is the total concentration of surfactants under the conditions:

If C = CMC, $(d^3F/dC_t^3) = 0$

F = a [micelle] + b [monomer]

C_t: total concentration and a, b are proportionality constants

Therefore, value of CMC depends on the method of measuring the samples, since a and b depend on the properties of the solution such as conductance and photochemical characteristics. When the degree of aggregation is monodispersion, the CMC is not related to the method of measurement. On the other hand, when the degree of aggregation is multidispersion, CMC is related to both the method of measurement and the dispersion. CMC is an important characteristic of a surfactant. Before CMC, the surface tension changes strongly with the concentration of the surfactant. After CMC, the surface tension remains almost constant. The CMC is the concentration of surfactants in the bulk at which micelles start forming. In most of the situations e.g. in surface tension measurements or conductivity measurements, the amount of surfactant at the interface is negligible as compared to that in the bulk and CMC is approximated by the total concentration. There are important situations where interfacial areas are large and the amount of surfactant at the interface can not be neglected. For example if we take a solution of a surfactant above CMC and start introducing air bubbles at the bottom of the

solution, these bubbles, as they rise to the surface, pull out the surfactants from the bulk to the top of the solution creating a foam column thus bringing down the concentration in bulk to below CMC. This is one of the easiest methods to remove surfactants from effluents (Foam Flotation). Thus in foams with sufficient interfacial area there will not be any micelles. Similar reasoning holds for emulsions. The other situation arises in detergency. One initially starts off with concentrations greater than CMC in water and on adding fabric with large interfacial area and waiting for equilibrium, the surfactant concentration goes below CMC and no micelles are left. Therefore the solubilization plays a minor role in detergency. Removal of oily soil is by modification of the contact angles and release of oil in the form of emulsion.

Factors affecting the CMC

1. Structure of the surfactant

In general, the CMC in aqueous media decreases as the hydrophobic character of the surfactant increases.

A. The hydrophobic group

In aqueous medium, the CMC decreases as the number of carbon atoms in the hydrophobic group increases to about 16 and a generally used rule for ionic surfactants is that CMC is halved by the addition of one methylene group to a straight-chain hydrophobic group attached to a single terminal hydrophilic group. For non-ionic the decrease with increase in hydrophobic group is somewhat larger, an increase by two methylene units reducing the CMC to about one-tenth compare to one-quarter in ionic. When the hydrophobic group is branched, the carbon atoms on the branches appear to have about one-half the effect of carbon atoms on a straight chain. When carbon-carbon double bond is present in the hydrophobic chain, the CMC is generally higher than that of the corresponding saturated compound, with the cis isomer generally having a higher CMC than the trans isomer. In the presence of polar group such as –O- or –OH the CMC of the hydrophobic chain increases. When the polar group and the hydrophilic group both attached to the same carbon atom, that carbon atom seems to have no effect on the value of the CMC. In propopylen oxide-ethylene oxide block copolymer surfactants, where the polyoxypropylene group act as a part of or as the entire hydrophobic group, the decrease in the CMC produced by one oxypropylene group has been stated to be equivalent to that produced by 0.4 methylene units when the polyoxypropylene chain is one to four units long.

B. The hydrophilic group

In aqueous medium, ionic surfactants have much higher CMC than non-ionic surfactants containing equivalent hydrophobic groups. Zwitter ionic have same CMC as for ionic surfactants. The CMC is higher when the charge on an ionic hydrophilic group is closer to the α-carbon atom of the alkyl hydrophobic group. An expected, surfactants containing more than one hydrophilic group in the molecule show larger CMC than those with one hydrophilic group and the equivalent hydrophobic group.

C. The Counter ion

The CMC in aqueous solution reflects the degree of binding of the counter ion to the micelle. Increased binding of the counter ion, in aqueous systems, causes to decrease in the CMC of the surfactant. The extent of binding of counter ion increases with increase in its polarizability and valence, and decrease with increase in its hydrated radius.

D. Empirical equation

Many investigators have developed empirical equations relating the CMC to the various structural units in surface-active agents. In aqueous medium, a relationship between the CMC, C_{CMC}, and the number of carbon atoms N in the hydrophobic chain was found: $\log CMC = A - BN$ Where A is a constant for a particular ionic head at given temperature and B is also a constant. In all these relationships the CMC in aqueous solution decreases as the hydrophobic character of the surfactant increases.

2. Electrolyte

In aqueous solution the presence of electrolyte causes a decrease in the CMC, the effect being more pronounced for anionic and cationic than for zwitter ionic surfactants and more pronounced for zwitter ionic than for non-ionic. Experimental data shows that for the anionic and cationic surfactants, the effect of the concentration of electrolyte is given by the following equation: $\log C_{CMC} = -a \log Ci + b$. where a and b are constants for a given ionic head at a particular temperature and C_i is the total counter ion concentration in mole per liter. The depression of CMC in these cases is due mainly to the decrease in the thickness of the ionic atmosphere surrounding the ionic head groups in the presence of the additional electrolyte and the consequent decreased electrical repulsion between them and the micelle.

3. Organic additives

Small amounts of organic materials may produce marked changes in the CMC in aqueous media. There are two types of materials which cause changes in the CMC. These materials are categorized as:

A. Class I materials

Materials that affect the CMC by incorporating into the micelle are considered as class I materials. These materials are generally polar organic compounds such as alcohols and amides. Compounds of this class operate at very low bulk phase. Members of class-I reduce the CMC. Shorter-chain members of the class- I are probably adsorbed mainly in the outer portion of the micelle close to the water-micelle "interface". The longer-chain members are probably adsorbed mainly in the outer portion of the core, between the surfactant molecules. Adsorption of the additives in these fashions decreases the work required for micellization. Depression of the CMC appears to be greater for straight-chain compounds than for branched ones and increases with chain length to a maximum when the length of the hydrophobic group of the additive approximates that of the surfactant. Additive that have more than one group capable of forming hydrogen bonds with water in a terminal polar grouping appear to produce greater depressions of the CMC than those with only one group capable of hydrogen bonding to water.

B. Class II materials

These types of materials change the CMC by modifying solvent-micelle or solvent-surfactant interactions. These materials change the CMC at higher bulk phase concentration than the class I materials. The members of this class change the CMC by modifying the interaction of water with the surfactant molecule or with the micelle, doing this by modifying the structure of the water, its dielectric constant, or its solubility parameter. Members of this class include urea, formamide, N-methylacetamide, short chain alcohols etc.

4. Temperature

The effect of temperature on CMC of surfactants in aqueous medium is complex, the value appearing first to decrease with temperature to some minimum and then to increase with further increase in temperature. Temperature increase causes decreased hydration of the hydrophilic group, which favor micellization. However, temperature increase also causes disruption of the structured water surrounding the hydrophobic group, an effect that disfavor micellization. The relative magnitude of these two

opposing effects determines whether the CMC increases or decreases over a particular temperature range.[5]

1.3 Polymer-Surfactant Interactions

1.3.1 Polymeric Surfactants as a Stable System with Right Consistency (Rheology) for Cosmetic Applications

Personal care formulations are designed to have a number of benefits, both functional and aesthetic.[9] For these reasons, many systems are designed to provide cleaning and protective barriers against damaging environment such as sunlight and they should have a pleasant odor, make the skin feel smooth, and appeal to the customer on applications. At present, personal formulations are based on oil-in-water (o/w) or water-in-oil (w/o) emulsions "structured" to produce creams with the right consistency that appeals to the customers. These systems are thermodynamically unstable, as their formation is accompanied by a large increase in the interfacial energy (small droplets) [10]. This can be understood from the free energy of formation of an emulsion.

$$\Delta G^{form} = \Delta A \gamma_{12} - T\Delta S^{conf}$$

Where ΔA is the increase in interfacial area, γ_{12} is the interfacial tension, T is the absolute temperature and ΔS^{conf} is the configurational entropy arising from the increase in the number of possible configuration due to the formation of a large number of droplets. With emulsions $|\Delta A_{12}| >> |-T\Delta S^{conf}|$ and hence $\Delta G^{form} > 0$; i.e., the formation of an emulsion is non-spontaneous and with time the emulsion tends to break down by flocculation and coalescence to reduce ΔA and hence ΔG.

The above thermodynamic explanation implies that to stabilize an emulsion against flocculation and coalescence, one need to create an energy barrier between the droplets to prevent their close approach (whereby the van der Waal attraction is strong). Several methods may be applied to produce such a high energy barrier. The most common procedure applied in many colloidal systems is to create an electrical double layer at the oil/water interface. When two droplets with such double layers (of the same charge) approach each other, separation of distance that is twice the double layer thickness causes strong repulsion which counteracts the van der Waal attraction. The energy distance curve for such system shows an energy barrier (maximum) at intermediate distances of separation, which has to overcome for flocculation and

coalescence to occur. The above method of stabilization is known as electrostatic stabilization. Electrostatic stabilization can be achieved by the use of ionic surfactants. However for a number of reasons this method of stabilization is not ideal for personal care formulation. First, the stabilization is influenced by the presence of electrolytes in the system, which reduces repulsion and may cause instability. In addition, many ionic surfactants cause skin irritation as a result of their penetration and interaction with the stratum corneum.[11] The stratum corneum is the main barrier to water loss and it consists of lipids that are organized in a bilayer structure, which at high water content is transparent and soft.[12] Surfactant that interact with the lipid bilayer and reduce its "liquid-like" nature (by disrupting the liquid crystalline structure) may cause crystallization of the lipids, and this has a drastic effect on the appearance of smoothness of the skin ("dry" skin feeling).

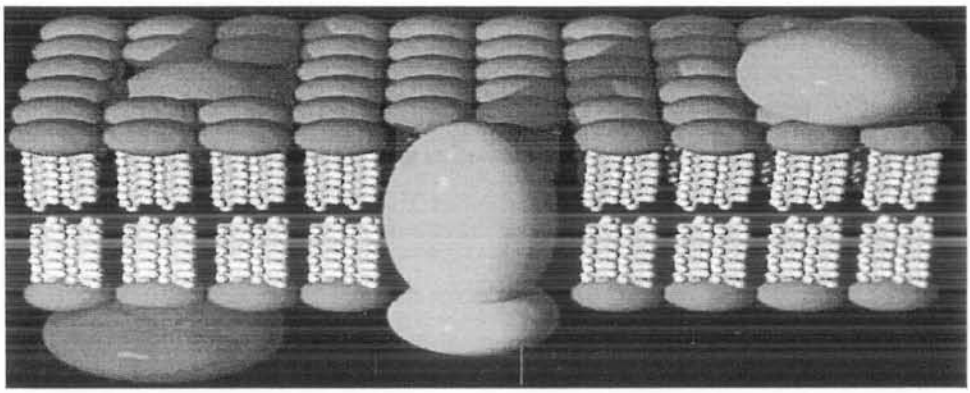

Fig 1.10: Schematic representation of Lipid Bilayer.

For the above reasons, many personal care emulsions are formulated using non-ionic surfactants usually polymeric surfactants. These surfactants adsorb at the oil/water interface with the hydrophobic group toward the oil phase while the hydrophilic group (mostly polyethylene oxide) remaining in the aqueous phase. These molecules produce a repulsive barrier as a result of the unfavorable mixing of the polar PEO chain (when these are in good solvent conditions) and the reduction in the configurational entropy of the chains by overlapping. Such repulsion is referred to as steric stabilization.[13] These non-ionic surfactants (used in mixtures) have been successfully applied to prepare stable o/w and w/o emulsions. In addition, in some cases, they form liquid crystalline structures at the o/w interface and these prevent coalescence of the oil droplets.[14] One of the main features of effective steric stabilization is strong adsorption of the chain to the interface. Apart from their effectiveness in prevention of flocculation and coalescence, they are also expected to cause no skin irritation. The high molecular weight of the polymeric

surfactant prevents their penetration through the skin and hence they do not cause any disruption of the stratum corneum. The most convenient polymeric surfactants are those of the block-and-graft copolymer type: ABA triblock copolymer, in which A- block represents lyophilic part while the B-block represents lyophobic part of the amphiphile. The hydrophobic chain (B-block) resides at the hydrophobic surface, leaving the two hydrophilic chains (A-block) dangling in aqueous solution (providing steric stabilization).

1.3.2 Adsorption at Interface

The process of polymer adsorption involves a number of interactions that must be separately considered. Three main interactions must be taken into account, namely

1. The interaction of the solvent molecule with surface (oil in the case of oil/water emulsion that needs to be displaced for the polymer segments to adsorb).
2. The interaction between the polymer chains and the solvent.
3. The interaction between the polymer and the surface.

Apart from knowing these interactions, one of the most fundamental considerations is the conformation of the polymer molecule at the interface. These molecules adopt various conformations depending on their structures. The ABA triblock copolymer arranged at the interface in such a way that its lyophobic part(the anchor chain B) make loops on the interface while the lyophilic part(A-chain tail) stabilizing the system.

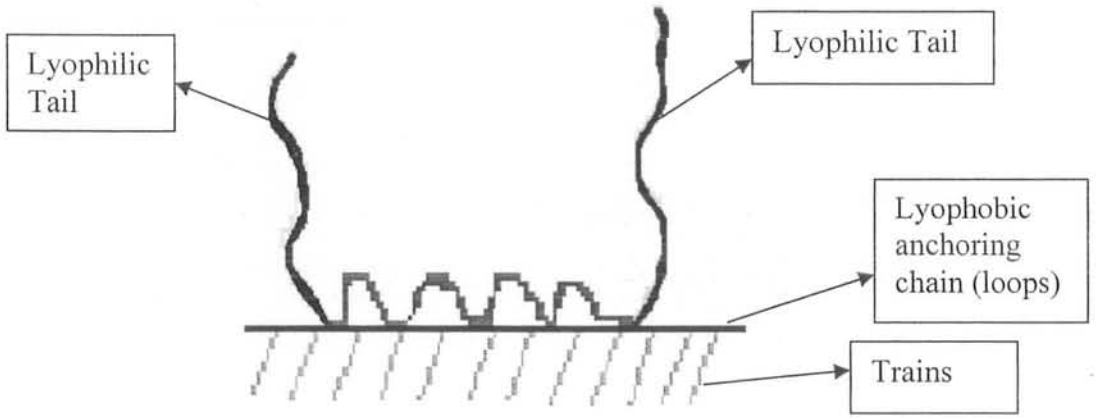

Fig 1.11: Conformation of Triblock copolymer of type ABA adsorbed on a plane surface.

Several theories describe the process of adsorption, which have been developed using either statistical mechanical approach or quasi-lattice models. In the statistical approach, the polymer is considered to consist of three types of structures with different energy states, trains, loops and tails.[15, 16] The structures closed to the surface (Trains) are adsorbed with an internal partition function determined by short-range forces between the segment and the surface. The segments in loops and tails are considered to have an internal partition function equivalent to that of segments in the bulk solution and these are assigned as segment-solvent interaction. By equating the chemical potential of the macromolecule in the adsorbed state and in the bulk solution, the adsorption isotherm can be determined.

The use of polymer and surfactant in the cosmetic industry is wide spread like in the formulation of shampoos, lotions etc these ingredients occur together. Through interaction, these ingredients affect the properties of each others and hence the overall properties of the formulation changed sometime beneficially and sometimes adversely. Therefore, it is very important to have a clear idea about the factors that govern the interaction of polymer and surfactant and also on the alteration of the properties that can be expected as a result of product formation through interactions.

This field of study is actually quite old. Interaction and complex formation between natural polymer (proteins) and "surfactants" (lipids) were recognized early in this century (1900) and much study on the mixtures of proteins and synthetic surfactants was carried out in the 1940s and 1950s.[17, 18]

1.3.3 Proposed Mechanism of Polymer-Surfactant Interactions

The field of polymer-surfactant interaction is very active among the colloidal scientists. For this purpose numerous types of experiments were performed to visualize the mechanism of polymer-surfactant interaction. The early explanation of polymer-surfactant mechanism was started from protein/surfactant system established binding of surfactant to sites along the polymer chain. On the basis of different experiments made by different scientists following types of mechanisms are proposed:

A. Cooperative mechanism

This type of mechanism is proposed on the basis of more recent data. In this type of mechanism the interaction involving "cooperativity" in binding of surfactant molecules.

B. Perturbation mechanism

This type of mechanism explains perturbation of aggregation or micellization of the surfactants.

C. Necklace mechanism

In this type of mechanism the micelles of surfactant are attached with the polymer chain in such a way as to produce a decorative necklace type of structure. This type of model is usually used for neutral triblock copolymer decorated with ionic surfactants like SDS, CTAB etc.

D. Mixed type mechanism

In this type of mechanism two polymer chains are attached to each other by surfactant monomers through hydrophobic forces.

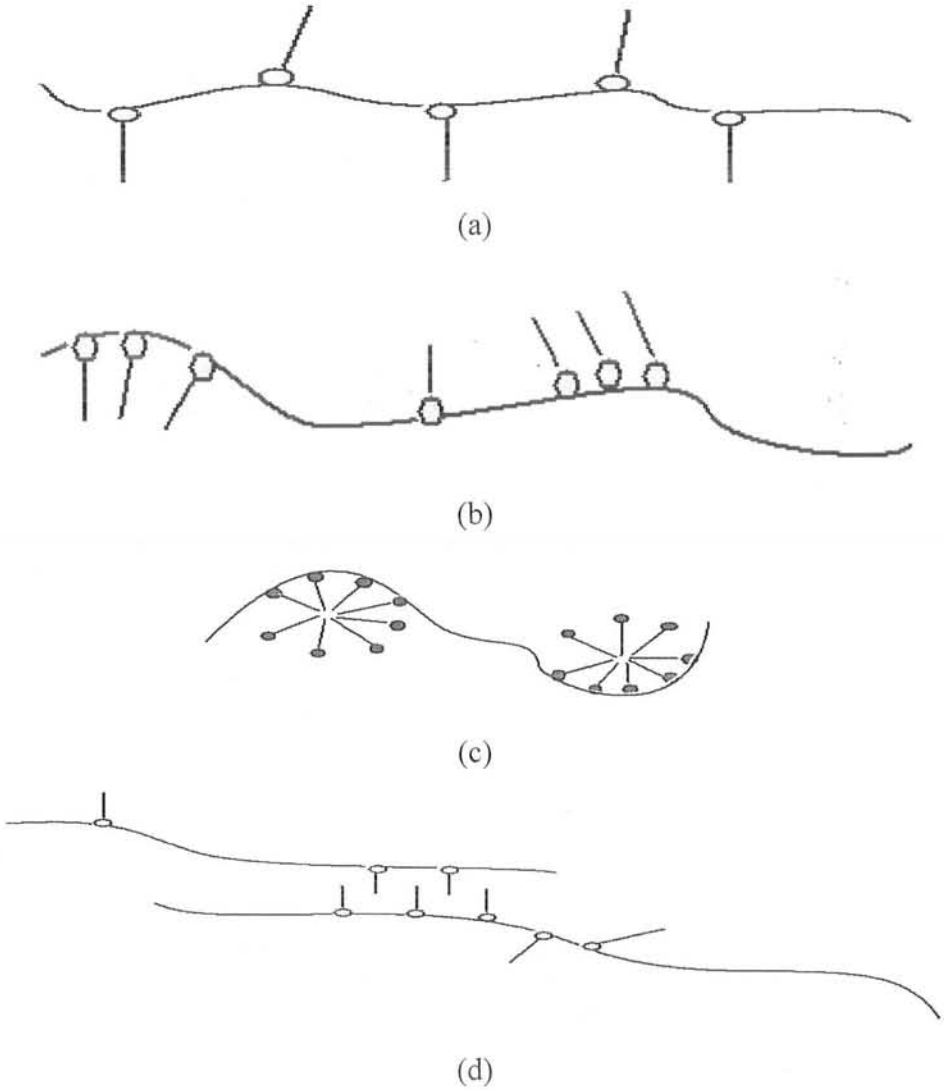

Fig 1.12: Schematic drawing of various modes of "binding" surfactants molecules by a polymer.

1.3.4 Factors Effecting Association of Surfactants with Polymers

As the polymer-surfactant interaction can be explained by different mechanisms. Among these, two mechanisms involve "cooperative" and "perturbed" aggregation of surfactant molecules. Factors which effect SDS micellization also influence the association of surfactant with polymer. The most important factors which have greater effect on the interaction of polymer-surfactant are summarized as:

A. Surfactant Chain Length

Studies with a number of surfactants show that polymer/surfactant interaction is most favorable under following conditions.

(a) Surfactants should have long hydrocarbon chain.

(b) Surfactants should have straight chain.

(c) The head group of surfactant should be terminal to the chain.[19]

For uncharged polymers the initial binding concentration or critical aggregation concentration (C.A.C) in homologous series of ionic surfactants decreases with increasing chain length of the surfactants. The linear relationship between log of C.A.C and n (number of carbon in the molecular chain), is same as between log CMC and n.

For PVP/SDS mixtures in 0.1 M NaCl solutions, Arai et .al[20], using the relationship ln T_1 = nw/kT+constant, found a value of w of -1.1kT. This correspond to the free energy change per -CH_2- group in two processes.i.e

a) Transferring the surfactant from unassociated state in solution to the complex and

b) Transferring the surfactant molecule to micelles.

The logarithm dependence of C.A.C (and CMC) can be related to Traube's rule.[21]

Traube's Rule: This rule was demonstrated by Traube's in 1891. This rule states that "the concentration of the compound required for equal lowering of surface tension diminish threefold for each -CH_2-group added to the chain".

Langmuir showed that Traube's rule can be stated in the form $\lambda n = \lambda o + 625n$, where λn = work done in bringing a mole of the molecule from the interior to the surface, n = number of carbon in the molecule chain and λ_o = constant depend on the end group of the series (for e.g. λ_o for CH_2OH end group = 575).

B. Surfactant Structure

The influence of surfactant structure, including the nature of the head group (and its charge) on polymer/surfactant interaction is very important in case of uncharged polymers. A general description that anionic surfactants are more reactive than cationic surfactants towards the uncharged water soluble polymers.[22] These effects are summarized in the following form

P^0:	SA^-	>	SA^+	>>	SA^0
P^{n+}	SA^-	>>	SA^+	>>	SA^0
P^{n-}	SA^-	>>	SA^+	>>	SA^0

This table shows that an anionic surfactant will react strongly with a polycation but will not react, or will react only weakly, with a polyanion, illustrating the potent effect of electrostatic forces. The adsorbed amount of surfactant was dependent upon the number of constituent groups such as $-CH_3$ present on the head group of the surfactant. Presence of more such shielding groups on the head group little will be the repulsion between the copolymer bound surfactant molecules and more will be its binding.[23, 24] The addition of SDS was found to melt the micellar cubic structures and while CTAB addition led to a phase separation (or precipitation).

C. Molecular Weight of the Polymer

Several studies have been published addressing various questions such as structure of polymer/surfactant complex[25], the effect of polymer molecular weight[26], the type of surfactant counter ion[27] and the effect of temperature.[28]

Despite the extensive experimental and theoretical research, there are still some important aspects of the polymer/surfactant interaction that have yet been hardly investigated. Such an aspect is the role of the polymer molecular weight, a parameter that is generally neglected. This approach is supported by the investigation of Schwuger[29] who found that the SDS does not interact with PEO if the PEO molecular weight is smaller than 1500. Above this molecular weight, the C.A.C first decreased slightly up to about M_{PEO} = 4000, then it became independent from the polymer molecular weight. Bernazanni et al. have very recently presented a combined isothermal titration calorimetry (ITC) and 13C, 1H, and 23Na NMR study[30]of the PEO/SDS interaction in

the low and moderate molecular weight ranges of the polymer. On the basis of their ITC measurements, the authors concluded that the minimum molar mass of the appearance of the PEO/SDS interaction is M_{PEO} = 350 and M_{PEO} = 3800 is the critical molecular weight above which the interaction is independent of M_{PEO}. The effect of polymer molecular weight on the polymer/surfactant interaction can be explained through following graph.

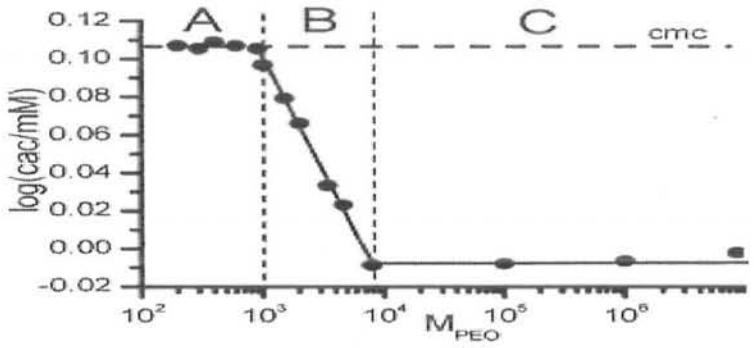

Fig 1.13: The effect of polymer molecular weight on the polymer/surfactant interaction.

In the above figure, the C.A.C is plotted as a function of PEO molecular weight. As reflected by the figure, the aggregation behavior of the SDS can be divided into three regions in the presence of PEO. Below M_{PEO} = 1000 (region A), the C.A.C of the surfactant corresponds to the CMC, which indicates that there is no complex formation in this molecular weight range. If the PEO molecular weight exceeds 1000, the C.A.C appears below the CMC, and it decreases as the polymer molecular weight increases. Finally, when the polymer molecular weight becomes large enough (larger than M_{PEO} = 8000), the C.A.C becomes practically constant (range C).

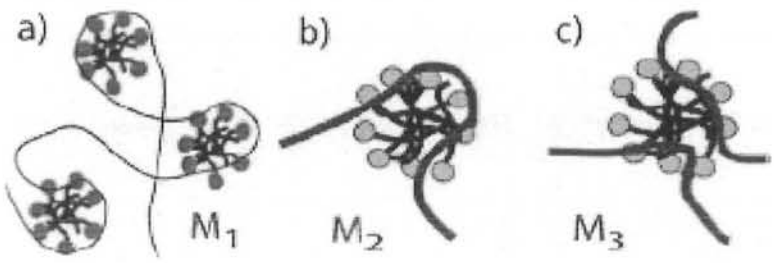

Figure 1.14: Schematic representation of the possible change of the polymer/surfactant complex structure with decreasing polymer molecular weight (M1 > M2 > M3):

(a) When M_{PEO} is large, several aggregates are connected by the polymer by wrapping around them (necklace model); (b) when the polymer chain length is comparable to the

chain length required for the formation of an optimal composition complex, only one aggregate forms in the coil; (c) in the case of short polymer chains, in principle, more than one polymer chain could be incorporated into the complex.[31]

D. Amount of Polymer

The polymer-surfactant interaction is influenced by amount of polymer. In case of surface tension measurement C.A.C is always less than the CMC. The dependence of polymer amount on the polymer/surfactant interaction can be explained on the basis of C.A.C. The position of C.A.C (T_1) is insensitive to polymer concentration, although in some systems it has been shown to decrease slightly with large increase in polymer concentration.[32, 33]Where as the saturation concentration increases linearly with polymer concentration. This linear increase in saturation concentration is only for uncharged polymers while in case of polyelectrolyte and proteins the system becomes more complicated.

E. Polymer Structure

During and after pioneering work of Saito[22] on the interaction between ionic surfactants and uncharged polymers it has been appreciated that there are definite difference in reaction affinity among polymers toward a given surfactant. For example, in cellulosic water soluble polymers it was known that MeC is more reactive than ethyl (hydroxyl) ethyl cellulose (EHEC); that polypropylene oxide is more reactive than polyethylene oxide. According to available informations Breuer and Robb[22]assigned reactivity sequence to a group of six in increasing order of reactivity as follows:

Interaction with anionic surfactants	PVA < PEO< MeC < PVAc ≤ PPO ~ PVP
Interaction with cationic surfactants	PVP < PEO < PVA < MeC < PVAc< PPO

The strongest interaction with lowest C.A.C and highest ionic dissociation (α) of the complex was obtained with the most hydrophobic member. Polymers with negligible surface activity (HEC, PAAm, dextrose) are generally unreactive; those with intermediate surface activity (PNIPAM, PVA, PEO) are more reactive; and those with pronounced surface activity (PPO, PVAc) are most reactive. On the basis of surface activity of polymer Lad et al.[34], Contractor and Bahadur[35] have also noted that in the mixed species of SDS and F68/L64/P85 strength of interaction increased with the increase in the chain length of hydrophobic PPO.

1.4 Literature Review

Micellization and gelation of triblock copolymer were investigated by surface tension, light scattering, and photon correlation spectroscopy.[36] Block copolymers of ethylene oxide and 1,2-butylene oxide i.e. diblock and triblock copolymers were introduced as commercial products by the Dow Chemical Company in 1993 with first description of these copolymers appearing in the commercial[37] and scientific[38] literature in 1994.

Yung-Wei Yang et.al studied the association of diblock and triblock copolymers in water by static and dynamic light scattering techniques. The critical micelle concentrations of diblock and triblock copolymer were compared and the effects of architecture were also investigated.[39] Tianbo Liu et.al used Laser Light Scattering and small angle neutron scattering to study poly (oxybutylene)-poly (oxyehtylene)-poly (oxybutylene) triblock copolymers ($B_6E_{46}B_6$) in aqueous solution from low to high concentrations and over a range of temperatures from 278K to 308K. At high concentration and low temperature these block copolymers associates in a small numbers and scattering evidence show that molecule associate with open structures. In this study it is also confirmed that the critical micelle concentration decreases with increasing temperature while the association number increases.[40]

Chiraphon Chaibundit et.al. used static and dynamic laser light scattering techniques for the study of micellization and micelle properties of block copolymer in dilute aqueous solutions, particularly the mass-average association number and thermodynamic and hydrodynamic radii. At a given temperature, the micelle association number decreased as the E-block length was increased while the radii decreased.[41] J. F. Holzwarth et.al, studied the binding of SDS to pluronic F127 using SDS surfactant selective electrode via electromotive force, isothermal titration calorimetry, and light scattering.[42]

Colin Booth et.al examines how composition, block length and block architecture govern two fundamental properties, critical micelle concentration and micelle association number, for a system which are in dynamic equilibrium.[43]

R. Zana et.al, studied the interaction between ethyl (hydroxyethyl) cellulose (EHEC) and two cationic surfactants hexadecyltrimethylammonium chloride and bromide (CTAC and CTAB) in aqueous solution as a function of temperature, by means

of electric conductivity and chloride ion self-diffusion measurement for CTAC and by time-resolved fluorescence quenching for CTAC and CTAB. The results shows that , in the presence of EHEC, the critical micelle concentration decreases, the micelle ionization degree increases, and the micelle aggregation number N decreases upon increasing temperature.[44] E. Hecht and H. Hoffmann studied the interaction of ABA block copolymers with ionic surfactants in aqueous solution. They investigated the influence of SDS on the aggregation behavior of F127 by static and dynamic light scattering, electric birefringence, and calorimetric methods. The results show that SDS binds to monomers of F127 and thereby suppresses completely the formation of F127 micelles.[45]

Kewei. Zhang et.al, studied the interaction between an anionic surfactant, sodium dodecyl sulfate (SDS), and a self-assembling ethylene oxide-propylene oxide-ethylene oxide triblock copolymer by phase diagram determination, NMR quadrupole splittings, and by self-diffusion. Addition of SDS induces a breakdown of anisotropic liquid crystalline phases into isotropic solutions, which especially at higher concentrations are bicontinuous. At moderately high copolymer concentrations there is a transition from bicontinuous isotropic solutions to solutions of discrete micelles on addition of SDS.[46]

Francoise. M. Wink and Sudarshi T. A. Regismond present a review for the application of fluorescence techniques to study polymer-surfactant system. In this review they discussed the critical aggregation concentration, aggregation number of the mixed micelles and the microenvironment within the micelles.[47]

Time-resolved fluorescence quenching of excited state pyrene by halothane was investigated in aqueous solutions of poly (oxyethylene)-poly (oxypropylene)-poly (oxyethylene) triblock copolymers, P84, P104, and F38, at 298K. The occupancy number of halothane in the block copolymer micelles and the dispersive factor were obtained from nonlinear least-squares fitting of the immobile quencher-probe and dispersive kinetic model respectively.[48]

N. J. Jain et.al., studied the micellization of an ethylene oxide-propylene oxide (PEO-PPO-PEO) symmetrical triblock copolymer (Pluronic) F127 ($EO_{99}PO_{65}EO_{99}$) in aqueous solution in the presence of various additives (i.e. sodium chloride, urea and SDS) by cloud point, surface tension, dye spectral change, sound velocity, viscosity and dynamic light scattering measurements over the temperature range 298K–323K. This

study shows that CMC of copolymer altered significantly in the presence of additives. The addition of SDS to aqueous copolymer solutions leads to the formation of copolymer-SDS complex (or mixed micelle) showing polyelectrolyte nature. Surface tension, dye spectral change measurements reveal aggregation of SDS taking place at concentration much below its CMC, indicating clearly SDS-copolymer interaction. The addition of SDS suppresses the micellization of copolymer and beyond a particular SDS concentration only; SDS micelles with one or two copolymers molecules are present predominantly.[49]

S. D. Wetting and R. E. Verrall investigated the physical interactions between cationic Gemini surfactants and triblock copolymers using specific conductance, fluorescence intensity, density, and equilibrium dialysis techniques. In this investigation it is confirmed that increased surfactant concentrations in the polymer coil region results in a gradual change from cluster of monomer surfactant bound to the polymer to the formation of regular micelles.[50]

J. F. Holzwarth at.el, investigated the mixed micelle compositions of various mixtures of the triblock copolymer (pluorinic F127) and SDS by Isothermal Titration Calorimetry (ITC), Surface Tension and Electromotive Force Measurement (emf). The CMC were determined using surface tension and ITC while small-angle neutron scattering (SANS) used for the structure and composition determination of the mixed micelles.[51] Karin Schillen et.al, investigated the properties of triblock copolymers in aqueous solution and their interaction with ionic surfactants SDS and CTAC by static and dynamic light scattering, high sensitivity differential scanning, and isothermal titration calorimetry.[52]

Mandeep Singh Bakshi et.al, studied the association behavior of triblock copolymers in aqueous solution with HTAB, TTAB and dimethylene bis (decylammonium bromide) (10-2-10) by fluorescence, viscosity, and Kraft temperature measurements.[53]

Asad Baran Mandal et.al investigated the interaction of water insoluble triblock copolymer with SDS by surface tension, conductivity and fluorescence measurements. In this study the CMC, counter ion association and the aggregation numbers for binary and ternary systems.[54] Self-diffusion coefficient (D^{o}_{m}), interaction parameter (k_f) and

hydrodynamic radius (R_h) of water insoluble triblock copolymer micelles in SDS micellar environment were determined by Cyclic Voltammetric (CV) technique.[55]

The fluorescence study of various zwitter ionic and triblock copolymer were carried out at 298K. From the variation of I_1/I_3 intensity ratio of pyrene fluorescence, the CMC and other related parameters were obtained. The nature of the mixed micelles was evaluated using regular solution and Motomura's approximations.[56]

Cyclic voltammeteric investigation of TTAB, HTAB and triblock copolymers reveal that variation in the peak current versus the total concentration of surfactant allowed us to evaluate the CMC and related parameters from regular solution theory along with the diffusion coefficient of the electroactive species. A variation in the micellar mole fraction of the ionic components suggests that the mixed micelles are rich in triblock copolymer component in the ionic surfactant rich region.[57]

Ornella Ortona et.al investigated the interaction between cationic, anionic, and non-ionic surfactants with ABA block copolymer Pluronic PE6200 and with BAB reverse block copolymer Pluronic 25R4 by using surface tensiometry, pyrene fluorescence and isothermal titration calorimetry. Pluronic in their non-aggregates form better interact with the anionic surfactant than with cationic and non-ionic ones as predicted by surface tension measurement.[58] Manuj Kumbhakar investigates the interaction mechanism of triblock copolymers (P123 and F127) with surfactants (SDS, CTAC and Triton X-100) by steady state fluorescence measurement. In this study three different concentration regions are studied. At low molar ratio of ionic surfactant to triblock copolymers (n) copolymer-surfactant micelles are basically copolymer-rich micelles with few surfactant molecules. At very high n values, copolymers-rich micelles are destroyed and surfactant-rich micelles with copolymer monomers are formed. At the intermediate n value there are two possibilities: the copolymer-rich micelles converted into surfactant-rich micelles by incorporation of surfactant to the copolymer-rich complex along with the release of free copolymer monomers or simultaneous buildup of surfactant-rich micelles together with the destruction of copolymer-rich micelles.[59]

I. Pepic explained the interactions in mixtures of nonionic surfactants, Lutrol F127, and cationic polyelectrolyte, chitosan from water solution and acetate buffer at two different temperatures. C.A.C, CMC and minimum area of Lutrol F127 molecule at the air/solution interface were determined by surface tension measurement.[60]

The interaction of SDS with diblock ($E_{18}B_{10}$, $B_{20}E_{610}$) and triblock copolymers ($B_{12}E_{227}B_{12}$, $E_{40}B_{10}E_{40}$, $E_{19}P_{43}E_{19}$) were investigated using surface tension, conductivity, dynamic light scattering, densities and ultrasonic velocities measurements. In this study it was observed that in the case of $B_{20}E_{610}$-SDS, $B_{12}E_{227}B_{12}$-SDS, $E_{40}B_{10}E_{40}$ and $E_{19}P_{43}E_{19}$ the formation of smaller particles compared to pure polymeric micelle point to micelle suppression induced by the ionic surfactants.[61]

Guiying Xu used the mesoscopic dynamic simulation method to simulate the aggregation behavior of Pluronic copolymer $E0_{13}PO_{30}EO_{13}$ (L64) and $EO_{26}PO_{40}EO_{26}$ (P85) solutions in the presence of SDS. The factors influencing the aggregation behavior like concentration, temperature and E0/PO ratio were discussed. Using simple copolymer model, the morphology and kinetic formation process of copolymer aggregates were obtained.[62] Praila K. Misra investigate the solution behavior of the mixture of CTAB and polyoxyethylene (30) octylphenol (OP-30) by using conductance, fluorescence intensity, and surface tension.[63]

Chapter – 2

THEORY OF CHARACTERIZATION TECHNIQUES

Chapter - 2

THEORY OF CHARACTERIZATION TECHNIQUES

2.1 Surface Tension

Surface tension is a property of the surface of a liquid. It causes the surface portion of liquid to be attracted to another surface, such as that of another portion of liquid (as in connecting bits of water or as in a drop of mercury that forms a cohesive ball). Applying Newtonian physics to the forces that arise due to surface tension accurately predicts many liquid behaviors that are so common place that most people take them for granted. Applying thermodynamics to those same forces further predicts other more subtle liquid behaviors. Surface tension has the dimension of force per unit length, or of energy per unit area. The two are equivalent, but when referring to energy per unit area, people use the term surface energy which is a more general term in the sense that it applies also to solids and not just liquids. If the value of force per unit length is denoted by γ, then the work done in extending that unit length area at a distance dx is

$$work = \gamma l dx \tag{2.1.1}$$

As $ldx = dA$ then the above equation can be written as

$$work = \gamma dA \tag{2.1.2}$$

The symbol γ represents the surface tension[64]. The unit of surface tension is either J/m^2 or N/m.[65] In materials science; surface tension is used for either surface stress or surface free energy.

2.1.1 Causes of Surface Tension

Surface-tension is caused by the attraction between the liquid's molecules by various intermolecular forces. In the bulk of the liquid, each molecule is pulled equally in every direction by neighboring liquid molecules, resulting in a net force of zero. At the surface of the liquid, the molecules are pulled inwards by other molecules deeper inside the liquid and are not attracted as intensely by the molecules in the neighboring medium (by vacuum, air or another liquid). Therefore, all of the molecules at the surface are subject to an inward force of molecular attraction which is balanced only by the liquid's resistance to compression, meaning there is no net inward force. However, there is a driving force to diminish the surface area, and in this respect a liquid surface resembles a

stretched elastic membrane. Thus the liquid squeezes itself together until it has the locally lowest surface area possible. Another way to view it is that a molecule in contact with a neighbor is in a lower state of energy than if it weren't in contact with a neighbor. The interior molecules all have as many neighbors as they can possibly have. But the boundary molecules have fewer neighbors than interior molecules and are therefore in a higher state of energy. For the liquid to minimize its energy state, it must minimize its number of boundary molecules and must therefore minimize its surface area.[66, 67] As a result of surface area minimization, a surface will assume the smoothest shape it can (mathematical proof that "smooth" shapes minimize surface area relies on use of the Euler–Lagrange equation). Since any curvature in the surface shape results in greater area, a higher energy will also result. Consequently the surface will push back against any curvature in much the same way as a ball pushed uphill will push back to minimize its gravitational potential energy.

2.1.2 Parameters Obtained from Surface Tensiometry

A. Critical Micelle Concentration (CMC)

By surface tensiometry, Critical Micelle Concentration (CMC) can be determined from the region where the surface tension remains constant and further adding of surfactants cause aggregation.

B. Surface excess concentration (Γ)

The concentration of the surfactant at the interface can be calculated from surface or interfacial tension data by the use of appropriate Gibb's equation

$$\Gamma = -\frac{1}{2.303RTx}\left(\frac{d\gamma}{d\log C}\right) \qquad (2.1.3)$$

$$\Gamma = -\frac{1}{RTx}\left(\frac{d\gamma}{d\ln C}\right)$$

Where x is a parameter which shows simultaneous adsorption of cations and anions

$$x = 1 + \frac{m}{m + m_s}$$

m = concentration of surfactant

m_s = concentration of electrolyte

In the absence of electrolyte $m_s = 0$ and $\frac{m}{m+m_s} = \frac{m}{m} = 1$ and x = 2

$$\Gamma = -\frac{1}{4.606RT}\left(\frac{d\gamma}{d\log C}\right) \tag{2.1.4}$$

From the plot of log C and γ we can calculate the value of Γ by putting the value of R, T and $\frac{d\gamma}{d\log C}$ =slope (obtained from the premicellar region).In the presence of excess amount of electrolyte $m_s = \infty$ and x = 1

C. Area per molecule (A)

From the surface excess concentration the area per molecule at the interface in square angstroms is calculated from the following equation

$$A = \frac{1}{\Gamma N_A} = \frac{1}{molm^{-2}.mol^{-1}} = m^2 \tag{2.1.5}$$

D. Free energy of adsorption (ΔG_{ad})

Free energy of adsorption can be calculated from the free energy of micellization (ΔG_m) and surface pressure (Π)

$$\Delta G_{ad} = \Delta G_m - \frac{\Pi_{cmc}}{\Gamma} \tag{2.1.6}$$

$$\Delta G_m = (1+\beta)RT \ln X_{cmc} \tag{2.1.7}$$

While surface pressure is $\Pi = \gamma_0 - \gamma_{cmc}$ where γ_0 the surface tension of the pure solvent and γ_{cmc} is the surface tension of the mixed system.[5]

2.2 Conductivity

Electrical conductivity or specific conductance is a measure of a material's ability to conduct an electric current. When an electrical potential difference is placed across a conductor, its movable charges flow, giving rise to an electric current. The conductivity σ is defined as the ratio of the current density J to the electric field strength E:

$$\sigma = \frac{J}{E} \tag{2.2.1}$$

It is also possible to have materials in which the conductivity is anisotropic, in which case σ is a 3×3 matrix (or more technically a rank-2 tensor) which is generally symmetric.

Conductivity is the reciprocal (inverse) of electrical resistivity, ρ, and has the SI unit of siemens per meter ($S \cdot m^{-1}$):

$$\sigma = \frac{1}{\rho} \tag{2.2.2}$$

Electrical conductivity is commonly represented by the Greek letter σ, but κ (esp. in electrical engineering science) or γ are also occasionally used.

Conductivity, i.e. measurement of the electrical conductivity, is used widely in fundamental investigations of electrolyte solutions and in tackling many applied problems. It is one of the simplest and yet most accurate method for the investigation and analysis of substances. It makes it possible to carry out studies over a wide range of temperatures, pressures, and electrolyte solutions (from strongly dilute to melts), and this can be done using practically any solvent.[68]

2.2.1 Parameters Obtained From Conductivity

A. CMC

By conductivity CMC is obtained from the intersection of the pre micellar and post micellar lines.

B. Degree of Ionization (α)

Ionization refers to the process whereby an atom or molecule loses an electron, resulting in two oppositely charged particles[69], a negatively charged electron and a positively charged ion. The degree of ionization, or α, is a way of representing the strength of an acid, often represented by the Greek letter alpha. It is defined as the ratio between the number of ionized molecules and the number of molecules dissolved in water. It can be represented as a decimal number or as a percentage. One can classify strong acids as having ionization degrees above 50%, weak acids with α below 5%, and the remaining as moderate acids, at a specified molar concentration. Actually, α is the ratio of the post micellar slope (S_1) to the pre micellar slope (S_2).[70]

$$\alpha = \frac{S1}{S2} \tag{2.2.3}$$

C. Degree of Counter Ion binding (β)

Many discussions have concentrated on the degree of counter ion binding to micelles, because comprehension of the specific binding of counter ions to micelles is a prerequisite for an understanding not only micellization but also of all kinds of

aggregation in aqueous solutions.[71] The degree of counter ion binding can be calculated from equation

$$\beta = 1 - \alpha \tag{2.2.4}$$

D. Free Energy of Micellization (ΔG_{mic})

The free energy of micellization can be explained on the basis of phase separation model. In micellization separate liquid phases formed. At low concentration the chemical potential of the dissolved surfactant can be described as

$$\mu_{sur}(solvent) = \mu^{o}{}_{sur} + RT \ln[S] \tag{2.2.5}$$

Where $\mu^{o}{}_{sur}$ is the effective standard chemical potential at dilute solution and [S] is the surfactant concentration. At $[S] = CMC$ the chemical potential of a surfactant in a micelle $\mu_{sur}(micelle)$ is equal to the chemical potential of a dissolved surfactant. This directly leads to

$$\mu_{sur}(micelle) = \mu^{o}{}_{sur} + RT \ln CMC \tag{2.2.6}$$

The molar Gibbs energy of micellization is the Gibbs energy difference between a mole of monomers in micelles and the standard chemical potential in dilute solution:

$$\Delta G^{mic} = \mu_{sur}(micelle) - \mu^{o}{}_{sur} = RT \ln CMC \tag{2.2.7}$$

For nonionic surfactant we can use this equation to calculate the change in Gibbs free energy of micellization.[72]

For ionic surfactant the Gibbs free energy of micellization can be calculated from the degree of counter ion binding (β)

$$\Delta G_{mic} = (1 + \beta) RT \ln CMC \tag{2.2.8}$$

$$\Delta G_{mic} = (1 + \beta) RT \ln Xcmc \tag{2.2.9}$$

Where $Xcmc = \dfrac{cmcofsurfac \tan t}{55.55}$

CMC are usually below 1M, for this reason Gibbs free energies of micellization are negative i.e. it is a spontaneous process.

2.3 Fluorescence Technique

Luminescence or Radiative Process

Emission of light from any substance by electronic excitation is called luminescence. In these processes the dissipation of energy takes place through the radiations.

Luminescence is further categorized as:

2.3.1 Fluorescence

The term 'fluorescence' was coined by George Gabriel Stokes in his 1852 paper[73]; the name was given as a description of the essence of the mineral fluorite, composed of calcium fluoride, which gave a visible emission when illuminated with "invisible radiation" (UV radiation).

"The emission transition process that occurs between the states having the same multiplicity". In the excited singlet state, the electron in the excited orbital is paired (by opposite spin) to the second electron in the ground state orbital. In fluorescence return of electron to the ground state is spin allowed and occur rapidly by the emission of photon ($h\nu$).[74]

Excitation: $S_0 + h\nu_{ex} \longrightarrow S_1$

Fluorescence (emission): $S_1 \longrightarrow S_0 + h\nu_{em}$

Fluorescence spectroscopy is usually the emission of visible light by a substance when absorbed light of invisible wavelength. Absorption of a photon triggers the emission of a photon with a longer (less energetic) wavelength. A shorter wavelength emission is sometimes observed from multiple photon absorption. The energy difference between the absorbed and emitted photons ends up as molecular rotations, vibrations or heat. Sometimes the absorbed photon is in the ultraviolet range, and the emitted light is in the visible range, but this depends on the characteristics of the particular fluorescent substance.[73]

2.3.2 Jablonski Diagram

A typical Jablonski diagram is shown in Figure.2.1. The singlet ground, first, and second electronic states are depicted by S_0, S_1, and S_2. At each of these electronic energy levels the fluorophores can exist in a number of vibrational energy levels, depicted by 0, 1, 2, etc. Transition occur in about 10^{-15} s, a time too short for significant displacement of

nuclei. This is the Frank-Cordon principle. Absorption and emission occur mostly from molecules with the lowest vibrational energy. The larger energy difference between the S_0 and S_1 excited states is too large for thermal population of S_1. For this reason we use light and not heat to induce fluorescence. Following light absorption several processes usually occur. A fluorophore is usually excited to some higher vibrational level of either S_1 or S_2. With a few rare exceptions, molecules in condensed phases rapidly relax to the lowest vibrational level of S_1.This process is called internal conversion and generally occurs within 10^{-12} s or less. Since fluorescence life times are typically near 10^{-8} s, internal conversion is generally complete prior to emission. Hence fluorescence emission generally results from a thermally equilibrated excited state, that is, the lowest energy vibrational state of S_1. Molecules in the S_1 state can also undergo a spin conversion to the first triplet stat T_1. Emission from T_1 is termed phosphorescence, and is generally shifted to longer wavelengths (lower energy) relative to the fluorescence. Conversion of S_1 to T_1 is called Inter System Crossing.[74]

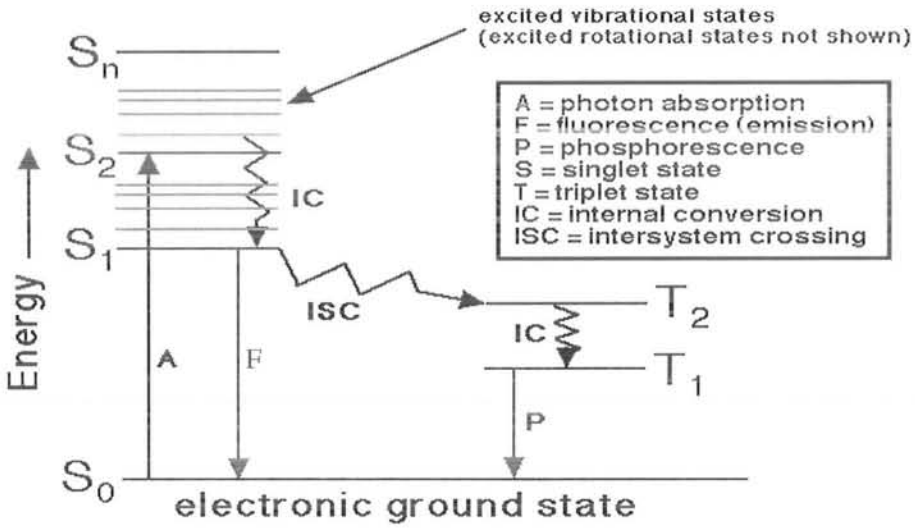

Fig. 2.1: Jablonski Diagram

2.3.3 Quantum Yield

The fluorescence quantum yield gives the efficiency of the fluorescence process. It is defined as the ratio of the number of photons emitted to the number of photons absorbed.

$$\Phi = \frac{\#\ photons emitted}{\#\ photons absorbed} \qquad (2.3.1)$$

The maximum fluorescence quantum yield is 1.0 (100%); every photon absorbed results in a photon emitted. Compounds with quantum yields of 0.10 are still considered quite fluorescent.[74] The higher the value of Φ, the greater the observed fluorescence of a compound. A non-fluorescent molecule is one whose quantum efficiency is zero or so close to zero that the fluorescence is not measurable(i.e., all energy absorbed by such a molecule is rapidly lost by collision deactivation).[75] Another way to define the quantum yield of fluorescence is by the rates excited state decay:

$$\frac{k_f}{\sum iki} \qquad (2.3.2)$$

Where k_f is the rate of spontaneous emission of radiation and $\sum_i ki$ is the sum of all rates of excited state decay. Other rates of excited state decay are caused by mechanisms other than photon emission and are therefore often called "non-radiative rates", which can include: dynamic collisional quenching, near-field dipole-dipole interaction (or resonance energy transfer), internal conversion and intersystem crossing. Thus, if the rate of any pathway changes, this will affect both the excited state lifetime and the fluorescence quantum yield. Fluorescence quantum yield are measured by comparison to a standard with known quantology; the quinine salt, quinine sulfate, in a sulfuric acid solution is a common fluorescence standard.

2.3.4 Types of Fluorescence

Fluorescence spectroscopy can be broadly classified into two types:

1. Steady State or Static Fluorescence Spectroscopy

That type of fluorescence spectroscopy which is performed with constant illumination and observation. In this type of fluorescence the sample is illuminated with a continuous beam of light, and the intensity or emission spectrum is recorded. Because of the nanosecond time scale of fluorescence most measurement are steady state measurements. When the sample is first exposed to light, steady state is reached almost immediately.[74]

2. Time resolved or Dynamic Fluorescence Spectroscopy

Time-resolved fluorescence spectroscopy is an extension of fluorescence spectroscopy. Here, the fluorescence of a sample is monitored as a function of time after excitation by a flash of light. The time resolution can be obtained in a number of ways,

depending on the required sensitivity and time resolution.While normal fluorescence spectroscopy is useful as a highly selective and sensitive non-invasive probe, better chemical information can often be gained from the same experiment by exploiting the time-dependent nature of fluorescence. Time-resolved fluorescence provides more information about the molecular environment of the fluorophore than steady state fluorescence measurements. Since the fluorescence lifetime of a molecule is very sensitive to its molecular environment, measurement of the fluorescence lifetime(s) reveals much about the state of the fluorophore. Many macromolecular events, such as rotational diffusion, resonance-energy transfer, and dynamic quenching, occur on the same time scale as the fluorescence decay. Thus, time-resolved fluorescence spectroscopy can be used to investigate these processes and gain insight into the chemical surroundings of the fluorophore. It is important to remember that the fluorescence lifetime is an average time for a molecule to remain in the excited state before emitting a photon. Each individual molecule emits randomly after excitation. Many excited molecules will fluoresce before the average lifetime, but some will also fluoresce long after the average lifetime. Fluorescence lifetimes are generally on the order of 1-10 n sec, although they can range from hundreds of nanoseconds to the sub-nanosecond time scale.

2.3.5 Basic Rules of Fluorescence

1. The Frank-Condon Principle

"The nuclei are stationary during electronic transitions, and so excitation occurs to vibrationally excited levels of the excited electronic state vertically".

2. The Kasha's Rules

"The fluorescence emission spectrum is generally observed irrespective of the excitation wavelength because the emission occurs from the lowest vibrational level of the lowest excited singlet state and relaxation from the excited vibrational levels is much faster than emission".

3. The Stokes Shift

"Emission is always of lower energy (longer wavelength) than absorption (shorter wavelength) due to nuclear relaxation in the excited state".

4. The Mirror Image Rule

"Emission spectra are mirror images of the lowest energy absorption band due to the same spacing of vibrational energy levels both in the ground and the excited states".[74]

2.3.6 Fluorescence Quenching

A quench refers to a rapid cooling. Quenching refers to any process which decreases the fluorescence intensity of a given substance. The substances which responsible for the decrease of fluorescence intensity are called quenchers. A variety of processes can result in quenching, such as excited state reactions, energy transfer, complex-formation and collisional quenching. As a consequence, quenching is often heavily dependent on pressure and temperature. Molecular oxygen and the iodide ion are common chemical quenchers. Quenching possess a problem for non-instant spectroscopic methods, such as laser-induced fluorescence.

Types of Fluorescence Quenching

A variety of molecular interactions can result in quenching. These include excited state reactions, molecule rearrangements, energy transfer, static and colliosional quenching. Among these quenching mechanism the static and colliosional (dynamic) are most important which produce valuable information about the binding between fluorescent sample and quencher.

A. Static Quenching

Quenching in which a nonfluorescent ground-state complex formed between the fluorophore and quencher is consider as static quenching. When this complex absorb light it immediately return to the ground state without the emission of a photon. For static quenching the dependence of the fluorescence intensity upon quencher concentration is easily derived by consideration of the association constant for the complex formation. This constant is given by

$$Ks = \frac{[I_Q - Q]}{[I_Q][Q]} \qquad (2.3.3)$$

Where $[I_Q\text{-}Q]$ is the concentration of the complex. $[I_Q]$ is the concentration of the uncomplexed fluorophore and [Q] is the concentration of the quencher. If the complex species is nonfluorescent then the fraction of the fluorescence that remains I_Q/I is given

by the fraction of the total fluorophores that are not complexed: $f = \frac{I_Q}{I}$. Recalling that the total concentration of fluorophore is given by

$$[I] = [I_Q] + [I_Q - Q] \text{ Or}$$

$$[I_Q - Q] = [I] - [I_Q] \tag{2.3.4}$$

Substituting the value of $[I_Q\text{-}Q]$ from equation (2.3.4) into equation (2.3.3)

$$K_s = \frac{[I] - [I_Q]}{[I_Q][Q]} = \frac{[I]}{[I_Q][Q]} - \frac{1}{[Q]} \tag{2.3.5}$$

Rearrangement of equation (2.3.5) gives following form

$$\frac{I}{I_Q} = 1 + K_s[Q] \tag{2.3.6}$$

Equation (2.3.6) explains the dependence of I/I_Q on [Q] is linear, which same both for static and dynamic quenching except that the quenching constant for static is now association constant.

B. Dynamic Quenching

That type of quenching that resulted from diffusive encounters between the fluorophore and quencher during the life time of the excited state called dynamic or colliosional quenching. In dynamic quenching, the quencher must diffuse to the fluorophore during the life time of the excited state. Upon contact, the fluorophore returns to the ground state, without emission of photon. In general quenching occurs without permanent change in the molecule that is without a photochemical reaction.

Dynamic quenching of fluorescence is described by the Stern-Volmer equation:

$$\frac{I}{I_Q} = 1 + K_q t_o[Q] = 1 + K_D[Q] \tag{2.3.7}$$

In this equation I an I_Q are the fluorescence intensities in the absence and presence of quencher. K_q is the bimolecular quenching constant, t_o is the life time of the fluorophore in the absence of quencher and [Q] is the quencher concentration. The Stern-Volmer quenching constant is given by $K_D = K_q t_o$. If the quenching is known to be dynamic, the Stern-Volmer constant will be represented by K_D. A plot of I/I_Q vs. [Q] gives an intercept one on the y-axis and a slope equal to K_D.[74]

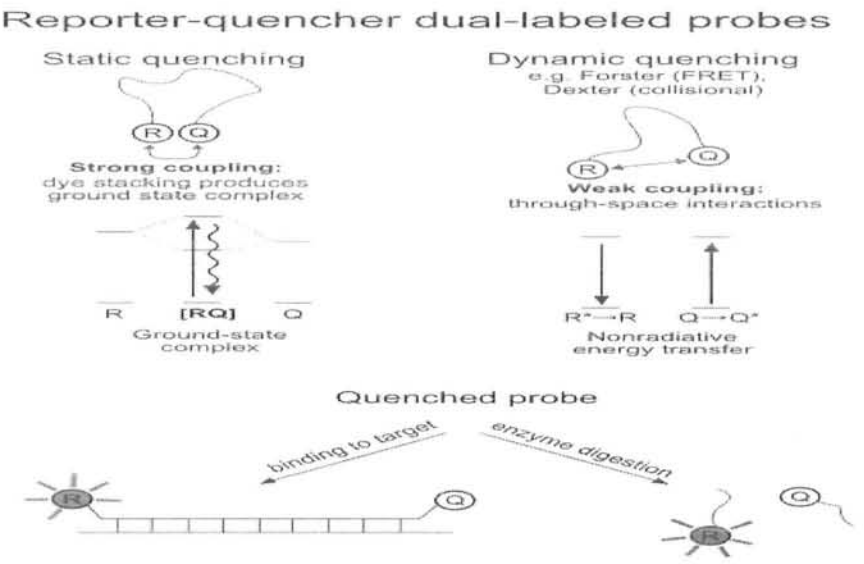

Fig. 2.2 Comparison of static and dynamic quenching

2.3.7 Parameters Obtained from Fluorescence

A. Aggregation Number (N_{agg})

The total number of molecules combine together to form a micelle called aggregation number. A typical experiment to determine the mean aggregation number would involve the use of a luminescent probe, quencher and a known concentration of surfactant. If the concentration of the quencher is varied, and the CMC of the surfactant is known, than from the decrease of fluorescence intensity the mean aggregation number can be calculated. The fluorescence intensities in the absence of quencher, Io, and in the presence of quencher, I_Q are related to the quencher concentration [Q] and micellar molar concentration [M] according to:

$$\ln \frac{I_o}{I_Q} = \frac{[Q]Nagg}{([S]-cmc)} \tag{2.3.8}$$

A plot of ln I_o/I_Q vs. [Q] gives slope $\frac{Nagg}{([S]-cmc)}$. From slope the N_{agg} can be calculated as: $slope = \frac{Nagg}{([S]-cmc)}$ and $N_{agg} = slope \times ([S]-cmc)$

Where [S] is the concentration of surfactant while CMC is the critical micellar concentration of the surfactant.

B. Binding Sites (n)

The binding sites can be calculated using following type of equation

$$\log(\frac{Io - I}{I}) = \log kb + n\log[Q] \qquad (2.3.9)$$

A plot of $\log(\frac{Io - I}{I})$ vs. log [Q] gives a slope and intercept. From the slope the binding constant can be calculated.

C. Binding constant (k_b)

From equation (2.3.9) we can also calculate the binding constant. The intercept of plot of $\log(\frac{I_o - I}{I})$ vs. log [Q] gives the binding constant.

D. Free energy of binding (ΔG_b)

The free energy of binding can be calculated using following equation

$$\Delta G_b = -RT \ln K_b \qquad (2.3.10)$$

Where R is the universal gas constant and T is the temperature.

2.4 Laser Light Scattering

2.4.1 Introduction

Light scattering is the alteration or change in the direction and the intensity of light beam that strikes an object. This alteration is due to the cumulative effects of reflection, refraction and diffraction (in the absence of absorption).Light scattering is an important tool for characterizing macromolecules for at least three decades. However, the replacement of the conventional light source by lasers in recent years has quantitatively changed the field and has sparked renowned interest. Through the use of coherent laser light, efficient spectrum analyzers and autocorrelations experiments in frequency and time domains one can study molecular motions, diffusion and other dynamic processes as well as equilibrium properties of solutions. The technology for clarifying samples has also significantly improved. Recirculation through submicron filters in closed loop system reduces the effect of dust and other contaminants and the new time domain techniques provide built in test for the presence of such particles. These advances make LLS a powerful form of spectroscopy for use of macromolecular characterization.

2.4.2 Types of Laser Light Scattering

2.4.2.1 Static Laser Light Scattering

In static laser light scattering the time averaged (or total) intensity of the scattered light is measured and for solution it is related to the time-averaged mean- square excess polarizability, which in turn is related to the time-averaged mean-square concentration fluctuation. The reduced integrated scattering intensity KC/R_{vv} (q) calculated from the absolute photon count, which is recorded with the measurement of the time correlation function (TCF).

Static light scattering is a useful technique that uses the intensity traces at a number of angles to get information about the molecular mass (Mw), radius of gyration (R_g), second viral coefficient (A_2) of the polymer or polymer complexes.[76-80]

A number of methods are developed to analyze the scattering of particles in solution to derive the above named physical characteristics of particles. A simple static light scattering experiment entails the average intensity of the sample that is corrected for the scattering of the solvent will yield the Raleigh ratio as a function of the angle or the wave vector q as follow.

$$R(\theta_{sample}) = R(\theta_{solvent})\, I_{sample}/I_{solvent} \qquad (2.4.1)$$

The difference in the Raleigh ratio $\Delta R(\theta)$ between the sample and solvent is given by

$$\Delta R(\theta) = R(\theta_{sample}) - R(\theta_{solvent}) \qquad (2.4.2)$$

In addition the setup of laser light scattering is corrected with a liquid of known refractive index and Raleigh ratio e.g. toluene, benzene or decalin.

The data analysis can be performed without a so called material constant K, which can lead to the calculation of other physical parameters of the system and is define below.

$$K=4\pi^2 n_o^2 (dn/dc)^2/N_A\lambda^4 \qquad (2.4.3)$$

Where (dn/dc) is the refractive index increment, n_o is the refractive index of the solvent, N_A is Avogadro's number and λ is the wavelength of the laser light.

Methods of Plots

The LLS data can be plotted by two ways:

Debye plot

This method is for dilute solutions of polymer (macromolecule), where additional scattering arises from concentration fluctuation, which is given by Raleigh Gans Debye as;

$$\Delta R_\theta = KcM \tag{2.4.4}$$

Where, ΔR_θ = Excess Rayleigh function

c = Concentration,

M = molar mass, K = optical constant.

For dilute solutions and polydisperse homopolymer of low molecular weight average molar mass M_w (for particle smaller than $\lambda/20$) above equation can be modified as;

$$\frac{KC}{\Delta R_\theta} = \frac{1}{M_w} + 2A_2C \tag{2.4.5}$$

This method is used to derive the molecular mass (Mw), and second viral coefficient (A_2) of polymer or polymer complex system by plotting a graph between KC/R_θ vs. C .This experiment is performed using a single angle (typically 90°).

Zimm plot

This is for particles or molecules with dimension exceeds $\lambda/20$; interference occurs between light scattered from different parts of the molecules and a reduction in ΔR_θ is observed. For dilute polymer solution the reduced integrated intensity, KC/R_{vv} (q) is related to molecular weight by Zimm equation;

$$\frac{KC}{R_{vv}(q)} = \frac{1}{M_w}\left(1 + \frac{1}{3}\langle R_g \rangle^2 q^2\right) + 2A_2C \tag{2.4.6}$$

Where K is optical constant ($K = \frac{4\Pi^2 (dn/dc)^2}{\lambda^4 N_A}$), here n is the refractive index, dn/dc is the refractive index increment of the solvent ,λ is the wavelength of laser used and N_A is Avogadro's constant, C is concentration, $R_{vv}(q)$ is Rayleigh ratio and q is the modulus of scattering vector ($q = \frac{4\pi n}{\lambda}\sin\frac{\theta}{2}$), θ is scattering angle. The variation of KC/R_{vv} (q) with C and θ can be expressed in terms of Zimm plot. Here KC/R_{vv} (q) is plotted vs. $q^2 + k'C$.

The results of each angle are plotted to zero concentration and those for each concentration to zero angle. The reciprocal of the weight average molar mass M_w, while the slope is a measure of second virial coefficient, A_2.[81] The experiment can be performed at several angles and at least four concentrations. A typical Zimm plot is shown in figure below.

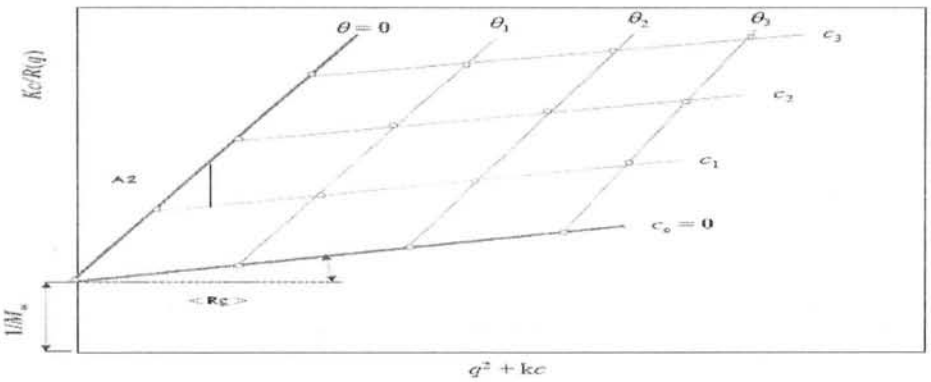

Fig. 2.3 Typical Zimm plot

Where C is concentration of the polymer and θ is angle. A_2, <Rg> and M_w are the second virial coefficient, radius of gyration and molar mass respectively. The extrapolation of both concentration and angle to zero is due to two reasons; (a) Non-ideal solution effect and (b) Large particle size effect. Thus extrapolation of concentration to zero can remove the non-ideal solution effect, while extrapolation of scattering angle to zero can remove large size effects. Hence we obtain second virial coefficient from the slope of concentration extrapolated to zero, radius of gyration from the slope of scattering angle extrapolated to zero and molecular weight from the intercept in both the cases .i.e. ($C \rightarrow 0$ & $\theta \rightarrow 0$).

2.4.2.2 Dynamic Laser Light Scattering

Dynamic light scattering (also known as Photon Correlation Spectroscopy or Quasi-Elastic Light Scattering) Information is extracted from correlating variation in the light intensity due to the Brownian movements of the particles. Here time dependent fluctuations in the scattered light signals are measured using fast photon counter. Dynamic LLS is used to determine diffusion coefficient, which can be converted to hydrodynamic radius through Stoke- Einstein/Debye-equation It is a technique in physics, which can be used to determine the size distribution profile of small particles in suspension or polymers in solution. It can also be used to probe the behavior of complex fluids such as concentrated polymer solutions.

Mechanism of dynamic light scattering

When light hits small particles the light scatters in all directions (Rayleigh scattering) for particles small compared to the wavelength (below 250 nm). If the light source is a laser, and thus is monochromatic and coherent, then one observes a time-dependent fluctuation in the scattering intensity. These fluctuations are due to the fact that the small molecules in solutions are undergoing brownian motion and so the distance between the scatterers in the solution is constantly changing with time. This scattered light then undergoes either constructive or destructive interference by the surrounding particles and within this intensity fluctuation, information is contained about the time scale of movement of the scatterers. There are several ways to derive dynamic information about particles' movement in solution by brownian motion. One such method is dynamic light scattering, also known as quasi-elastic laser light scattering.

Intensity correlation function

The dynamic information of the particles is derived from an autocorrelation of the intensity trace recorded during the experiment. The second order autocorrelation curve is generated from the intensity trace as follows:

$$g^2(q;\tau) = \frac{\langle I(t)I(t+\tau)\rangle}{\langle I(t)\rangle^2} \qquad (2.4.7)$$

Where g^2 (q; τ) is the autocorrelation function at a particular wave vector, q, and delay time, τ, and I is the intensity. At short time delays, the correlation is high because the particles do not have a chance to move to a great extent from the initial state. The two signals are thus essentially unchanged when compared after only a very short time interval. As the time delays become longer, the correlation starts to exponentially decay to zero, meaning that after a long time period has elapsed, there is no correlation between the scattered intensity of the initial and final states. This exponential decay is related to the motion of the particles, specifically to the diffusion coefficient. To fit the decay (i.e., the autocorrelation function), numerical methods are used, based on calculations of assumed distributions. If the sample is monodisperse then the decay is simply a single exponential. The Siegert equation relates the second order autocorrelation function with the first order autocorrelation function g^1 (q; τ) as follows:

$$g^2(q;\tau) = 1+\beta\,[g^1(q;\tau)]^2 \qquad (2.4.8)$$

Where the parameter β is a correction factor that depends on the geometry and alignment of the laser beam in the light scattering set up.

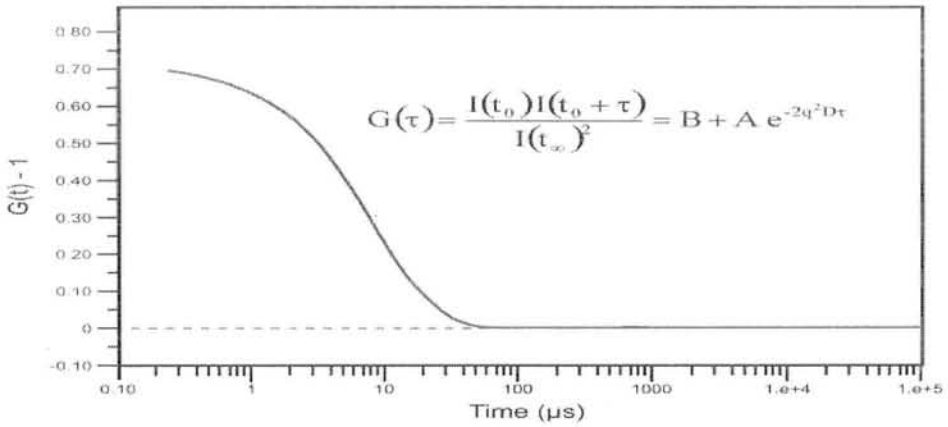

Fig. 2.4 Representative Correlation function measured during dynamic light scattering

Data analysis

The simplest approach is to treat the first order autocorrelation function as a single exponential decay. This is appropriate for a monodisperse population.

$$g^1(q;\tau) = \exp(-\Gamma\tau) \qquad (2.4.9)$$

Where Γ is the decay rate. The translational diffusion coefficient D_t may be derived at a single angle or at a range of angles depending on the wave vector q.

$$\Gamma = q^2 D_t$$

$$q = \frac{4\pi n_o}{\lambda}\sin\left(\frac{\theta}{2}\right) \qquad (2.4.10)$$

Where λ is the incident laser wavelength, n_0 is the refractive index of the sample and θ is angle at which the detector is located with respect to the sample cell. Depending on the anisotropy and polydispersity of the system, a resulting plot of Γ/q^2 vs. q^2 may or may not show an angular dependence. Small spherical particles will show no angular dependence, hence no anisotropy. A plot of Γ/q^2 vs. q^2 will result in a horizontal line. Particles with a shape other than a sphere will show anisotropy and thus an angular dependence[82].The intercept is equal to D_t and often used to calculate the hydrodynamic radius of a sphere through the Stokes-Einstein equation. It is important to note that the size determined by dynamic light scattering is the size of a sphere that moves in the same manner as the scatterer. So, for example, if the scatterer is a random coil polymer, the determined size is not the same as the radius of gyration determined by static scattering.

In most cases, samples are polydisperse. Thus, the autocorrelation function is a sum of the exponential decays corresponding to each of the species in the population.

$$g^1(q;\tau) = \sum_{i=1}^{n} G(\Gamma_i)\exp(-\Gamma_i\tau) = \int G(\Gamma)\exp(-\Gamma\tau)d\Gamma \qquad (2.4.11)$$

It is tempting to obtain data for g^1 (q; τ) and attempt to invert the above to extract G (Γ). Since G (Γ) is proportional to the relative scattering from each species, it contains information on the distribution of sizes.

Chapter – 3

METHODS AND MATERIALS

Chapter - 3

METHODS AND MATERIALS

3.1 Materials and apparatus used

To study the interactions of polymers with surfactants, two triblock copolymers $E_{30}B_{10}E_{30}$ and $E_{48}B_{10}E_{48}$ and two ionic surfactants Sodium Dodecyl Sulphate (SDS) and Cetyl Trimethyl Ammonium Bromide (CTAB) were used. The formulas of chemicals used are given below.

1. Triblock copolymers: $E_{30}B_{10}E_{30}$ and $E_{48}B_{10}E_{48}$.
2. Anionic surfactant Sodium Dodecyl Sulphate (SDS).

Fig. 3.1 Structure of SDS

3. Cationic surfactant Cetyl Trimethyl Ammonium Bromide (CTAB)

Fig. 3.2 Structure of CTAB

4. Pyrene

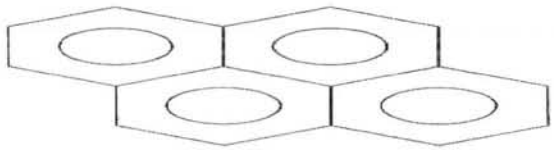

Figure. 3.3 Structure of Pyrene

5 Cetyl Pyridinium Chloride (CPC)

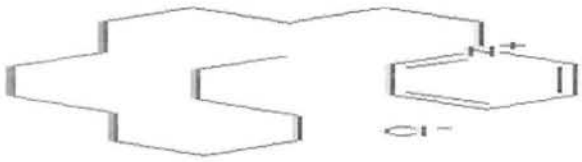

Figure. 3.4 Structure of CPC

All experiments were carried out with analytical reagent grade chemicals using doubly distilled deionized water having almost zero conductivity. The apparatus used

was water deionizer, analytical balance of ±0.001 g accuracy, conductivity meter Jenway 4310, torsion balance (White Elec. Inst. Co. Ltd.), PTFE 1.0 μm filter, commercial LLS Spectrometer (ALV/DLS/SLS-5022F), water circulating bath (IRMECO I-2400 GmbH Germany and Perkin Elmer Luminescence spectrometer Model LS 55(Serial Number 73135).The cell used for measuring fluorescence was 10 mm path length quartz cell and was clear in all dimensions.

3.2 Surface tension measurements

For measurement of surface tension, 0.1g/L and 2g/L stock solutions of triblock copolymers were prepared by dissolving 0.0015g polymer in 15mL(0.1g/L) and 0.03g in 15mL(2g/L) deionized water. Stock solutions of SDS and CTAB were prepared by dissolving 1.44g/100mL (50mM) and 0.27g/50mM (15mM).First the surface tension of pure components in aqueous solutions i.e. pure polymer and surfactants were measured at 303K. Then Surface tension for surfactant/polymer mixed system were measured by diluting the stock solution of SDS(50mM) from 50mM to 1mM and CTAB(15mM) from 15mM to 0.1mM with the polymer stock solution as a solvent. Surface tension was measured with the help of Torsion Balance (White Elec. Inst. Co. Ltd.) equipped with a platinum ring (4 cm circumference) along with temperature controlled water circulating bath (IRMECO I-2400 GmbH Germany). For sample a special homemade glass was used, the cell had hollow space for circulation of water, and there was an inlet and outlet for water circulation. The sample was taken in the cell around which water with 303K temperature, was circulated in the hollow portion of the cell in order to achieve the desired temperature.

On smooth supporting surface the Torsion Balance was placed in such a position to view the dial easily and accurately. By means of two leveling screws in the tripod base so that the bubble in the spirit level was adjusted exactly in the center. To the extension hook platinum ring (4cm circumference) was attached. The instrument was kept free from vibrations. It is necessary that the platinum wire of the ring must be circular in one plane and free from bends. The torsion balance was checked for zero and calibrated with water. Chromic acid was used for washing all glassware followed by rinsing with deionized water and dried in oven.

Stock solution was taken in the measuring cell (having water circulation through hollow space around measuring sample) and placed on the platform below the ring after

calibration of the instrument. Adjusted the position of the cell on platform in such a way that the sample surface was 10mm below the platinum ring. Then beam was unclamped and with the help of special screw at the base of platform the cell was moved so that the ring was dipped in sample surface. The index pointer was gradually moved along to maintain zero at vernier' s scale. After reaching the corresponding surface tension of the sample, the ring was suddenly detached from the liquid surface and the reading on the outer main scale was noted, which gives surface tension (γ) in N/m. At least three readings were noted for each solution.

3.3 Conductivity measurements

The conductance data were recorded by a digital conductivity meter Jenway-4310. This instrument has auto ranging from 0.01μS to 199.9mS and temperature control accuracy of 273.5K. The measurement cell was immersed in a water circulating bath (IRMECO I-2400 GmbH Germany) in order to hold a constant temperature. Conductivity cell was equipped with electrode, temperature sensor and magnetic stirrer. Conductivity of each solution was measured at temperature range 303K. Prior to measurement calibration was made with KCl aqueous solution by using the normal concentration data keeping the cell constant 1.04. After calibration the measurement of samples were made by immersing the cell in the samples using water circulating bath keeping temperature constant allowing the read out to stabilize, and then result was recorded.

3.4 Steady State Fluorescence Spectroscopy

Steady State Fluorescence Spectroscopy was performed using a Perkin Elmer Luminescence spectrometer Model LS 55(Serial Number 73135).The cell used for measuring fluorescence was 10 mm path length quartz cell and was clear in all dimensions. Different stock solution of 0.1g/L and 2g/L of triblock copolymers were prepared. A very low concentration ($1x10^{-6}$M) of pyrene was used. The pyrene solution of 1×10^{-03}M was prepared by dissolving 0.02g of pyrene in 100mL of ethanol. This solution was further diluted up to 1×10^{-06}M by dissolving 0.2ml of 1×10^{-03}M pyrene in 200ml of polymer stock solution. These polymers stock solutions were then used for the preparation of 25mM SDS and 15mM CTAB. Different concentrations of Cetyl Pyridinium Chloride (CPC) varying from $3x10^{-4}$M to$2.8x10^{-5}$M were prepared using 25mM SDS and 15mM CTAB by dilution method. Luminescence spectrometer was used

in Fluor mode to perform the fluorescence spectroscopy. The parameters used were as follow:

The scan rate was kept at 600 nm minute^{-1}, λ_{exc} was 340 nm, and scan range was 350- 600nm.Excitation slit was fixed at 7 nm and emission slits were fixed at2.5nm. Photomultiplier voltage was fixed at 65V. Polarizer was kept clear and no cutoff was operating during scan.

3.5 Dynamic Light Scattering measurements

Dynamic light scattering experiment was carried out by a commercial LLS spectrometer BI-200SM motor-driven goniometer equipped with BI-9000AT digital autocorrelator or the BI-9025AT photon counter and a cylindrical 22mW uniphase He–Ne laser (wave length = 637nm) and BI-ISTW software was used. The spectrometer has a high coherence factor of $\beta \sim 0.95$ because of a novel single- mode fiber optic coupled with an efficient avalanche- photodiode.

The instrument is very sensitive to dust particle so as to avoid discrepancy, all the glassware were washed with acetone before use and dried carefully in oven. Solutions analyzed contain fixed amount of triblock copolymer (3g/L) and varying concentrations of surfactant SDS (0.01M to 0.15M).The deionized water was first filter with PTFE 0.1μm filter. The polymer and surfactant solutions were filtered into quartz LLS cell (10mm in diameter) by PTFE 0.22μm filter. The experiment duration was 5 min. Each experiment was repeated two or more times. In the dynamic light scattering, the measurements were carried out at a scattering angle of 90°. Scattering intensities were measured at a temperature 303K for various concentrations. Other solutions were prepared by diluting the stock solutions for each copolymer-surfactant system, about 18 solutions for each copolymer – surfactant system were studied by light scattering at 303K. The data was treated by a procedure given in section 2.4.2.2.

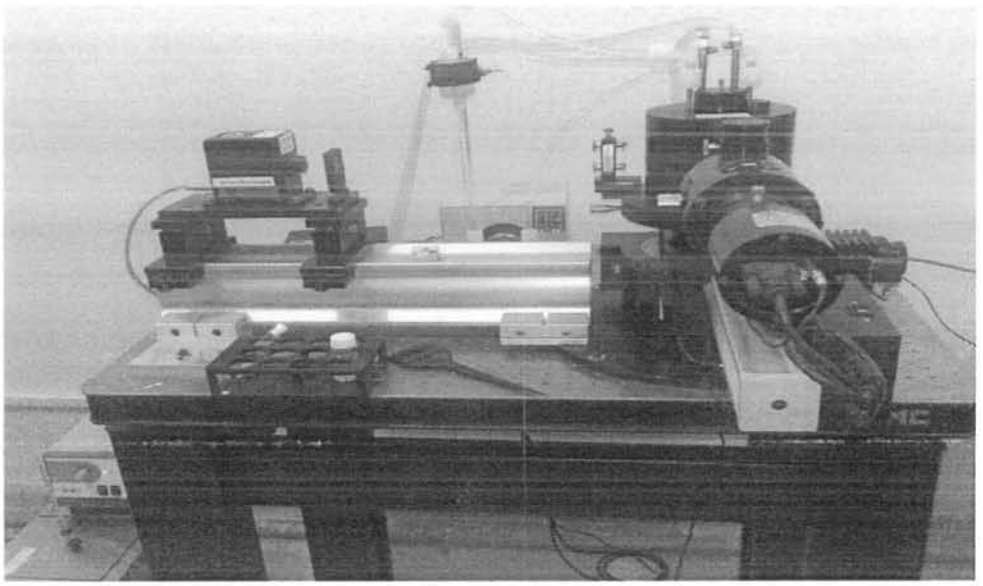

Fig. 3.5 A Commercial laser light scattering spectrophotometer

Chapter – 4

RESULTS AND DISCUSSION

Chapter - 4

RESULTS AND DISCUSSIONS

4.1 Surface tension measurements

Surface tension is one of the important tools to investigate surface properties of the single components (pure polymer or pure surfactant) as well as of the mixture of two or more components. The surface tension results were obtained using semi log plots of surfactant concentration and surface tension as shown in Figures 4.1 to 4.12. In case of triblock copolymers ($E_{30}B_{10}E_{30}$ and $E_{48}B_{10}E_{48}$), the surface tension of the solution at low polymer concentration is greater but as the concentration of the polymer increases, the surface tension gradually decrease until a point reach where the surface tension remain constant and further increase of polymer concentration cause aggregation of the polymer. This point corresponds to the Critical Micelle Concentration (CMC). The CMC values were obtained for $E_{30}B_{10}E_{30}$ (0.8g/L) and $E_{48}B_{10}E_{48}$ (0.94g/L) in close agreement reported for other EBE triblock copolymers having a comparable hydrophilic length.[61, 83, 84] Similarly CMC values for SDS (8mM) and CTAB (0.9mM) were obtained in the same fashions (Fig 4.3, 4.4) which are also in close agreement with literature values.[85, 86]

In case of pure triblock copolymer and pure surfactant the semi log plot look simple, but in case of mixture these plots look complicated and one may expect to see a decrease in surface tension with added surfactant. Two or more plateaus values corresponding to polymer rich aggregates and to surfactant rich aggregates may be observed.

In our case the semi log plots were obtained for fixed concentrations of triblock copolymers (0.1g/L and 2g/L) and varying concentration of surfactants (SDS and CTAB). These plots (Fig 4.5 to 4.12) give four different surfactant concentration regions. Region I correspond to low surfactant concentration region in which surfactant is present in the monomer form and the surface tension is little affected. In this region surfactant competes polymer for adsorption at the air/water interface. In region II the surfactant starts binding with the monomer of the polymer and a complex with low surface activity formed at enhanced surfactant concentration. A number of polymer molecules are initially placed at the interface, but the introduction of SDS makes those molecules to be desorbed back to bulk, possibly as a result of polymer-surfactant complexation. Due to

formation of less surface active complex, the polymer desorbed from the surface will cause surface tension to increase. In Region III the interaction between polymer and surfactant strengthen and greater number of surfactant molecules bind to polymer causing a decrease in surface tension with further increase in surfactant concentration. Region IV corresponds to normal micellization of surfactant as a result of polymer/surfactant complex break down with decrease in surface tension.[87] In region II the increase in surface tension causes binding of surfactant aggregates to monomeric $E_{30}B_{10}E_{30}$ and $E_{48}B_{10}E_{48}$ which is due to the loss in the surface activity of the triblock copolymer monomer (contain bound surfactant aggregates) and behave as polyelectrolyte, leaving the air/water interface.[88]

From the semi log plot of surface tension vs. surfactant concentration, three important parameters can be obtained.

1. Critical Aggregation Concentration (CAC)

The CAC corresponds to the first break point on the semi log plot at low concentration of surfactant. It is the concentration at which binding of surfactant onto the polymer in bulk phase just started. CAC is shown on the semi log plot as T_1. Below T_1, the surfactant and polymer together adsorbed at the air/water interface showing very weak interaction.[89]

2. Polymer Saturation Point (PSP)

This point corresponds to the region where the polymer saturation with surfactant takes place. At this point polymer/micelle aggregates are present in the bulk solution. This point is less defined than CAC (T_1) and CMC (T_3).

3. Critical Micelle Concentration (CMC)

This point or region corresponds to normal surfactant micellization in the bulk.[90, 91] The CMC values of triblock copolymer/surfactant systems were tabulated in table 4.1.In our case from the results of semi log plot, parameters like surface excess concentration (Γ), Area per molecule (A^2) cannot be calculated using Gibb's Equations as reported in literature.[91] The reason for this is the exact activity of different species (surfactant ion, surfactant micelle, and polymer/micelle complex) are not known.

From Table 4.1 the comparison of CMC for triblock copolymers ($E_{30}B_{10}E_{30}$ and $E_{48}B_{10}E_{48}$) and surfactants (SDS and CTAB) are summarized as:

The CMC of both SDS and CTAB increased with polymer concentration but it is more pronounced in case of 2.0g/L. Concentrated solutions of triblock copolymer will reach to equilibrium values relatively quick, but dilute solutions of triblocks would require long times (even a whole day) due to slow diffusion of the polymer chains.

The increase in CMC due to $E_{48}B_{10}E_{48}$ is greater as compared to that of $E_{30}B_{10}E_{30}$ both in case of SDS and CTAB. The reason for this is the high molecular weight of $E_{48}B_{10}E_{48}$. The effect of molecular weight in our case is counted because the hydrophobic/hydrophilic ratio are not same ($E_{30}B_{10}E_{30}$ = B/E=0.166 and $E_{48}B_{10}E_{48}$ = B/E = 0.104).

The change in CMC for SDS in the presence of polymer is greater than for CTAB because in CTAB the number of $-CH_2-$ groups (16) are greater than that of SDS (12). This can be explained on the basis of Traube's rule[92] "the concentration of the compound required for equal lowering of surface tension diminishes three fold for each $-CH_2-$ group added to the chain" therefore the change in CMC of CTAB in the presence of polymer is lower than that of SDS. This can also be explained on the basis of head group of surfactant according to a general description that anionic surfactants are more reactive than cationic surfactants towards the uncharged water soluble polymers.[93] The effects of anionic and cationic group towards different polymers are given as:

P^0:	SA^-	>	SA^+	>>	SA^0
P^{n+}	SA^-	>>	SA^+	>>	SA^0
P^{n-}	SA^-	>>	SA^+	>>	SA^0

Effect of polymer concentration on the surface tension of the mixed system

The rise in surface tension in case of dilute polymer solution is more as compare to concentrated polymer solution because in dilute polymer solution the change in surface tension is only due to the surface activity of the surfactant while in case of concentrated polymer solution this change is due to both the surface activity of the polymer and surfactant. The greater rise of surface tension observed in case of SDS as compare to CTAB is due to less surface activity of CTAB as compare to SDS.

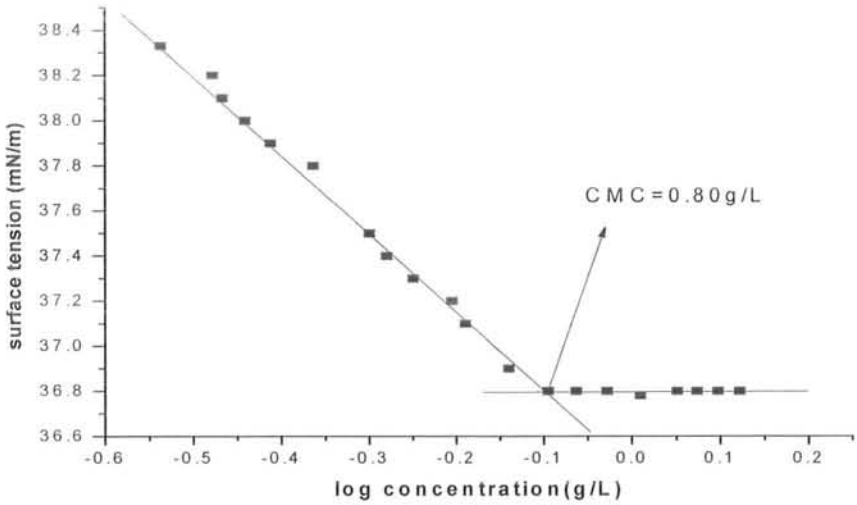

Fig. 4.1: Semi log plot of surface tension vs. concentration of pure $E_{30}B_{10}E_{30}$ at 303K.

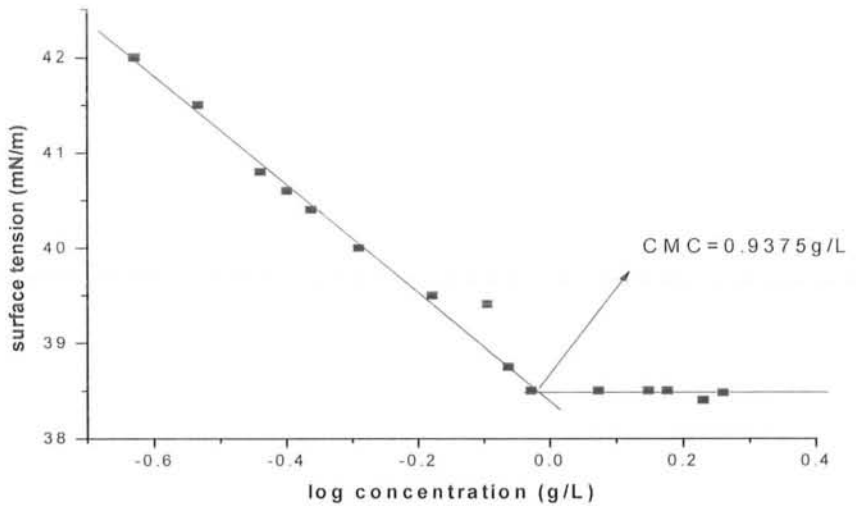

Fig 4.2: Semi log plot of surface tension vs. concentration of pure $E_{48}B_{10}E_{48}$ at 303K.

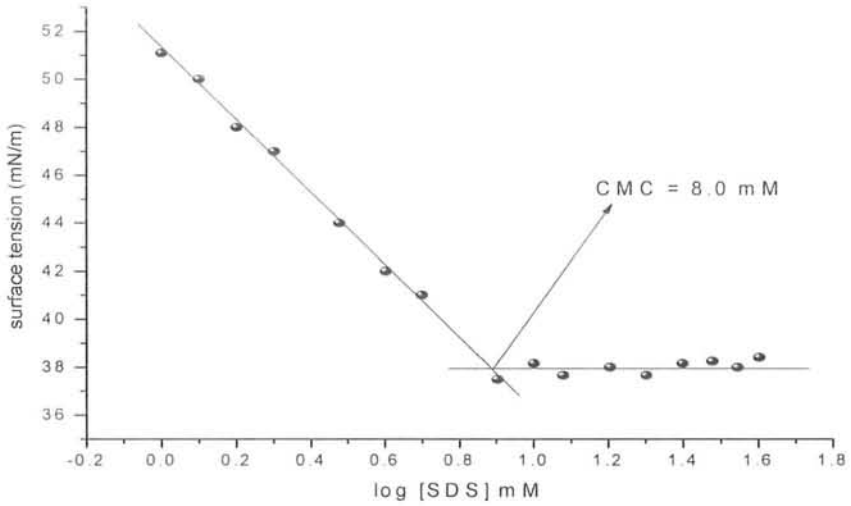

Fig 4.3: Semi log plot of surface tension vs. concentration of pure SDS at 303K.

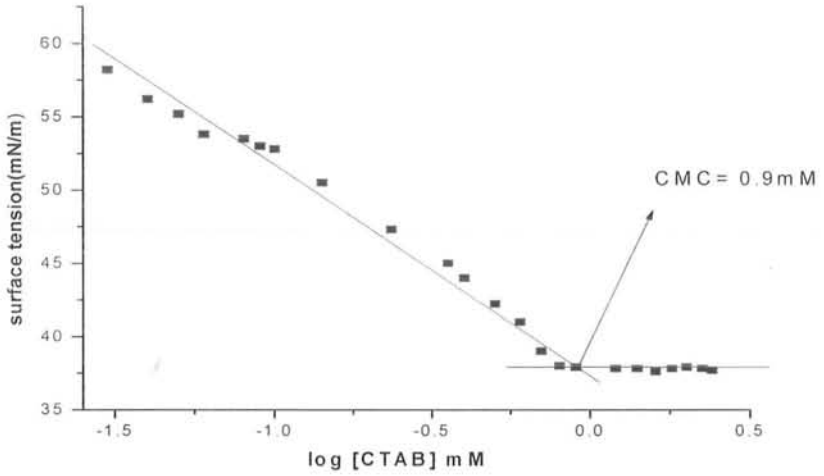

Fig 4.4: Semi log plot of surface tension vs. concentration of pure CTAB at 303K.

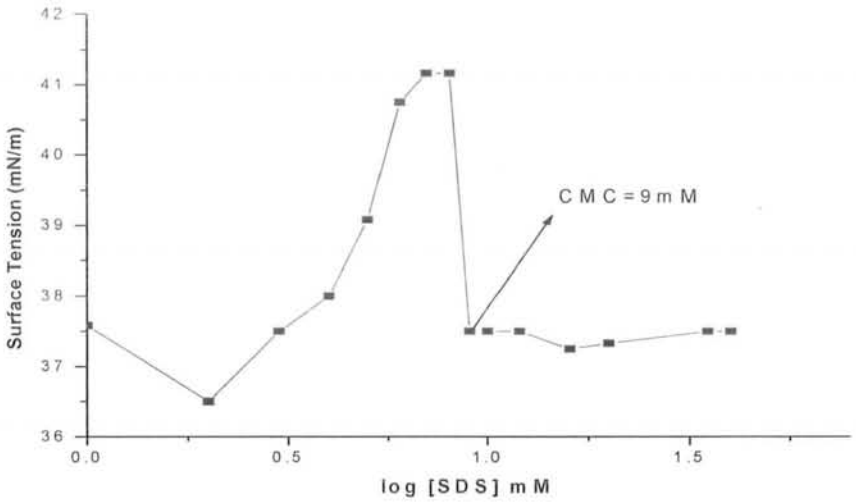

Fig 4.5: Semi log plot of surface tension vs. concentration of SDS in 0.1g/L $E_{30}B_{10}E_{30}$ at 303K.

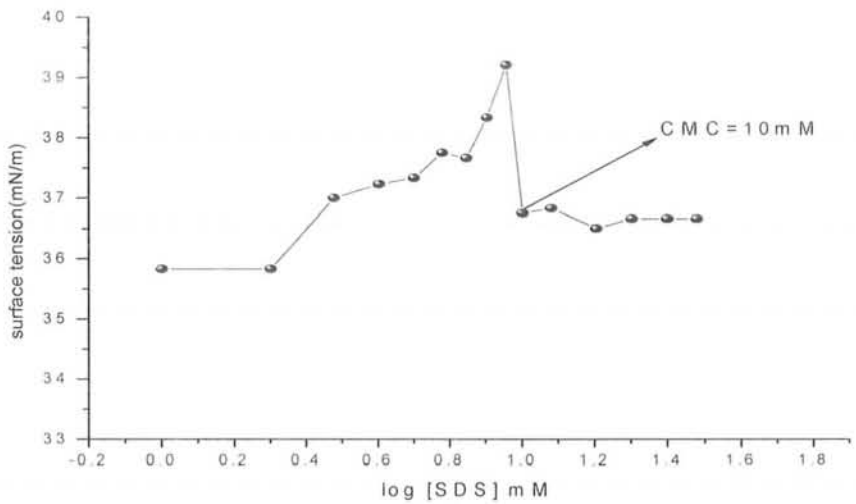

Fig 4.6: Semi log plot of surface tension vs. concentration of SDS in 2g/L $E_{30}B_{10}E_{30}$ at 303K.

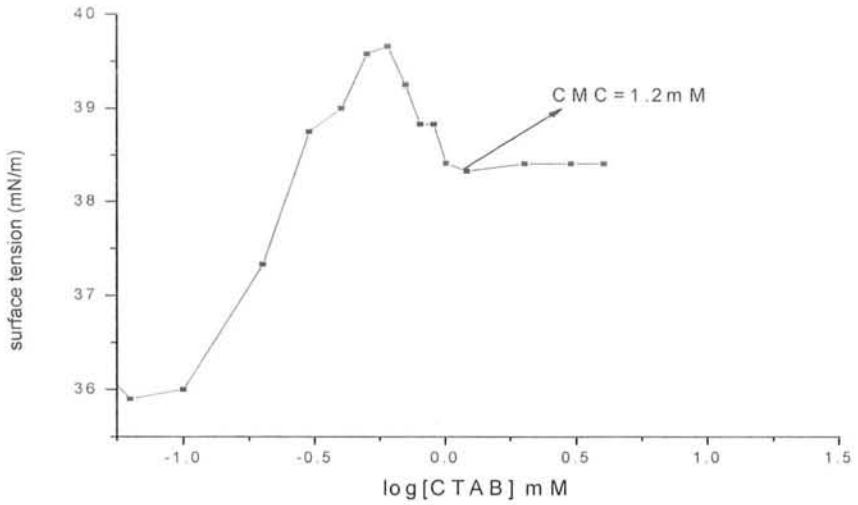

Fig 4.7: Semi log plot of surface tension vs. concentration of CTAB in 0.1g/L $E_{30}B_{10}E_{30}$ at 303K.

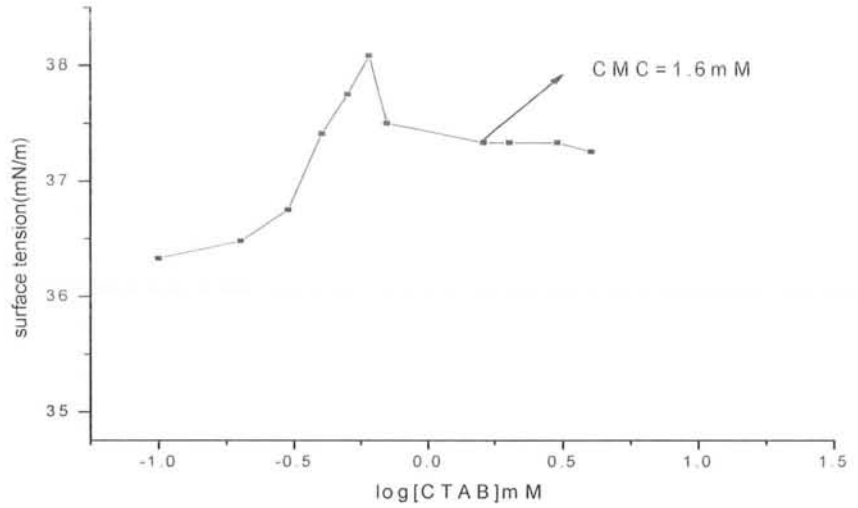

Fig 4.8: Semi log plot of surface tension vs. concentration of CTAB in 2g/L $E_{30}B_{10}E_{30}$ at 303K.

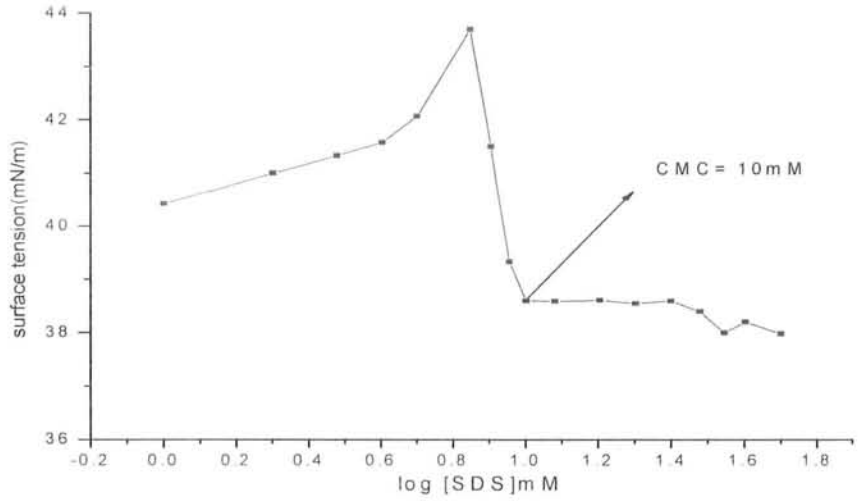

Fig 4.9: Semi log plot of surface tension vs. concentration of SDS in 0.1g/L $E_{48}B_{10}E_{48}$ at 303K.

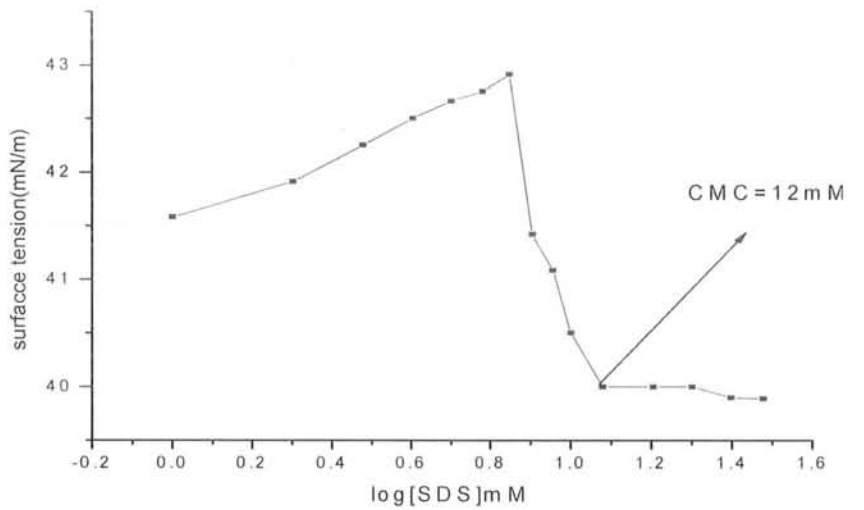

Fig 4.10: Semi log plot of surface tension vs. concentration of SDS in 2g/L $E_{48}B_{10}E_{48}$ at 303K.

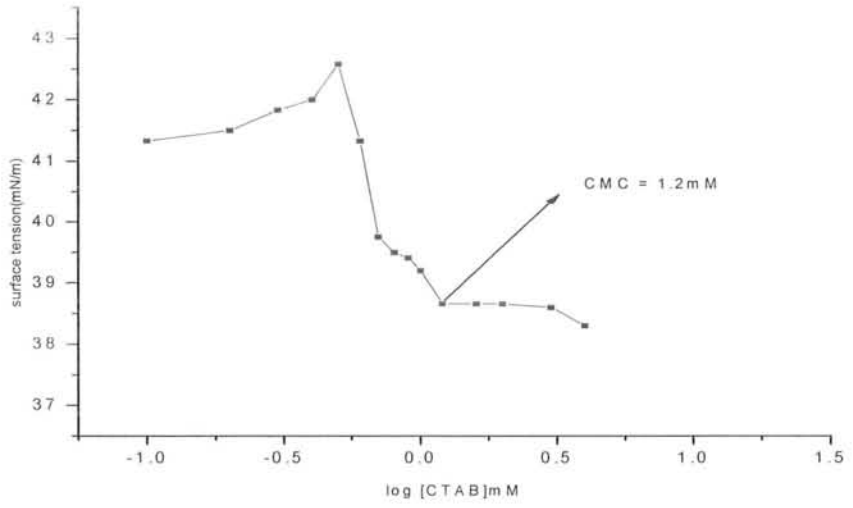

Fig 4.11: Semi log plot of surface tension vs. concentration of CTAB in 0.1g/L $E_{48}B_{10}E_{48}$ at 303K.

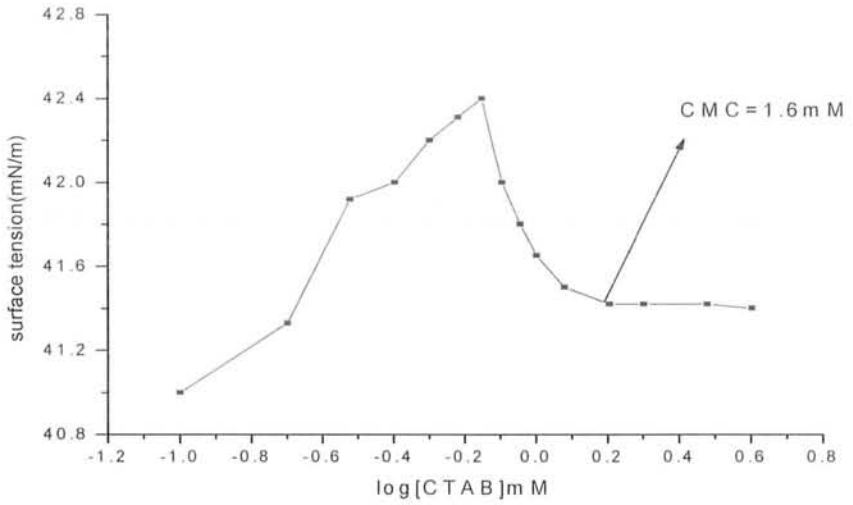

Fig 4.12: Semi log plot of surface tension vs. concentration for CTAB in 2g/L $E_{48}B_{10}E_{48}$ at 303K.

Table 4.1: CMC of the mixed system of SDS and CTAB with triblock $E_{30}B_{10}E_{30}$ and $E_{48}B_{10}E_{48}$ at 303k measured by surface tensiometry.

S.#	SAMPLE	CMC(mM)
01	SDS	8.0
02	$E_{30}B_{10}E_{30}$	0.238
03	$E_{48}B_{10}E_{48}$	0.189
04	SDS +0.1g/L $E_{30}B_{10}E_{30}$	9.0
05	SDS + 2.0g/L $E_{30}B_{10}E_{30}$	10.0
06	SDS + 0.1g/L $E_{48}B_{10}E_{48}$	10.0
07	SDS +2.0g/L $E_{48}B_{10}E_{48}$	12.0
08	CTAB	0.9
09	CTAB +0.1g/L $E_{30}B_{10}E_{30}$	1.20
10	CTAB + 2.0g/L $E_{30}B_{10}E_{30}$	1.60
11	CTAB+ 0.1g/L $E_{48}B_{10}E_{48}$	1.20
12	CTAB +2.0g/L $E_{48}B_{10}E_{48}$	1.60

4.2 Conductivity measurements

A. CMC

The CMC values were obtained for pure surfactants as well as for mixed systems of polymer/surfactant from the intersection of the two lines as shown in Figures 4.13 to 4.22. The CMC values obtained by conductivity are shown in Table 4.2. In the pre micellar region the conductivity is linearly increased with surfactant concentration but in post micellar region there is somewhat less increase in conductivity. Above the CMC, the rate of increase of conductivity is slow because micelles are being formed.

The increase in the conductance in pre micellar region is due to availability of free surfactant ions but in the post micellar region the movement of surfactant free ions are slow down due to interaction with polymer. This increase in conductance in the pre micellar region as compared to that in post micellar one is greater in case of SDS as compared to CTAB.

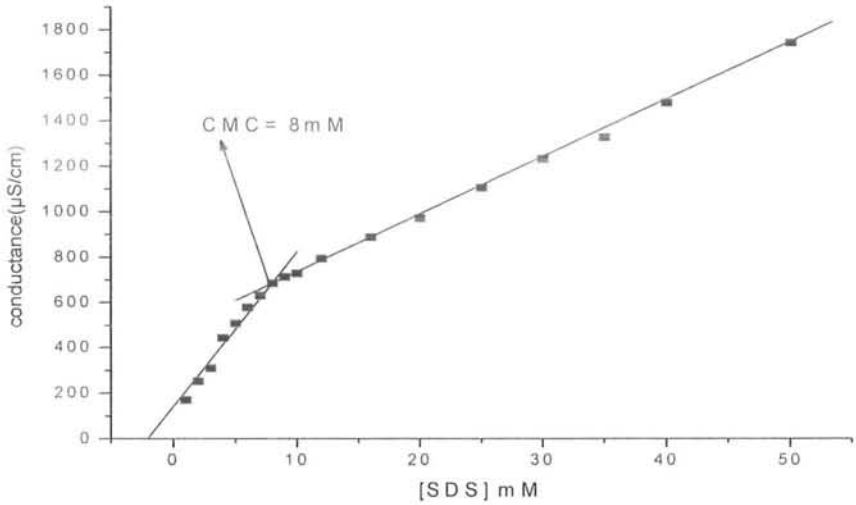

Fig 4.13: Conductance vs. concentration plot of pure SDS at 303K.

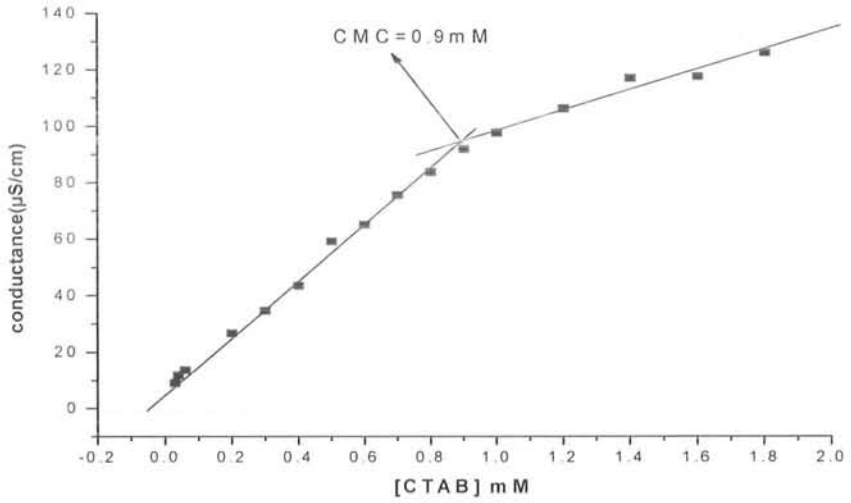

Fig 4.14: Conductance vs. concentration plot of pure CTAB at 303K.

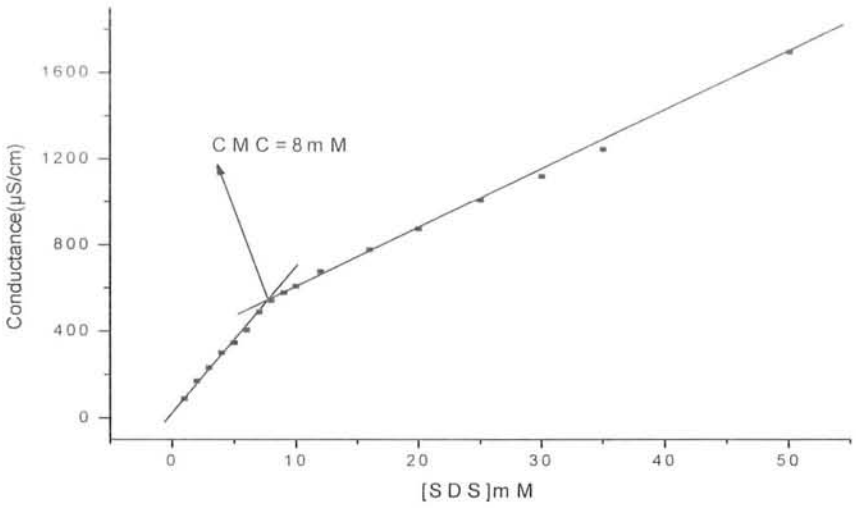

Fig 4.15: Conductance vs. concentration plot of SDS in 0.1g/L $E_{30}B_{10}E_{30}$ at 303K.

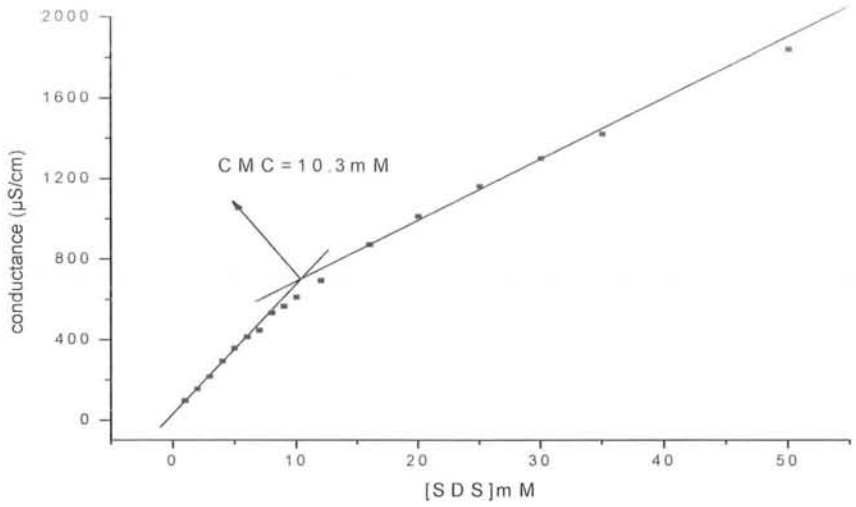

Fig 4.16: Conductance vs. concentration plot of SDS in 2g/L $E_{30}B_{10}E_{30}$ at 303K.

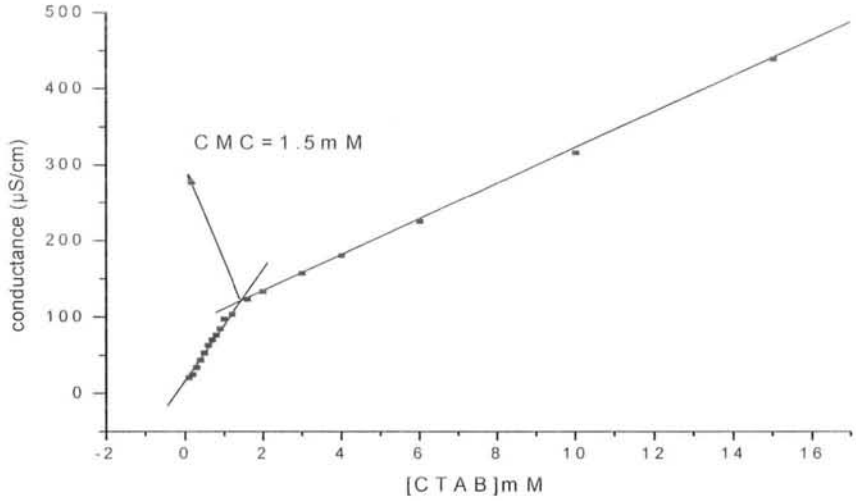

Fig 4.17: Conductance vs. concentration plot of CTAB in 0.1g/L $E_{30}B_{10}E_{30}$ at 303K.

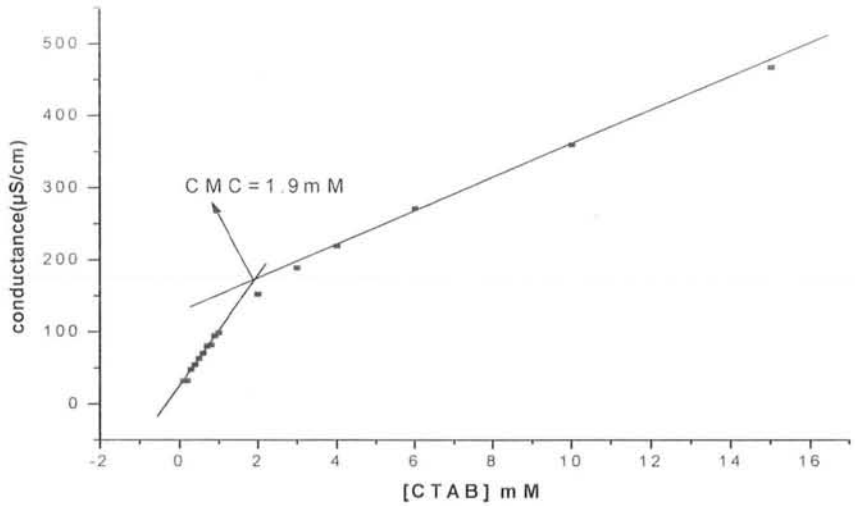

Fig 4.18: Conductance vs. concentration plot of CTAB in 2g/L $E_{30}B_{10}E_{30}$ at 303K.

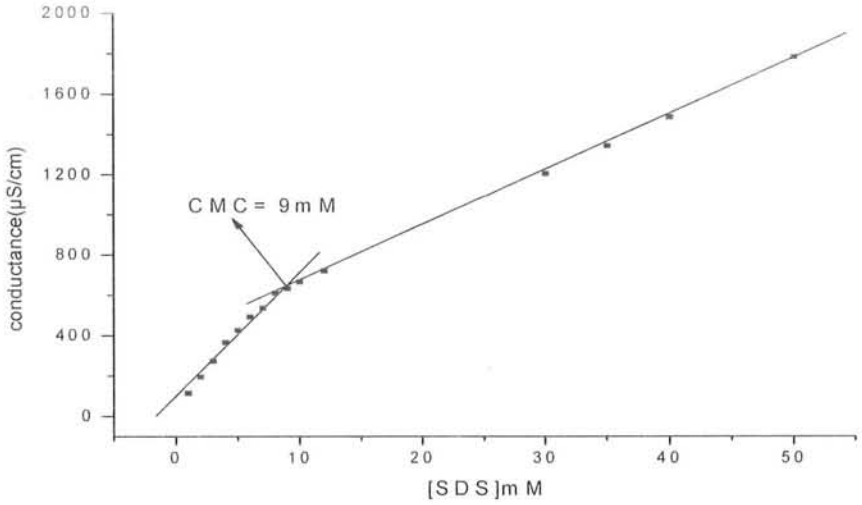

Fig 4.19: Conductance vs. concentration plot of SDS in 0.1g/L $E_{48}B_{10}E_{48}$ at 303K.

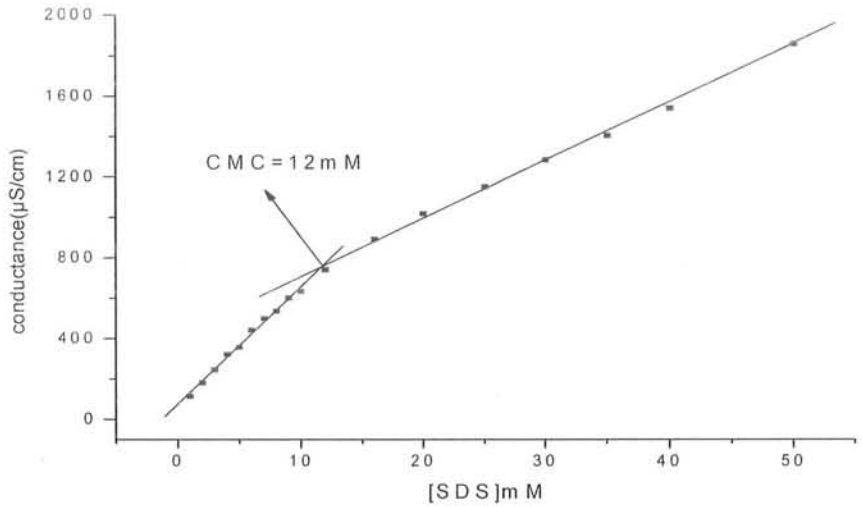

Fig 4.20: Conductance vs. concentration plot of SDS in 2g/L $E_{48}B_{10}E_{48}$ at 303K.

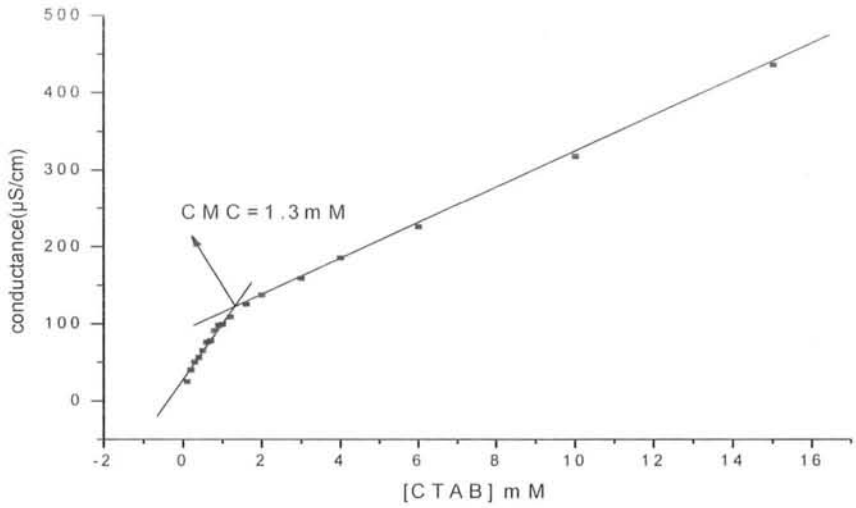

Fig 4.21: Conductance vs. concentration plot of CTAB in 0.1g/L $E_{48}B_{10}E_{48}$ at 303K.

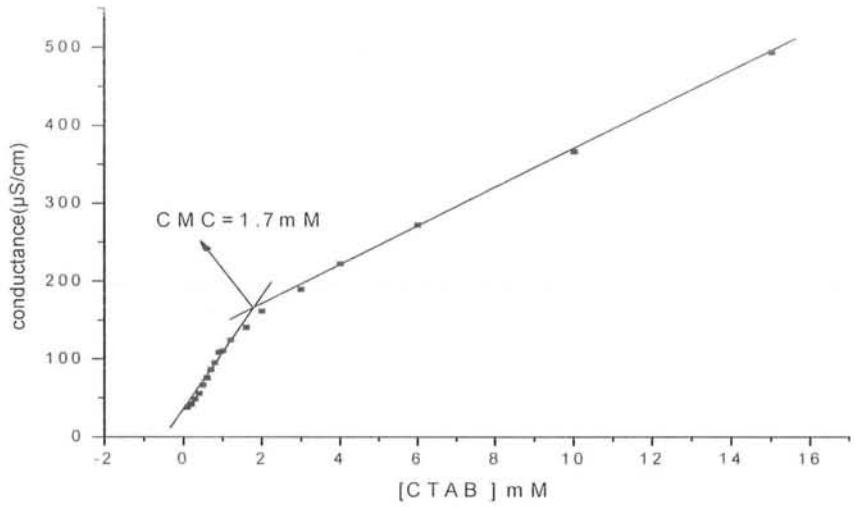

Fig 4.22: Conductance vs. concentration plot of CTAB in 2g/L $E_{48}B_{10}E_{48}$ at 303K.

Table 4.2: CMC of the mixed system of surfactants with Triblock copolymers at 303K by conductivity

S.#	SAMPLE	CMC (mM)
01	SDS	8.0
02	$E_{30}B_{10}E_{30}$	-----
03	$E_{48}B_{10}E_{48}$	-----
04	SDS +0.1g/L $E_{30}B_{10}E_{30}$	8.0
05	SDS + 2.0g/L $E_{30}B_{10}E_{30}$	10.30
06	SDS + 0.1g/L $E_{48}B_{10}E_{48}$	09.0
07	SDS +2.0g/L $E_{48}B_{10}E_{48}$	12.0
08	CTAB	0.9
09	CTAB +0.1g/L $E_{30}B_{10}E_{30}$	1.50
10	CTAB + 2.0g/L $E_{30}B_{10}E_{30}$	1.90
11	CTAB+ 0.1g/L $E_{48}B_{10}E_{48}$	1.30
12	CTAB +2.0g/L $E_{48}B_{10}E_{48}$	1.70

Table 4.3: Comparison of CMC by surface tensiometry and conductivity.

S.#	SAMPLE	CMC (mM) by surface tension	CMC(mM) by conductivity
01	SDS	8.0	8.0
02	$E_{30}B_{10}E_{30}$	0.238	-----
03	$E_{48}B_{10}E_{48}$	0.189	-----
04	SDS +0.1g/L $E_{30}B_{10}E_{30}$	9.0	8.0
05	SDS + 2.0g/L $E_{30}B_{10}E_{30}$	10.0	10.3
06	SDS + 0.1g/L $E_{48}B_{10}E_{48}$	10.0	9.0
07	SDS +2.0g/L $E_{48}B_{10}E_{48}$	12.0	12.0
08	CTAB	0.9	0.9
09	CTAB +0.1g/L $E_{30}B_{10}E_{30}$	1.2	1.5
10	CTAB + 2.0g/L $E_{30}B_{10}E_{30}$	1.6	1.9
11	CTAB+ 0.1g/L $E_{48}B_{10}E_{48}$	1.2	1.3
12	CTAB +2.0g/L $E_{48}B_{10}E_{48}$	1.6	1.7

B. Degree of Protonation or Degree of Ionization (α)

The degree of dissociation (degree of protonation) α, of the micelle was determined from the specific conductance vs. concentration of surfactant (mM) plots Figures 4.13 to 4.22. Actually, α is the ratio of the post micellar slope (S_1) to the pre micellar slope (S_2)[94] as shown in Figures 4.23 and 4.24.

$$\alpha = \frac{S1}{S2} \tag{2.2.3}$$

The degrees of ionization were calculated for pure SDS and CTAB are in closed agreement with literature reported values.[95, 96] The higher value obtained for Triblock copolymer/SDS system as compared to pure SDS shown in Table 4.4 by conductivity method supports the explanation that SDS micelles are responsible for the stronger rate enhancement effect observed in the rate constant vs. [SDS] profile.[97] It was previously reported that the increase in stabilization of the micellar charge stems from an increasing reduction of electrostatic repulsion. Especially at higher micellar charge, the formation of smaller polymer-bound micelles (confirmed from the Fluorescence data) will be favored, since electrostatic repulsion is diminished and the increase in hydrocarbon-water contact area is stabilized by the polymer.[98] In case of CTAB, the degree of ionization of mixed system is less than that of pure CTAB due to decrease in micellar charge and hence the size of the polymer-bound micelle remains greater than in case of SDS.

C. Degree of counter ion binding or counter ion association (β)

The degree of counter ion binding is obtained from the equation 2.2.4

$$\beta = 1 - \alpha \tag{2.2.4}$$

The degree of micelle charge neutralization (β) for SDS and CTAB were calculated from equation (2.2.4) which is in close agreement with literature reported value.[99,86] The values of β obtained for the mixtures of polymers and SDS were less than that of pure SDS, confirming that addition of polymer increase micellar ionization.[99]

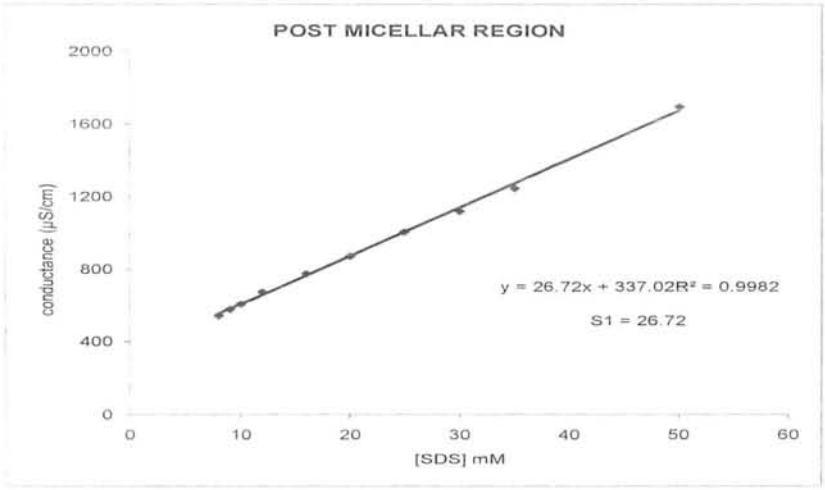

Fig 4.23: Slope of the post micellar region calculated from the plot of conductance vs. concentration of SDS in 0.1g/L $E_{30}B_{10}E_{30}$ at 303K.

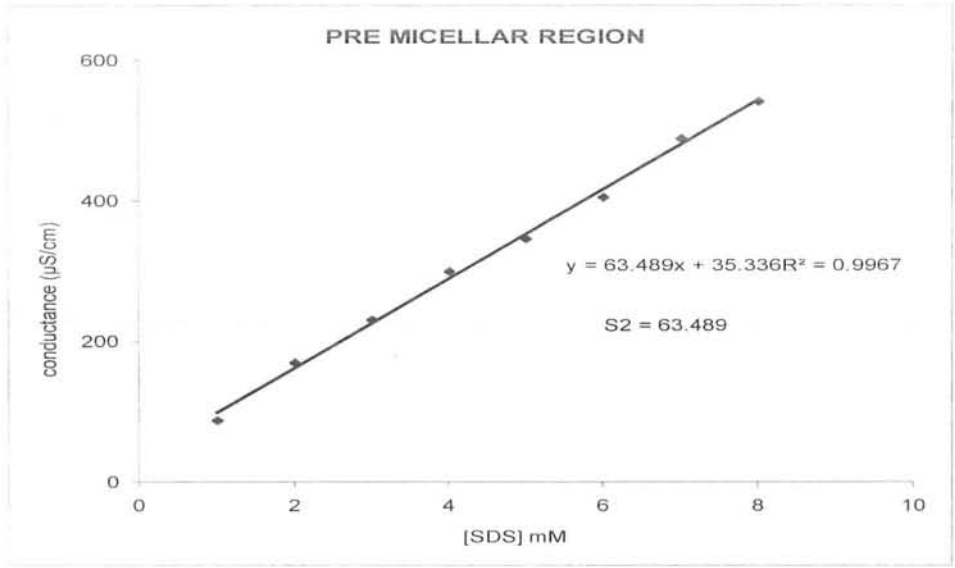

Fig 4.24: Slope of the pre micellar region calculated from the plot of conductance vs. concentration of SDS in 0.1g/L $E_{30}B_{10}E_{30}$ at 303K.

D. Free Energy of Micellization (ΔG_m)

The free energy of micellization for both pure surfactants and mixed systems obtained using equation (2.2.9)

$$\Delta G_m^{\circ} = (1+\beta)RT \ln Xcmc \qquad (2.2.9)$$

According to Table 4.4, the negative values of free energy of micellization show spontaneous process. The free energy of micellization in the presence of higher concentration of TBP was less negative as compared to pure surfactants. The free energy of micellization in the case of CTAB +TBP system is more negative as compare to SDS +TBP system prefer association of TBP among themselves than interacting with the surrounding CTAB monomers.[100] From these results of free energy of micellization it was concluded that SDS interacts strongly with TBP than CTAB.

Table 4.4: Degree of ionization (α), counter ion binding (β) and free energy of micellization (ΔG_m) for the mixed system of surfactant with triblock copolymer at 303K.

S.#	SAMPLE	α	β	ΔG_m(KJ/mol)
01	SDS	0.33	0.67	-37.21
02	$E_{30}B_{10}E_{30}$	-----	------	------
03	$E_{48}B_{10}E_{48}$	------	------	------
04	SDS +0.1g/L $E_{30}B_{10}E_{30}$	0.42	0.58	-35.20
05	SDS + 2g/L $E_{30}B_{10}E_{30}$	0.54	0.46	-31.60
06	SDS + 0.1g/L $E_{48}B_{10}E_{48}$	0.41	0.59	-34.95
07	SDS +2g/L $E_{48}B_{10}E_{48}$	0.50	0.50	-31.89
08	CTAB	0.38	0.62	-45.01
09	CTAB +0.1g/L $E_{30}B_{10}E_{30}$	0.32	0.68	-44.52
10	CTAB + 2g/L $E_{30}B_{10}E_{30}$	0.38	0.62	-41.96
11	CTAB+ 0.1g/L $E_{48}B_{10}E_{48}$	0.35	0.65	-44.32
12	CTAB +2g/L $E_{48}B_{10}E_{48}$	0.37	0.63	-42.68

4.3 Fluorescence Technique

Parameters Obtained from Fluorescence

A. Microenvironment

Pyrene is a spectroscopic probe that exhibits fluorescence emission spectrum consisting of five peaks. The I_1/I_3 ratio of this vibronic fine structures indicate the polarity of the pyrene micro environment and used for the detection of micelle as well as polymer-surfactant interactions.[101] The values of I_1/I_3 range from 1.9 in polar solvent to 0.6 in hydrocarbon. The bands I and III correspond to $S_1^{v=0} \rightarrow S_0^{v=0}(0,0)$ and $S_1^{v=0} \rightarrow S_0^{v=1}(0, 1)$ transitions. The decrease in the values of vibronic ratio (I_1/I_3) in the presence of TBP as compared to aqueous surfactant provides strong evidence for interaction of surfactant and TBP.[102] The smaller I_1/I_3 value in case of CTAB +TBP as compared to pure CTAB, suggests the presence of low micro polarity or higher hydrophobic environment. On the other hand in case of SDS + TBP, the I_1/I_3 values are greater than SDS+ H_2O suggests higher micro polarity or higher hydrophilic environment.[103] In case of either SDS or CTAB, the pyrene resides in the hydrophobic environment of complexes (produced as a result of surfactant /TBP interactions) compared to water. The effect of Cetyl Pyridinium Chloride (CPC) on the fluorescence intensity of the pyrene was also studied. The plot of fluorescence intensity versus wavelength (nm) Figures.4.25 to 4.34 shows spectral change of pyrene in the presence of varying concentrations of quencher. These plots show that as the quencher concentration increases the pyrene emission intensities decreases.

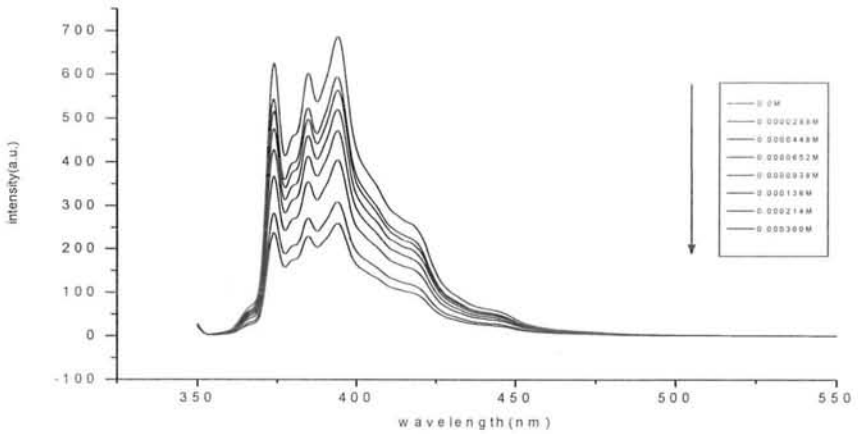

Fig. 4.25: Spectral change of pyrene emission spectrum in the presence of various concentrations of Quencher and fixed amount of 25mM SDS at 303K.

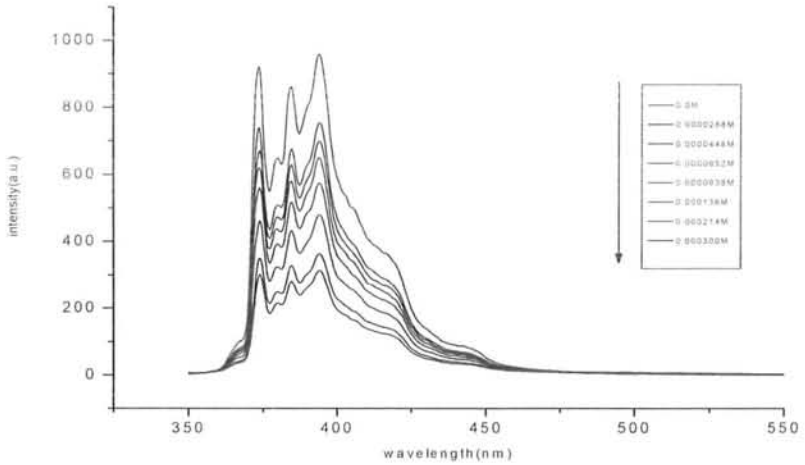

Fig 4.26: Spectral change of pyrene emission spectrum in the presence of various concentrations of Quencher and fixed amount of 25mM SDS and 0.1g/L $E_{30}B_{10}E_{30}$ at 303K.

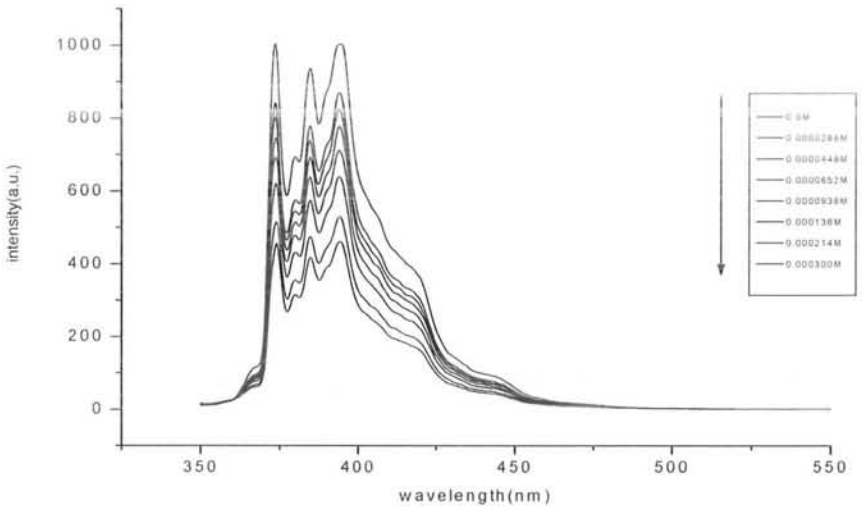

Fig 4.27: Spectral change of pyrene emission spectrum in the presence of various concentrations of Quencher and fixed amount of 25mM SDS and 2.0g/L $E_{30}B_{10}E_{30}$ at 303K.

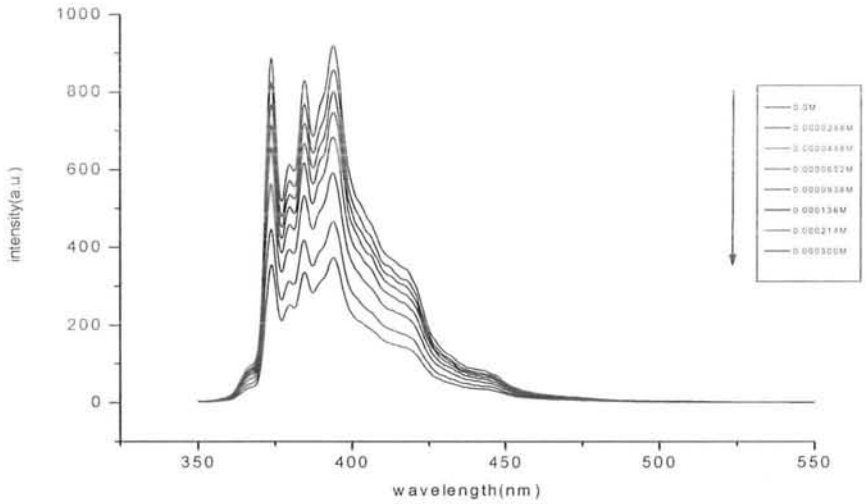

Fig 4.28: Spectral change of pyrene emission spectrum in the presence of various concentrations of Quencher and fixed amount of 25mM SDS and 0.1g/L $E_{48}B_{10}E_{48}$ at 303K.

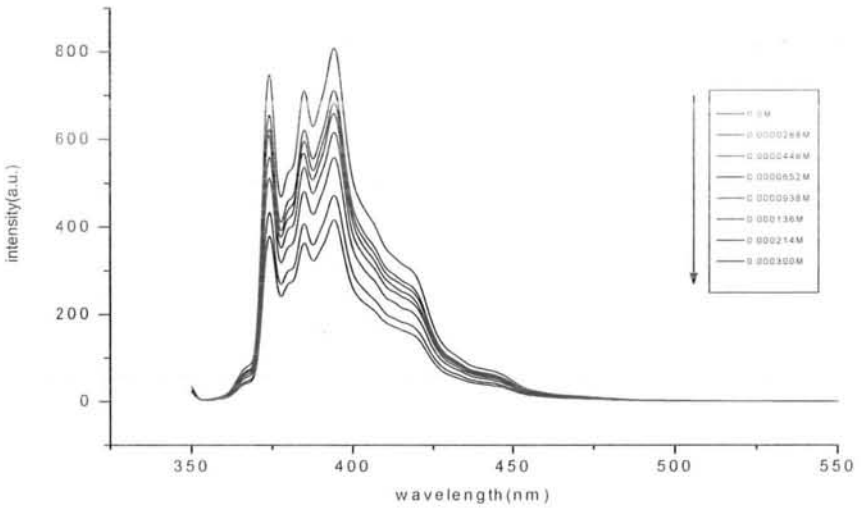

Fig 4.29: Spectral change of pyrene emission spectrum in the presence of various concentrations of Quencher and fixed amount of 25mM SDS and 2.0g/L $E_{48}B_{10}E_{48}$ at303K.

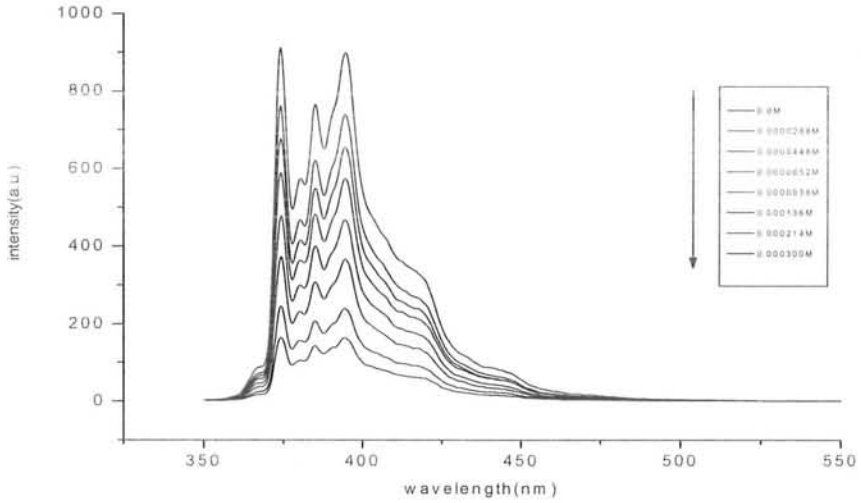

Fig 4.30: Spectral change of pyrene emission spectrum in the presence of various concentrations of Quencher and fixed amount of 15mM CTAB at 303K.

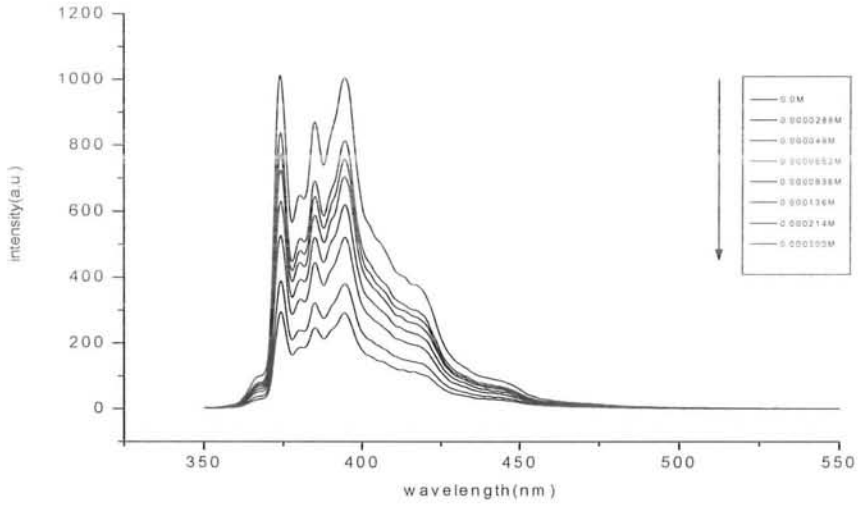

Fig 4.31: Spectral change of pyrene emission spectrum in the presence of various concentrations of Quencher and fixed amount of 15mM CTAB and 0.1g/L $E_{30}B_{10}E_{30}$at 303K.

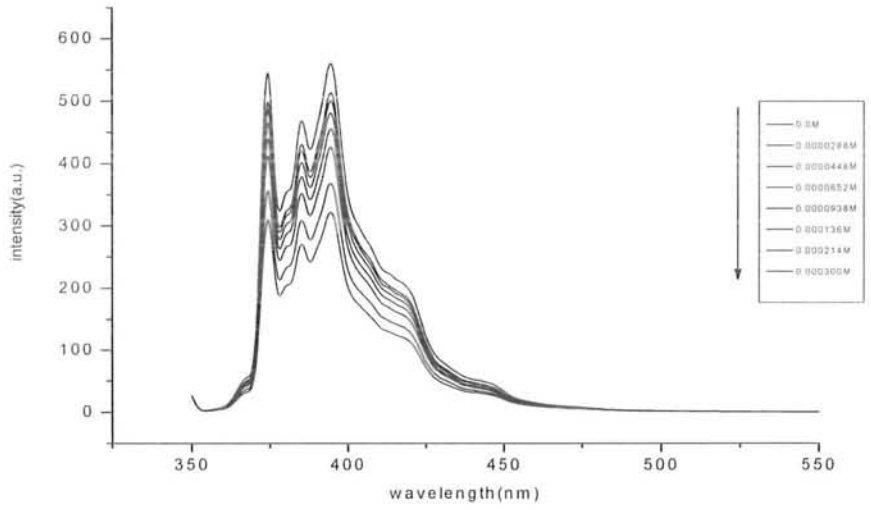

Fig 4.32: Spectral change of pyrene emission spectrum in the presence of various concentrations of Quencher and fixed amount of 15mM CTAB and 2.0g/L $E_{30}B_{10}E_{30}$at 303K.

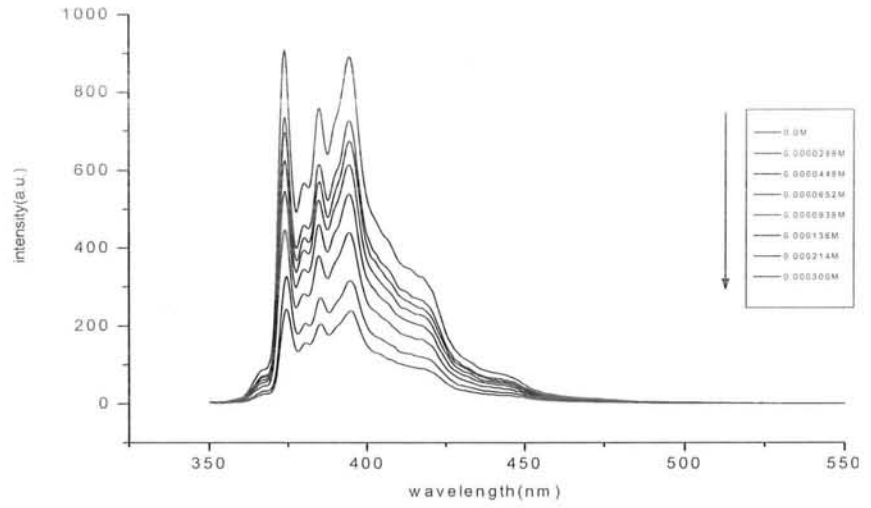

Fig 4.33: Spectral change of pyrene emission spectrum in the presence of various concentrations of Quencher and fixed amount of 15mM CTAB and 0.1g/L $E_{48}B_{10}E_{48}$ at 303K.

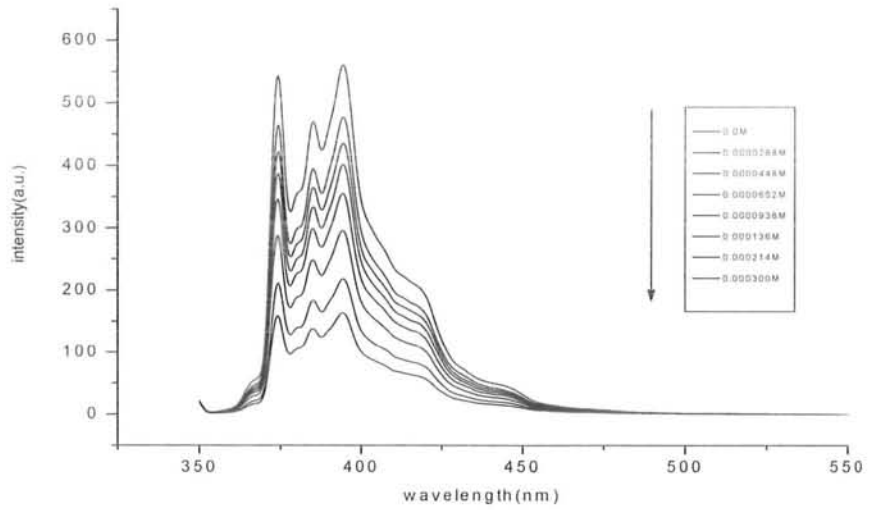

Fig 4.34: Spectral change of pyrene emission spectrum in the presence of various concentrations of Quencher and fixed amount of 15mM CTAB and 2.0g/L $E_{48}B_{10}E_{48}$ at 303K.

B. Aggregation Number (N_{agg})

The aggregation numbers of surfactant micelles, both in binary and ternary systems was measured by Static Fluorescence Quenching through the general method proposed by Turro and Yekta[104] in 1978. On the assumptions based on Tachiya[105] model, the aggregation number is determined from equation (2.3.8):

$$\ln \frac{I_o}{I_Q} = \frac{[Q]Nagg}{([S]-cmc)} \qquad (2.3.8)$$

From the slope of the plot of ln I_1/I_3 vs. [Q], the aggregation numbers both for binary and ternary systems were determined as shown in Figures 4.35 to 4.44.[106] The aggregation number calculated for SDS + H_2O, was 62 that agree well with the literature reported values 57 and 62.[107,108] Similarly the values of aggregation number calculated for CTAB + H_2O was 87 which is also in close agreement with literature reported values 80 and 95.[109,110] The aggregation numbers for ternary system i.e. surfactant + TBP (both surfactant and TBP micelles present) were determined in the same manner. According to an expectation that for highly polar polymers the aggregation numbers would be rather close to those in the absence of polymer, while for a non-polar polymer, the aggregation number is much lower.[111] In case of both SDS and CTAB, the aggregation numbers decreases which show interaction of surfactant with TBP. In this study the effect of block

copolymer architecture was also observed. It was generally believed that the aggregation numbers is influenced by the length of hydrophilic block. In our case the decrease in the aggregation number of $E_{48}B_{10}E_{48}$ is greater than $E_{30}B_{10}E_{30}$ because in the former case the hydrophilic block length is greater. This can also be explained on the basis of polymer hydrophobic/hydrophilic ratio. The aggregation number decreases with decrease in the hydrophobic/hydrophilic ratio.[112] In case of $E_{30}B_{10}E_{30}$; the hydrophobic/hydrophilic ratio is 0.166 which is greater than the same value for $E_{48}B_{10}E_{48}$ that is 0.104.

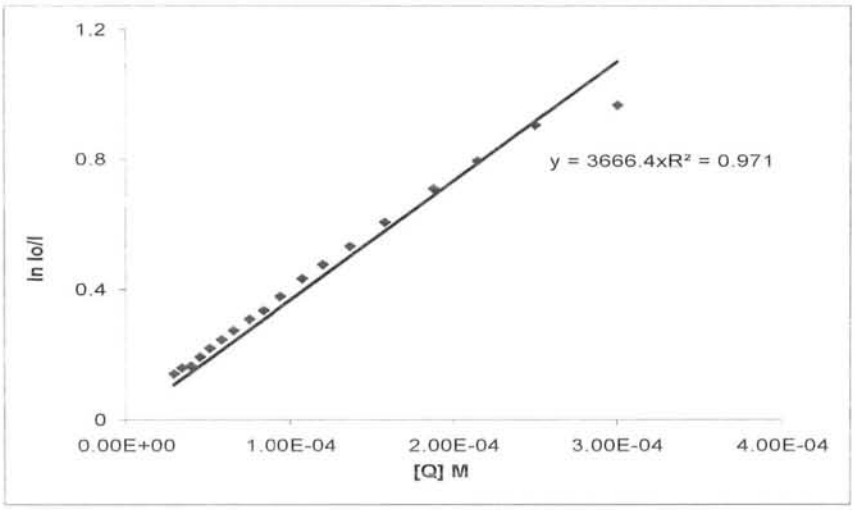

Fig 4.35: Plot of Q [M] vs. ln Io/I for pure 25mM SDS aqueous solution at 303K

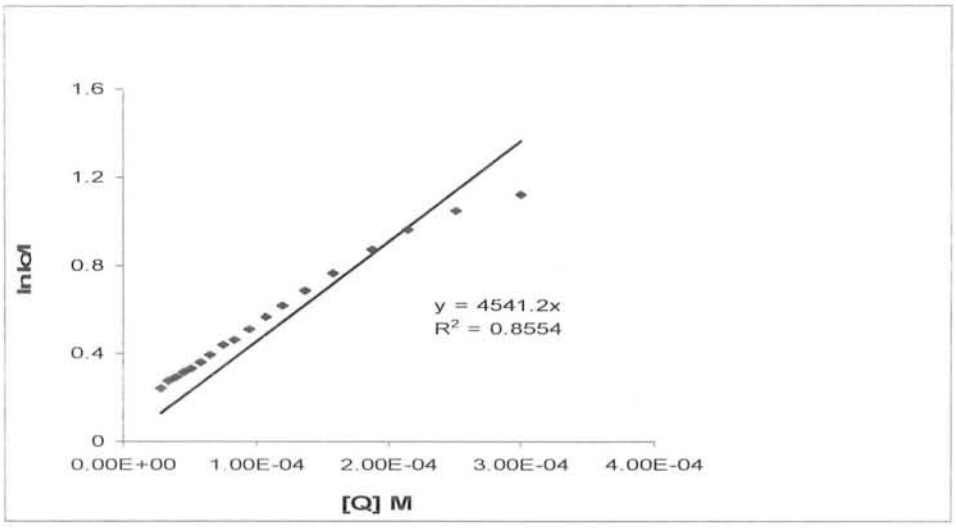

Fig 4.36: Plot of Q [M] vs. ln Io/I for 0.1g/L $E_{30}B_{10}E_{30}$ and 25mM SDS at 303K.

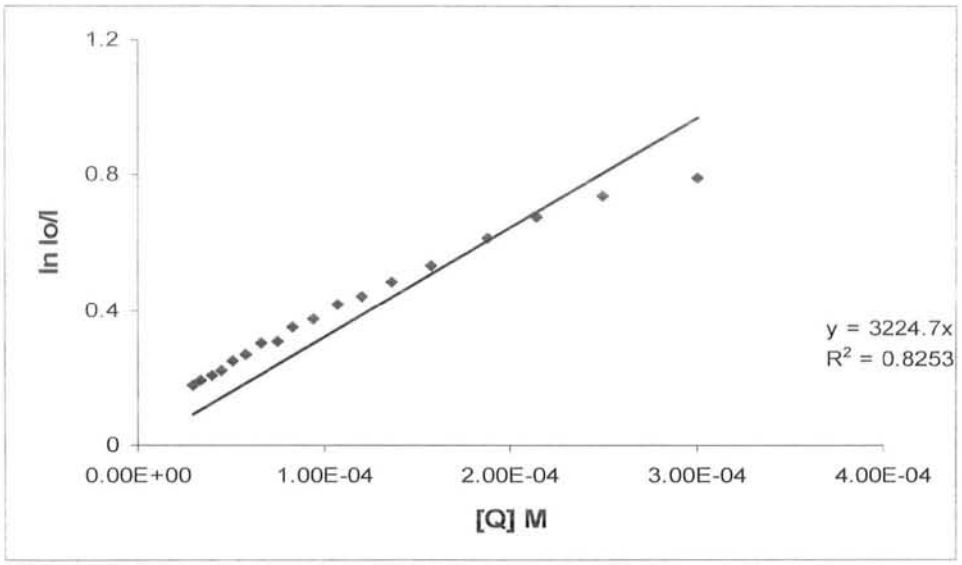

Fig 4.37: Plot of Q [M] vs. ln Io/I for 2g/L $E_{30}B_{10}E_{30}$ and 25mM SDS at 303K

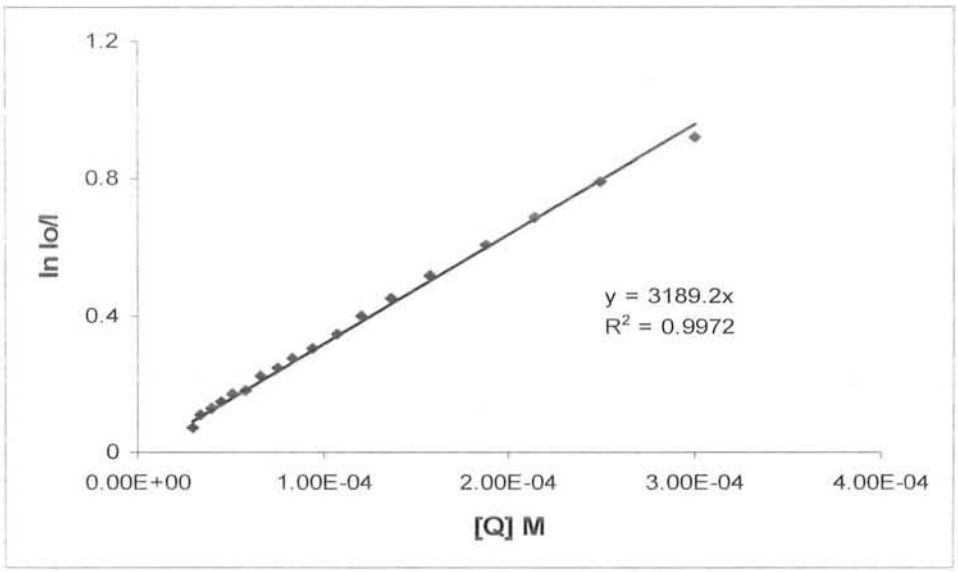

Fig 4.38: Plot of Q [M] vs. ln Io/I for 0.1g/L $E_{48}B_{10}E_{48}$ and 25mM SDS at 303K.

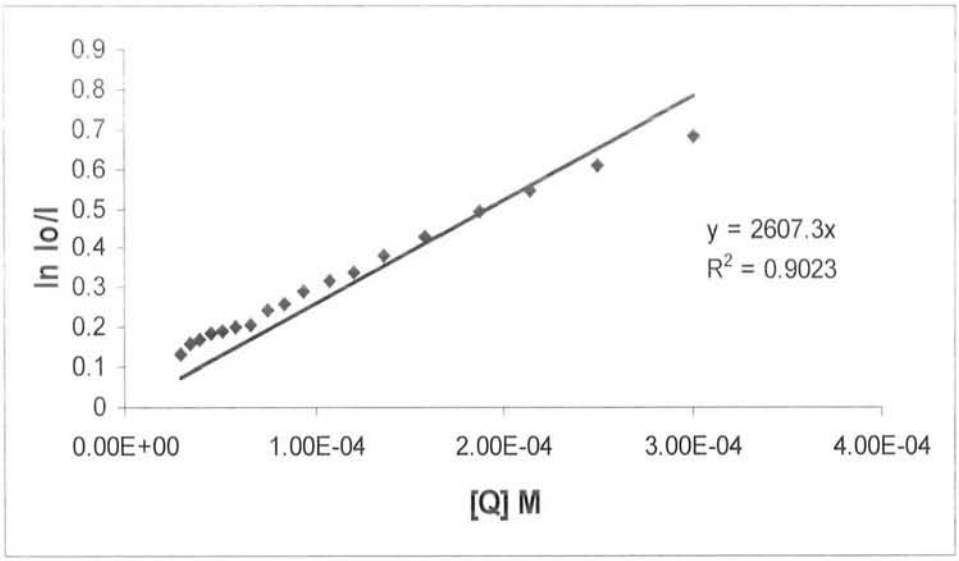

Fig 4.39: Plot of Q [M] vs. ln Io/I for 2g/L $E_{48}B_{10}E_{48}$ and 25mM SDS at 303K

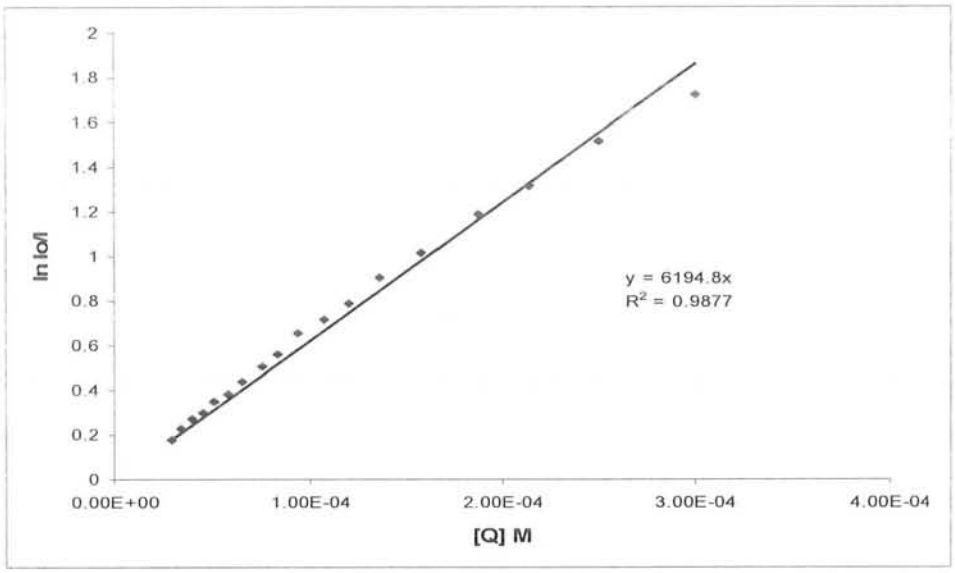

Fig 4.40: Plot of Q [M] vs. ln Io/I for 15mM pure CTAB aqueous solution at 303K.

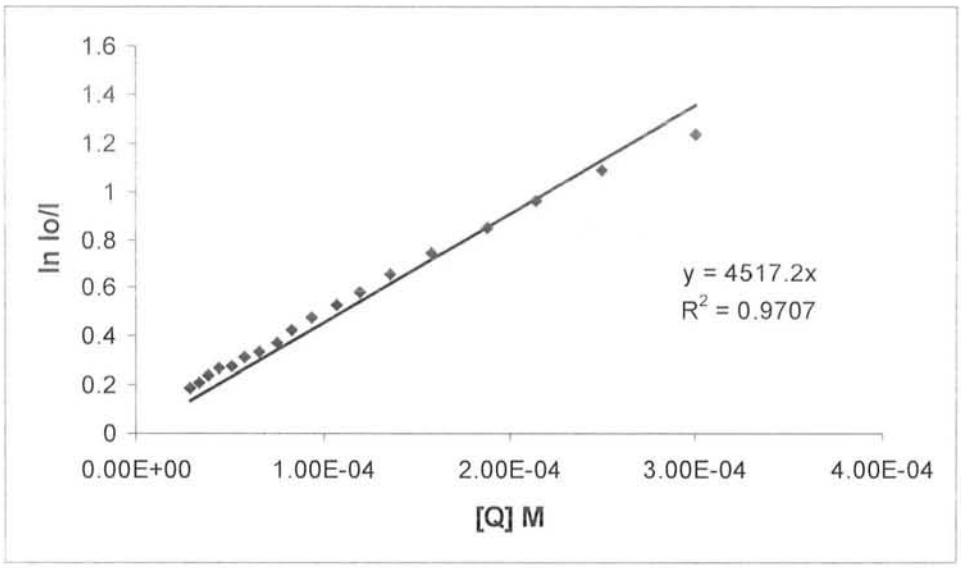

Fig 4.41: Plot of Q [M] vs. ln Io/I for 0.1g/L $E_{30}B_{10}E_{30}$ and 15mM CTAB at 303K.

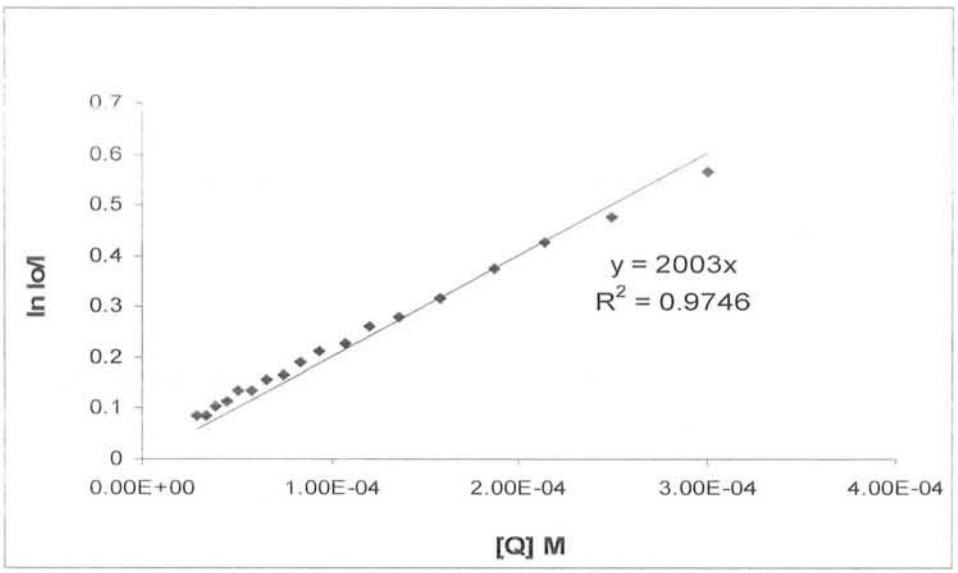

Fig 4.42: Plot of Q [M] vs. ln Io/I for 2g/L $E_{30}B_{10}E_{30}$ and 15mM CTAB at 303K.

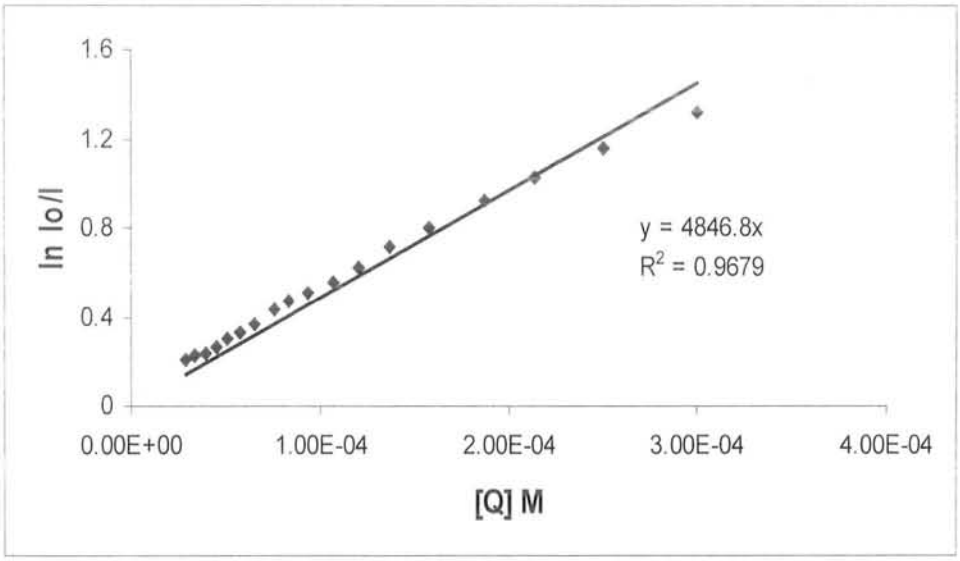

Fig 4.43: Plot of Q [M] vs. ln Io/I for 0.1g/L $E_{48}B_{10}E_{48}$ and 15mM CTAB at 303K.

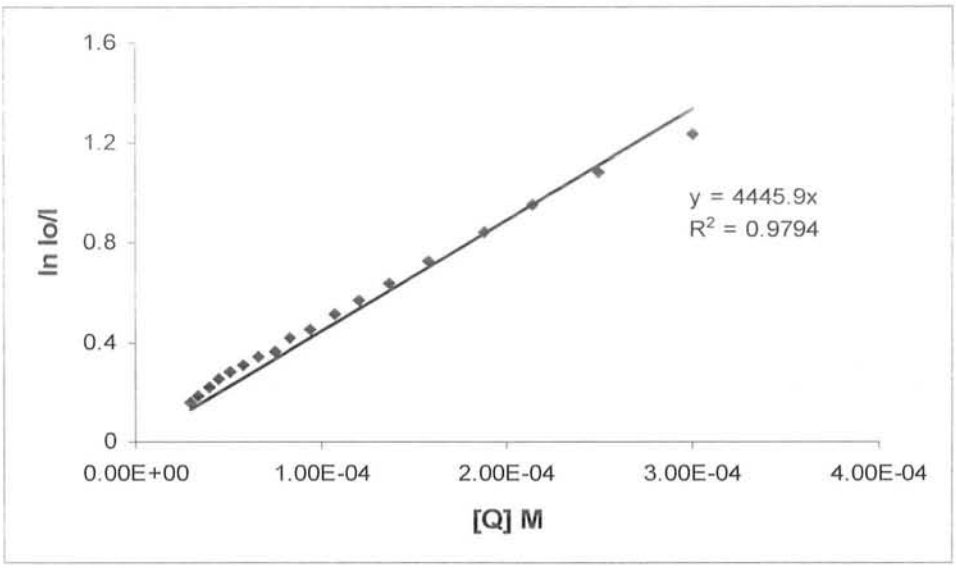

Fig 4.44: Plot of Q [M] vs. ln Io/I for 2g/L $E_{48}B_{10}E_{48}$ and 15mM CTAB at 303K.

C. **Binding Sites (n).**

The binding sites were calculated using equation 2.3.9

$$\log(\frac{Io-I}{I}) = \log kb + n\log[Q] \qquad (2.3.9)$$

The values of n were calculated from the slope of the plot of log $(I_o\text{-}I)/I$ vs. [Q] as shown in Figures 4.45 to 4.54 .The values of n were approximately equal to unity which indicates that the association of surfactant monomer with TBP micelles is in 1:1 ratio.[100] The positive values of n signifies that the interaction of surfactant with the corresponding TBP is by desorption process.[94]

D. **Binding Constant (K_b)**

The binding constant (K_b) were calculated from the intercept of the plot of $\log(\frac{I_o - I_Q}{I_Q})$ vs. [Q] using equation 2.3.9.

E. **Free Energy of Binding (ΔG_b)**

The free energy of binding can be calculated from equation (2.3.10) given as

$$\Delta G_b = -RT\ln K_b \qquad (2.3.10)$$

A negative value of ΔG_b for all systems indicates spontaneity of process.

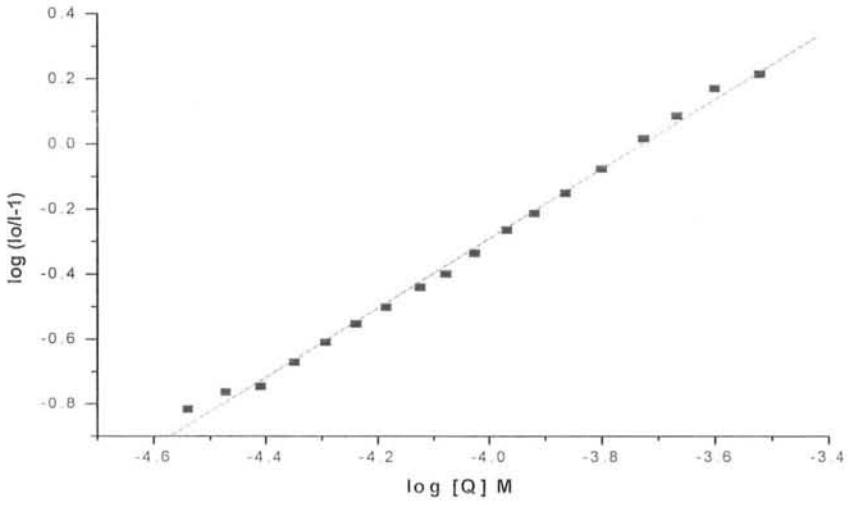

Fig 4.45: Plot of log Q [M] vs. log (Io/I-1) for 25mM pure SDS at 303K.

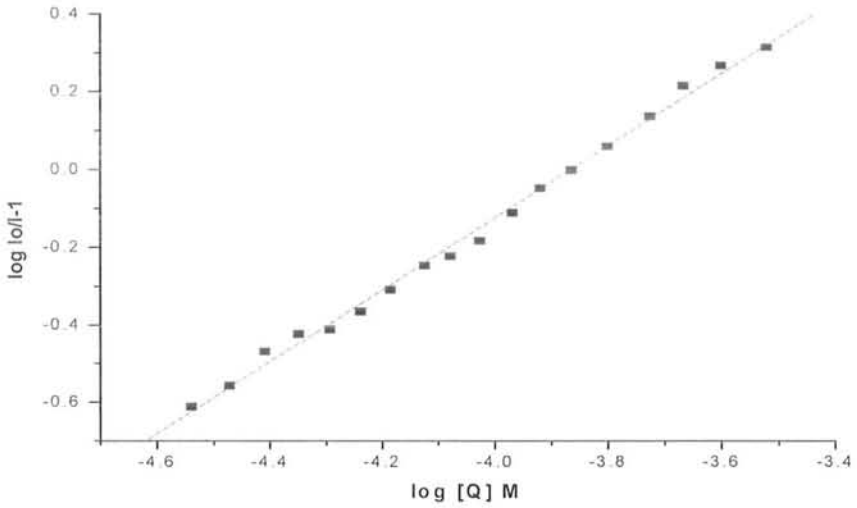

Fig 4.46: Plot of log Q [M] vs. log (Io/I-1) for 0.1g/L $E_{30}B_{10}E_{30}$ and 25mM SDS at303K.

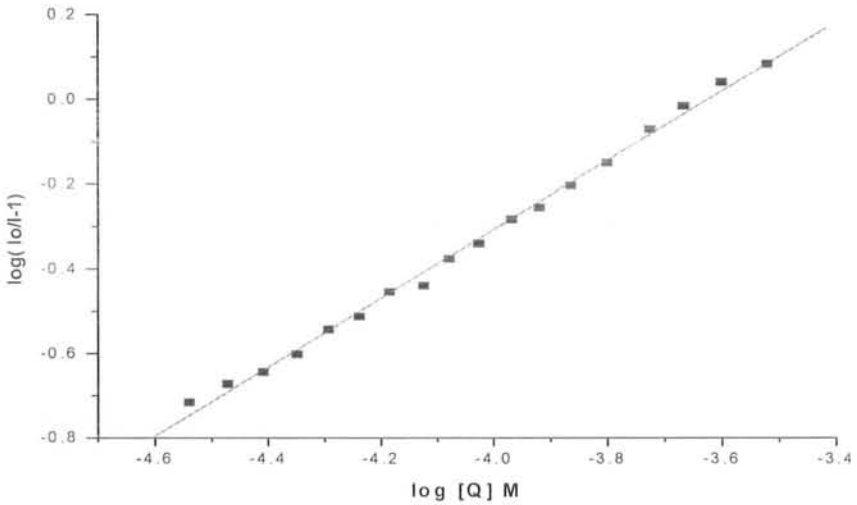

Fig 4.47: Plot of log Q [M] vs. log (Io/I-1) for 2g/L $E_{30}B_{10}E_{30}$ and 25mM SDS at 303K.

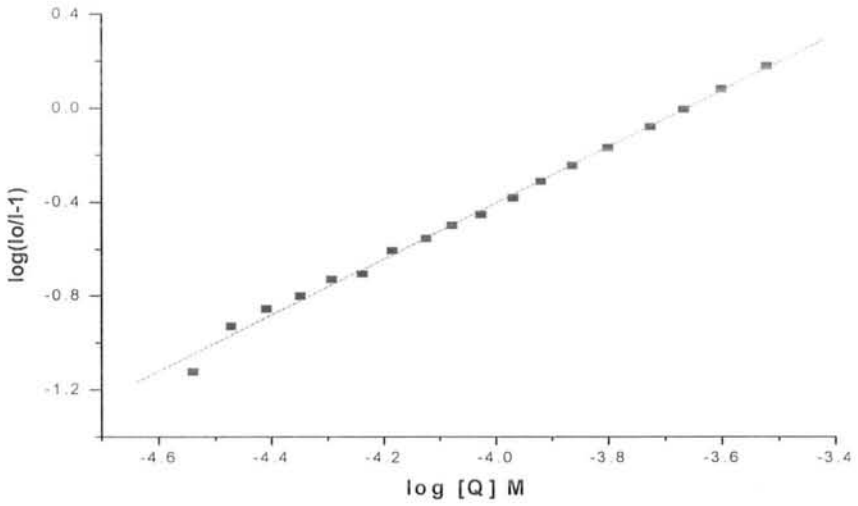

Fig 4.48: Plot of log Q [M] vs. log (Io/I-1) for 0.1g/L $E_{48}B_{10}E_{48}$ and 25mM SDS at 303K.

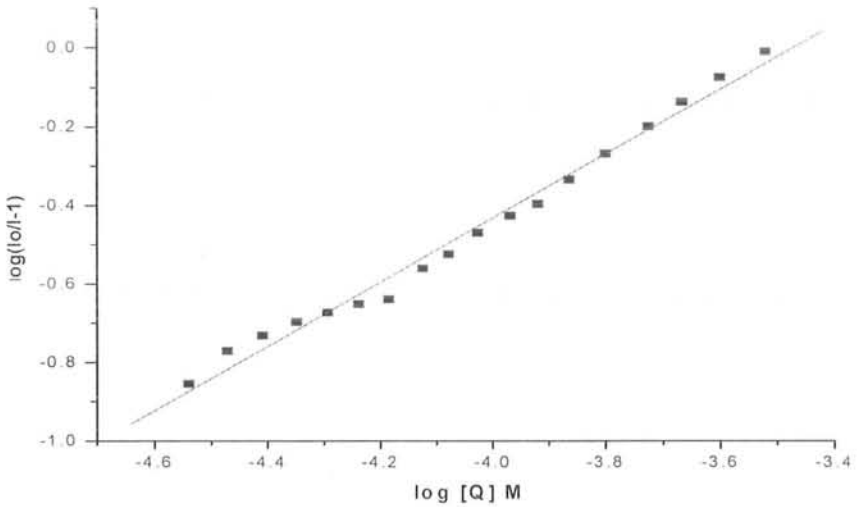

Fig 4.49: Plot of log Q [M] vs. log (Io/I-1) for 2g/L $E_{48}B_{10}E_{48}$ and 25mM SDS at 303K.

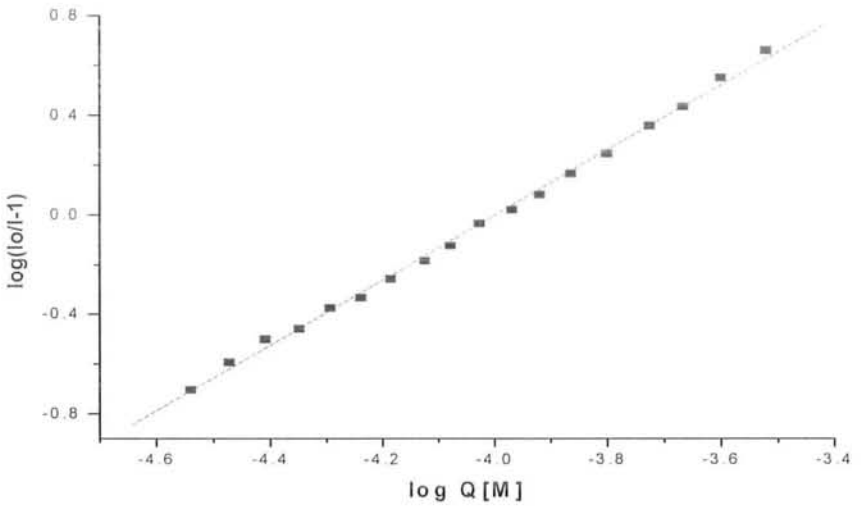

Fig 4.50: Plot of log Q [M] vs. log (Io/I-1) for 15mM pure CTAB at 303K.

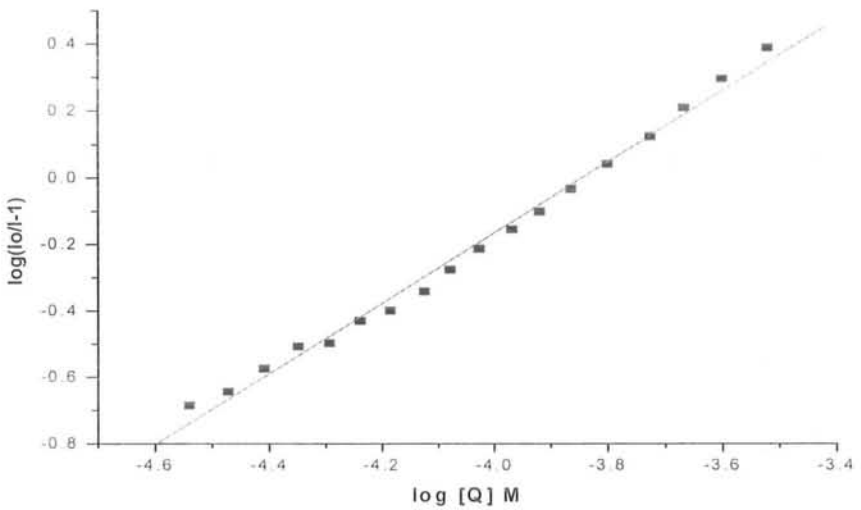

Fig 4.51: Plot of log Q [M] vs. log (Io/I-1) for 0.1g/L $E_{30}B_{10}E_{30}$ and 15mM CTAB at 303K.

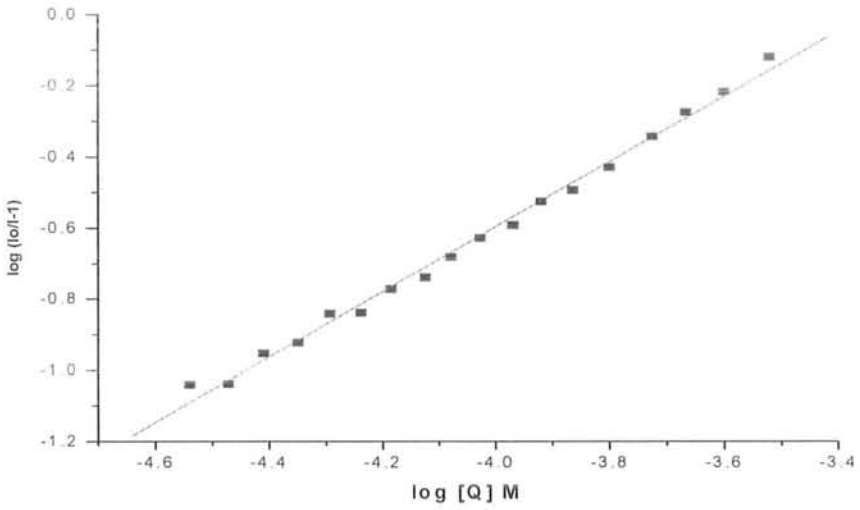

Fig 4.52: Plot of log Q [M] vs. log (Io/I-1) for 2g/L $E_{30}B_{10}E_{30}$ and 15mM CTAB at 303K.

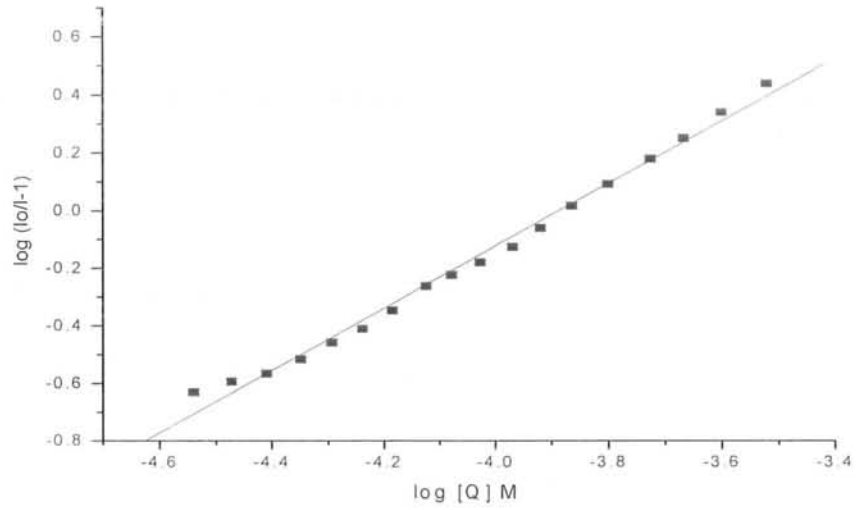

Fig 4.53: Plot of log Q [M] vs. log (Io/I-1) for 0.1g/L $E_{48}B_{10}E_{48}$ and 15mM CTAB at 303K.

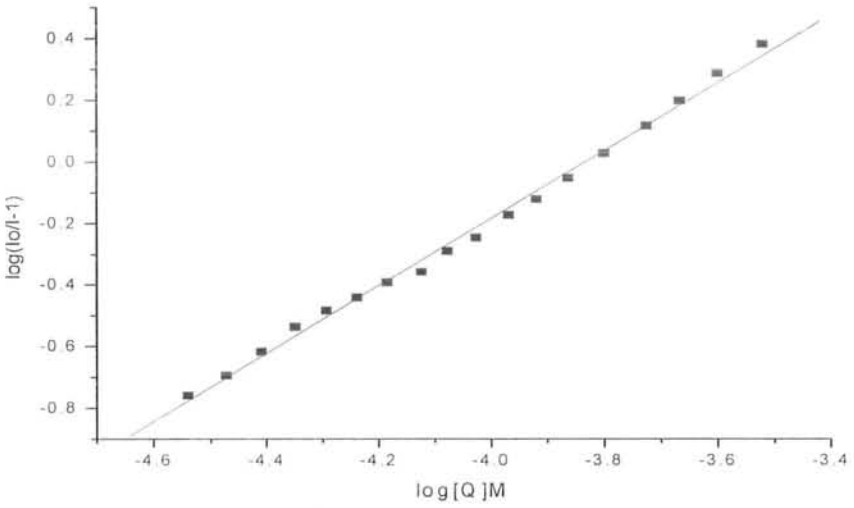

Fig 4.54: Plot of log Q [M] vs. log (Io/I-1) for 2 g/L $E_{48}B_{10}E_{48}$ and 15mM CTAB at 303K.

Table 4.5: Parameters obtained from static fluorescence spectroscopy

S.#	Sample	Conc.	I_1/I_3	N_{agg}	n	ΔG_b(KJ/mol)	K_b
01	SDS	25mM	1.04	62	1	-23.06	9473.9
02	SDS+$E_{30}B_{10}E_{30}$	25mM+2g/L	1.07	55	1	-17.17	913.88
03	SDS+$E_{48}B_{10}E_{48}$	25mM+0.1g/L	1.07	54	1	-25.49	24801.6
04	SDS+$E_{48}B_{10}E_{48}$	25mM+2g/L	1.06	44	1	-16.51	702.26
05	CTAB	15mM	1.20	87	1	-30.46	179023.4
06	CTAB+$E_{30}B_{10}E_{30}$	15mM+0.1g/L	1.17	64	1	-23.70	12219.6
07	CTAB+$E_{30}B_{10}E_{30}$	15mM+2g/L	1.16	28	1	-17.85	1197.62
08	CTAB+$E_{48}B_{10}E_{48}$	15mM+0.1g/L	1.2	68	1	-24.41	16178.9
09	CTAB+$E_{48}B_{10}E_{48}$	15mM+2g/L	1.15	62	1	-24.53	16941.4

4.4 Dynamic Laser Light Scattering

Fig. 4.55 shows the intensity fraction distribution of the apparent hydrodynamic radius (R_h) of 3.0g/dm^3 $E_{30}B_{10}E_{30}$ aqueous solution with various SDS concentrations ranging from 0.01M to 0.15M. This figure shows multimodal distribution for $E_{30}B_{10}E_{30}$-SDS system.[61] The hydrodynamic radius of pure $E_{30}B_{10}E_{30}$ micelles with R_h = 6.0 nm. Initially at very low surfactant concentration, 0.01M-0.05M, the apparent hydrodynamic radii of the polymer micelles remains invariable indicating weak interaction between polymer micelle and surfactant monomer with no disruption in their structures.[113] Further loading of SDS, from 0.06M to 0.1M, leads to decrease in the R_h of the polymeric micelles till1.0 nm. This decrease in size is due to increase in the amount of negatively charged head group (degree of ionization increases confirm from conductivity data table 4.3) in the copolymer micelles by avoiding the SDS direct contact with water due to their hydrophobicity. Due to unfavorable environment for SDS in water, it penetrates into the core of the polymer micelle. The head groups repulsion of SDS inside the core of the polymer micelle cause disruption of the polymer structure allowing water penetration, and thus gives rise to a less dense packing of the micelle, resulting in decrease in the aggregation number.[113] (Fluorescence work Table 4.5) Within this concentration range we also observed other peaks with higher R_h values in the range of 50-60nm which correspond to the mixed micelles of block copolymer and SDS with larger aggregation number. Increase in the concentration of surfactant equal or greater than 0.1M causes formation of regular surfactant micelles which remain stable up to 0.15M. The mechanism proposed[61] for the above system is that initially at low surfactant concentration the surfactant hydrophobic tail start binding with block copolymer hydrophobic part (unassociated form), followed by the formation of polymer-surfactant complexes which break down on further loading of surfactant and regular micelles of surfactant are produced.

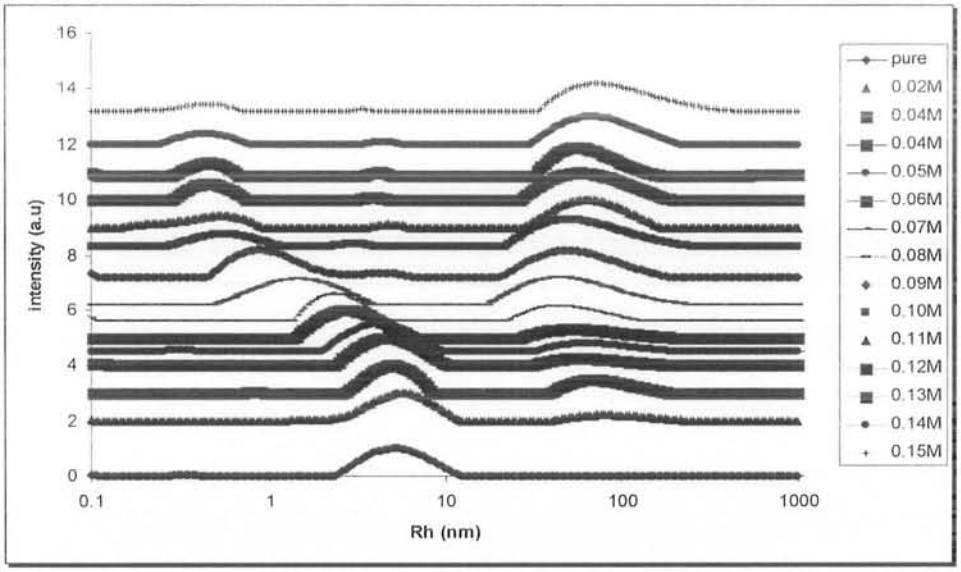

Fig 4.55: Normalized intensity fraction distributions of apparent hydrodynamic radius (R_h) for aqueous solutions of $E_{30}B_{10}E_{30}$-SDS complexes (copolymer concentration was kept constant i.e. 3g/dm^3) at 303K.

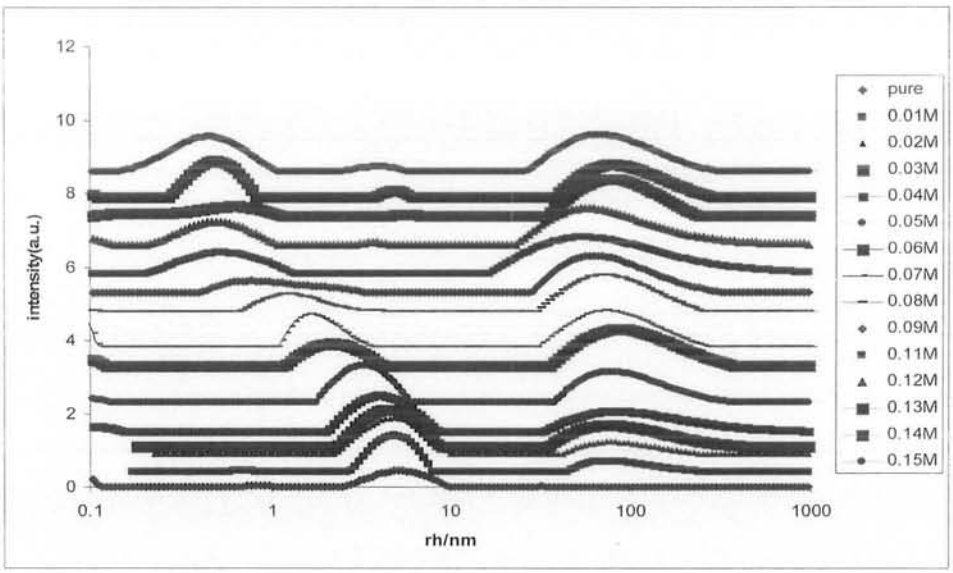

Fig 4.56: Normalized intensity fraction distribution of apparent hydrodynamic radius (Rh) for aqueous solutions of $E_{20}B_{10}E_{20}$-SDS complexes (copolymer concentration was kept constant i.e. 3g/dm^3) at 303K.

CONCLUSIONS

1. CMC increase both in case of SDS and CTAB but increase in the presence of concentrated polymer solutions are more as compare to dilute polymer solutions.

2. Degree of ionization increase in the case of SDS + TBP as compare to CTAB + TBP.

3. Degree of counter ion binding in case of SDS + TBP decrease as compare to CTAB+ TBP.

4. Increase of free energies of micellization both in the case of SDS + TBP and CTAB + TBP is observed.

5. Aggregation numbers decrease both in the case of SDS + TBP and CTAB + TBP but greater decrease observed in the case of $E_{48}B_{10}E_{48}$ + surfactants.

6. The unit values of binding sites both for SDS + TBP and CTAB + TBP confirm the association of surfactant monomer with TBP micelles in 1:1 ratio.

7. The free energies of binding both for SDS + TBP and CTAB + TBP shows similar trend as that for free energies of micellization of the same systems.

8. The hydrodynamic radius of the polymeric micelles decrease with increase in the surfactant concentrations confirming the strong interactions of surfactant with TBP.

REFERENCES

REFERENCES

1. Swarbrick, J.; Boylan, J.C.; *Encyclopedia of pharmaceutical technology* ISBN 0-8247-2824-6 volume 3 third edition **2000**.
2. Cosgrove, T.; *Colloidal science principles, methods and applications* ISBN-13:978-14051-2673-1 **2005**.
3. Billmeyer, F.W.; *Text book of polymer science*, third edition ISBN 9971-51-141-X **1984**, P101.
4. Farn, R.J.; *Chemistry and technology of surfactants* **2006** P1.
5. Rosen, M.J.; *Surfactants and Interfacial Phenomena* ISBN 0-471-73600-7 **1978**, pp. 1-122.
6. Aniansson, E. A. G.; Wall, S. N. *J. Phys. Chem.* **1976**, 80, 905.
7. Goddard, E. D.; Hoeve, C. A. J.; Benson, G. C. *J. Phys. Chem.* **1957**, 61, 593.
8. Goddard, E. D, Benson, G. C.; *Can J Chem* **1957**; 35, 986.
9. Bruer, M.M.; *Cosmetic emulsion.* In: Becher P.ed. *Encyclopedia of Emulsion Technology*, Vol 2. New York: Marcel Dekker, **1985**, 385.
10. Tadros, Th.F; Vincent, B.; In: Becher P, ed. *Encyclopedia of Emulsion Technology*, Vol 1. New York: Marcel Dekker, **1983**: Chapter 3.
11. Friberg, S. E. *J. Soc Cosmet Chem* **1990**, 41,155.
12. Kilgman, A. M.; In: Montagna W, ed. *Biology of the Stratnum Corneum in Epidermis*. New York: Academic Press, **1964**, 421.
13. Napper, D. H.; *Polymeric Stabilization of Dispersions*. London: Academic Press, **1983**.
14. Friberg, S. E.; Jansson, P. O.; Cederberg, E. *J. Colloidal Interface Science*. **1976**, 55, 614.
15. Silberberg, A. *J. Chem. Phys.* **1968**, 48, 2835.
16. Hoeve, C. A. *J. Polym. Sci.* **1970**, 30,361; **1971**, 34, 1.
17. Putnam, F. W. *Adv. Protein. Chem.* **1948**, 4, 79.

18. Steinhardt, J.; Reynolds, *J. Multiple Equilibria in Proteins*. New York: Academic Press, **1969.**

19. Goddard, E. D.; Hannan, R. B. *J. American Oil chemist's society*. 54, **1977**, 561.

20. Arai, H.; Murata, M.; Shinoda, K. *J. Colloid Interface Sci* **1971**, 37, 223.

21. Traube, I. *Ann. Chem. Liebigs*.**1891**, 27, 265.

22. Breuer, M. M.; Robb, I. D. *Chem Ind* **1972**, 530.

23. Brackman, J. C.; Engberts, J.B.F.N. *Langmuir* **1991**, 7, 2097.

24. Brackman, J.C. ; Engberts, J.B.F.N. *Langmuir* **1992**, 8, 424.

25. Gjerde, M. I.; Hoilanad, H. *J. Colloid. Interface. Sci.* **1996**, 183, 285.

26. Dai, S., Tam, K. C. *J. Phys. Chem. B* **2001**, 105, 10759.

27. Wang, Y.; Han.; Yan, H.; Cooke, D. J,; Lu, J.; Thomas, R. K. *Langmuir* **1998**, 14, 6054.

28. Da Silva, R. C.; Loh, W.; Olofsson, G. *Thermochim. Acta* **2004**, 417, 295.

29. Schwuger, M. J. *J. Colloid. Interface. Sci.* **1973**, 43, 491.

30. Bernazzani, L.; Borsacchi, S.; Catalano, D.; Gianni, P.; Mollica, V.; Vitelli, M.; Asaro, F.; Feruglio, L. *J. Phys. Chem*. B **2004**, 108, 8960.

31. Meszoras, R.; Varga, I.; Gilanyi, T. *J. Phys. Chem. B* **2005,** *109,* 13538.

32. Jones, M. N. *J. Colloid. Interface. Sci.* **1967**, 23, 36.

33. Lang, H. ; Kolloid, Z. Z. *Polym.* **1971**, 243, 101.

34. Lad, K.; Bahadur, A.; Pandya, K.; Bahadur, P. *Ind. J. Chem*. **1995**, 34A, 938.

35. Contractor, K.; Bahadur, P. *Eur. Polym. J.* 34, **1998**, 225.

36. Luo, Y. Z.; Nicholos, C. V.; Attwood. D.; Collett. J. H.; Price. C.; Booth. C. *Colloid. Polym. Sci.* **1992**, 270, 1094.

37. Dow Chemical Co., Freeport, Texas, Technical Literature, B-Series *Polyglycols. Butylenes Oxide/Ethylene Oxide Block Copolymers,* **1994**.

38. Nace, V. M.; Whitmarsh, R. H.; Edens, M. W. *J. American. Oil Chemist's. Society*. **1994**, 71, 777.

39. Yang, Y-W.; Deng, N-J.; Yu, G-E.; Zhou, Z-K.; Attwood, D.; Booth, C. *Langmuir*, **1995**, 11, 4703.

40. Liu,T.; Zhou, Z.; Wu, C.; Schneider, D. K.; Nace, V. M. *J. Phys. Chem. B* **1997**, 101, 8808.

41. Chaibundit, C.; Mai, S-M.; Heatley, F.; Booth, C. *Langmuir* **2000**, 16, 9645.

42. Li, Y.; Xu, D.; Bloor, M.; Holzwarth, J. F.; Wyn-Jones, E. *Langmuir* **2000**, 16, 10515.

43. Booth, C.; Attwood, D.; Price, C. *Phys. Chem. Chem. Phys.*, **2006**, 8, 3612-3622.

44. Zana, R.; Binana-Limbele, W.; Kamenka, N.; Lindman,B. *J. Phys. Cem.* **1992**, 96, 5461.

45. Hecht, E.; Hoffmann, H. *Langmuir* **1994**, 10, 86.

46. Zhang, K.; Lindman, B.; Copolla, L. *Langmuir* **1995**, 11, 538.

47. Winnik, F. M.; Regismond, S. T. A. *Colloids and Surfaces A: Physiochemical and Engineering Aspects* **1996**, 118, 1-39.

48. Wen, X.; Sikorski, M.; Khmilinskii, I. V.; Verrall, R. E. *J. Phys. Chem. B* **1999**,103, 10092.

49. Desai, P. R.; Jain, N. J.; Sharma, R. K.; Bahadur, P. *Colloid and Surfaces A: Physiochemical and Engineering Aspects* **2001**, 178, 57.

50. Wetting, S. D.; Verrall, R. E. *Journal of Colloid and Interface Science* **2001**, 244, 377.

51. Thurn, T.; Couderc, S.; Sidhu, J.; Bloor, D. M.; Penfold, J.; Holzwarth, J. F.; Wynes-Jones, E. *Langmuir* **2002**, 18, 9267.

52. Jansson, J.; Schillen, K.; Olofsson, G.; Silve, R. C. d.; Loh, W. *J. Phys. Chem. B* **2004**, 108, 82.

53. Bakshi, M. S.; Sachar, S.; Yoshimura, T.; Esumi, K. *Journal of Colloid and Interface Science* **2004**, 278, 224.

54. James, J.; Vellaichami, S.; Krishnan, R. S. G.; Samikannu, S.; Mandal, A. B.

Chemical Physics **2005**, 312, 275.

55. James, J.; Ramalechume, C.; Mandal, A. B. *Chemical Physics Letters* **2005**, 405, 84.

56. Bakshi, M. S.; Kaur, G.; Kaura, A. *Colloids and Surfaces A: Physiochemical. Eng. Aspects* **2005**, 269, 72.

57. Mahajan, K. R.; Kaur, N.; Bakshi, M. S. *Colloids and Surfaces A: Physiochemical. Eng. Aspects* **2006**, 276, 221.

58. Ortona, O.; D'Errico, G.; Paduano, L.; Vitagliano, V. *Journal of Colloid and Interface Science* **2006**, 301, 63.

59. Kumbhakar, M. *J. Phys. Chem. B* **2007**,111, 14250.

60. Pepic, I.; Filipovic-Grcic, J.; Jalsenjak, I. *Colloids and Surfaces A: Physiochem. Eng. Aspects* **2008**, 327, 95.

61. Kelarakis, A.; Chaibundit, C.; Krysmann, M. J.; Havredaki, V.; Viras, K.; Hamley, I. W. *Journal of Colloid and Interface Science* **2009**, 330, 67.

62. Li, Y.; Xu, G.; Zhu, Y.; Wang, Y.; Gong, H. *Colloids and Surfaces A: Physiochemical. Eng. Aspects* **2009**, 334, 124.

63. Misra, P. K.; Mishra, H. P.; Dash, U.; Mandal, A. B. *Journal of Colloid and Interface Science* **2009**, 333, 590.

64. Adamson, A. W. *Physical Chemistry of Surfaces Third Edition April* **1976** P 2.

65. Hans-Jurgen, B,; Karlheinz, G,; Michael, K. *Physics and Chemistry of Interfaces August* **2003** P6.

66. Pierre-Gilles, D. G.; Françoise, B-W.; David, Q. ; **2002**. *Capillary and Wetting Phenomena — Drops, Bubbles, Pearls, Waves*. Springer. ISBN 0-387-00592-7.

67. White, H. E. **1948**. *Modern College Physics*. Van Nostrand. ISBN 0442294018.

68. Safonova, L. P.; Kolker, A. M. *Russian Chemical Reviews* **1992**, 61, 9.

69. Brian, C. *Glow discharge plasmas*. **1995** 74, 49.

70. Breuer, M. M.; Robb, I. D. *Chem Ind* **1972**, 530.

71. Moroi, Y. *Theoretical and Applied Aspects, Plenum, New York*, **1992**, 61.

72. Butt, H. J.; Graf, K.; Kappl, M.; **2003,** 253.

73. Stokes, G. G. (**1852**). "On the Change of Refrangibility of Light". *Philosophical Transactions of the Royal Society of London* 142: 463.

74. Joseph, R. L. principal of fluorescence spectroscopy 3rd edition by Center of Fluorescence Spectroscopy University of Maryland School of Medicine, Baltimore, MD 21201 USA **2006.**

75. Guilbault, G. G. Practical fluorescence second edition **1990**.

76. Einstein *Ann. Phys.* **1910**, 33, 1275.

77. Raman, C. V. *Indian J. Phys* **1927**, 2, 1.

78. Debye, P. Light Scattering in Solutions. *J. Appl. Phys.***1944**, 15, 338. doi:10.1063/1.1707436.

79. Zimm, B. H. *J. Chem. Phys.***1945** 13.

80. Zimm, B. H. *J. Chem. Phys.* **1948**, 16, 1093.

81. Zim, B.H. *J. Chem. Phys.* **1948,** 16, 1099.

82. Jean-François, G. *Macromolecule* **2000,** 34, 3361.

83. Yu, G-E.; Yang, Y-W.; Atwood, D.; Booth, C.; Nace, V. M. *Langmuir* **1996**, 12, 3404.

84. Yu, G-E.; Li, H.; Price, C.; Booth, C. *Langmuir* **2002**, 18, 7756.

85. Hai, M.; Han, B.*J. Chem. Eng. Data* **2006**, 51, 1498-1501.

86. Chakraborty, T.; Chakraborty, I.; Ghosh, S. *Langmuir* **2006**, 22, 9905.

87. Hecht, E.; Hoffmann, H. *Langmuir* **1994**, 10, 86.

88. Thurn, T.; Couderc, S.; Sidhu, J.; Bloor, D.M.; Penfold, J.; Holzwarth, J.F.; Wyn-Jones, E. *Langmuir* **2002,** 18, 9267.

89. Goddard, E.D.*Colloids Surf* **1986**, 19, 255.

90. Jones, M.N. *J. Colloid Interface* Sci **1967**, 23, 36.

91. Lange, H.; Kolloid, Z. Z. *Polym* **1971**, 243, 101.

92. Traube, I. *Ann.Chem. Liebigs*.**1891**, 27, 265.

93. Breuer, M.M.; Robb, I.D. *Chem Ind* **1972**, 530.

94. James, J.; Vellaichami, S.; Krishnan, R.S.G.; Samikannu, S.; Mandal, A.B. *Chemical Physics* **2005**,312, 275.

95. Dominguez, A.; Fernandez, A.; Iglesias, E.; Montenegro, L. *J. Chem. Educ.*, **1997**, 74, 1227.

96. Nawja, K.E.; Fanny, M.; Daniele, C.; Pablo, S.C. *Colloid. Polym Sci* **2003**, 281, 353.

97. Zanette, D.; Ruzza, A.A.; Frehner, S.J.; Minatti, E. *Physicochemical and Engineering Aspects* **1996,** 108, 91.

98. Brackman, J. C.; Engberts, J. B. F. N. *Langmuir* **1992**, 8, 424.

99. Bravo, C.; Leis, J.R.; Pena, M.E. *J. Phys. Chem.* **1992**, 96, 1957.

100. Misra, P. K.; Mishra, H. P.; Dash, U.;Mandal, A. B. *J. Colloid and Interface Science* **2009**, 333, 590.

101. Bakshi, M.S.; Sachar, S.; Yoshimura, T.; Esumi, K. *J Colloid and Interface Science*. **2004**, 278, 224.

102. Wetting, S.D.; Verrall, E. *J Colloid and Interface Science*. **2001**, 244, 377.

103. Bakshi, M.S.; Kaur, G.; Kaura, A. *Colloids and Surfaces A: Physicochem. Eng. Aspects* **2005**, 269, 72.

104. Turro, N.J.; Yekta, A. *J. Am. Chem. B* **1978**,100, 5951.

105. Tachiya, M. *Chem. Phys. Lett.* **1975**, 33, 289.

106. Ortona, O.; D'Errico, G.; Paduano, L.; Vitagliano, V. *J. Colloid and Interface Science* **2006**, 301, 63.

107. Reiss-Husson, F.; Luzzati, V. *J. Colloid Interface Science* **1966**, 21,534.

108. Mysels, K. J.; Princen, L. *J. Phys. Chem* **1959**, 63, 1696.

109. Tartar, H. V. *J. Colloid. Sci* **1959**, 14, 115.

110. Ekwall, P.; Mandell, L.; Solyom, P. *J. Colloid Interface Sci.* **1971**, 35, 519.

111. Zana, R.; Binana-Limbele, W.; Kamenka, N.; Lindman, B. *J. Phys. Chem* **1992**, 96, 5461.

112. Lin, C-M.; Chen, Y-Z.; Sheng, Y-J.; Tsao, H-K. *J. Reactive and Functional Polymers* **2009**, 69, 539.

113. Castro, E.; Taboada, P.; Barbosa, S.; Mosquera, V. *Bio macromolecules* **2005**, 6, 1438.